**The Thesis Committee for Ellen Elizabeth Reid**
**Certifies that this is the approved version of the following thesis:**

# The effect of temperature and terrace geometry on carbonate precipitation rate in an experimental setting

**APPROVED BY**
**SUPERVISING COMMITTEE:**

**Supervisor:**

Wonsuck Kim

Joel Johnson

David Mohrig

# The effect of temperature and terrace geometry on carbonate precipitation rate in an experimental setting

**by**

**Ellen Elizabeth Reid, B.S.Geo.Sci.**

**Thesis**

Presented to the Faculty of the Graduate School of

The University of Texas at Austin

in Partial Fulfillment

of the Requirements

for the Degree of

**Master of Science in Geological Sciences**

**The University of Texas at Austin**

**August 2012**

# Dedication

This thesis is dedicated to my parents, who have never stopped supporting me and believing in me during my pursuit of higher education.

# Acknowledgements

First and foremost, I would like to acknowledge my adviser Wonsuck Kim, who aided me in every way from the initial concept of my research to writing the thesis. My research would not have been possible without him. Wonsuck, I appreciate your gracious patience and guidance. I'd also like to thank my committee of David Mohrig and Joel Johnson, for visiting my flume, generating ideas for what direction to take my experiments, and revising my thesis. I would like to thank my lab assistant Eric Swanson for countless hours constructing and refining the flume and assisting in conducting the experiments. I would like to thank Jake Jordan and Kiran Sathaye for their constant encouragement and input (and MATLAB assistance). Finally, I would like to thank the Jackson School of Geosciences for their support during my undergraduate and graduate career, and shaping me into the geologist that I am today.

# Abstract

## The effect of temperature and terrace geometry on carbonate precipitation rate in an experimental setting

Ellen Elizabeth Reid, M.S.Geo.Sci.

The University of Texas at Austin, 2012

Supervisor: Wonsuck Kim

Through flume experiments we demonstrate the calcite precipitation process seen at geothermal hot springs in the lab setting. A series of four experiments were run, varying temperature and terrace ridge height while all other experimental parameters, including initial substrate slope, spring water discharge, and $CO_2$ input were kept constant. The goal of the experiments was to measure the temperature and terrace height control quantitatively in terms of the amount of overall travertine aggradation, aggradation rate changes in time and downstream direction, as well as to observe the effect of these parameters on processes occurring during precipitation. Using the final deposit thickness measured manually at the end of each experiment and elevation data obtained from a laser topographic profiler, I conclude that high temperature and small terrace heights favor increased precipitation of travertine. However, the amount of precipitation also depends on location within a terrace pond. Flow velocity increases as it approaches a terrace lip, resulting in enhanced precipitation and greater thicknesses in the

downstream direction through increased $CO_2$ degassing, a process called downstream coarsening.

# Table of Contents

# List of Tables

## List of Figures

# Chapter 1: Introduction

I have conducted a series of experiments precipitating calcite in the laboratory setting using a flume. Water discharge and initial substrate slope were held constant while temperature and terrace height were varied for each experiment, and the resulting deposit was analyzed. The field process analogue for setting parameter standards in the hot water experiments is a hot springs environment, such as Mammoth Hot Springs, Yellowstone National Park. Travertine here forms as terraces, which is the morphology I attempted to recreate in the experiments. Studying the travertine precipitation process and its resulting deposits is useful in a number of applications. Travertine deposits are very sensitive to water chemistry, transport conditions, and climate. Therefore, travertine serves as a reliable source for reconstructing paleoenvironments (Fouke 2000). Some hot springs are in particularly harsh, unusual environments and contain unique microorganisms; these can be used for discern information about primordial life on Earth as well as potential life on other planets (Fouke 2000). Travertine also has industrial application. When urban settings sit on top of limestone/carbonate rocks or karst environments, limestone precipitation in pipes and boilers is a major issue and source of financial loss for cities (Hammer 2008). Travertine also can serve as a reservoir for hydrocarbons, for example, the Itaborai Basin in Southeastern Brazil was a carbonate hot spring in the Paleocene (Sant' Anna 2004).

In this study, we focus on the temperature and terrace geometry controls on carbonate precipitation patterns to enhance our ability to utilize carbonate sedimentary records for reconstructing paleoenvironments.

**Travertine environments and associated patterns**

Travertine is a type of carbonate, a precipitated form of limestone with the chemical formula $CaCO_3$, and includes all deposits in non-marine settings in its strictest definition. Travertine will precipitate in an array of environments, including hot springs, mountainous streams, caves, and waterfalls (Hammer 2008; Fouke 2000). It forms in predictable yet poorly understood morphologies based on the surrounding environment and local conditions. For example, in hot springs such as Mammoth Hot Springs in Yellowstone, much work has been done studying travertine terraces, also known as cascading dams (Hammer 2008), rimstone (Goldenfeld 2006), or barrages (Pentecost 1994). Travertine terraces appear as a series of steps: laterally extensive, vertical ridges with flat tops that cover most of the surface area (Figure 1.1). A second dominant morphology present in hot springs is travertine domes, for which Goldenfeld (2006) provides a growth model. Other potential morphologies of travertine include needle-like speleothems in caves and tufa in low-temperature locations (Fouke 2000). Travertine morphology depends on environmental conditions. Chavetz (1984) classifies five morphological variations for all travertine deposits, including cascade, lake-fill, sloping mound, cone or fan, terraced mound, and fissure ridge. All of these classifications are informal; there is currently no systematic way of naming or organizing travertine deposits (Pentecost 1994). For example, in some literature "tufa" refers to cold water carbonate precipitate (Hammer 2007). In other literature, whether a deposit is classified as travertine or tufa depends on the degree of cementation (Pentecost 1994).

Travertine can form in a wide range of temperatures, from 5 degrees to 95 degrees Celsius, though most environments are within the 10-30 degree Celsius range (Chavetz 1984). When travertine is deposited it is fragile, friable, poorly cemented, and subject to degradation

from external environmental forces. For this reason travertine deposits in tectonically active areas are relatively young, Quaternary age and younger (Sant'Anna 2004). Many travertine deposits have a high proportion of sand and mud grains in their composition, especially in turbulent, high-energy environments (Pentecost 1994). Travertine is also more commonly found in warm, tropical climates than in high latitude locations (Pentecost 2000). Travertine deposits can be deposited very rapidly, up to five millimeters per day. This is a million-fold difference compared to the rates of classic depositional environments and erosional landscapes, however travertine precipitates on much shorter time scales (Veysey 2008). The thickness of these terrace deposits can be over a variety of scales, from millimeters to hundreds of meters (Goldenfeld 2006).

Travertine precipitation and local topography feedback on one another (Goldenfeld 2006) – the geomorphology of the location can influence the morphology of the travertine deposit that forms as a result, but deposits can also have an effect on water flow and as a result the topography of the evolving surface. Its presence can also change the slope of the land, and the overlying pattern of erosion and accumulation, including protecting the underlying surface from erosion (Pentecost 1994). Because of the resulting irregular topography and the rapid formation of deposit, it is often difficult if not impossible to correlate between travertine layers in stratigraphy (Sant'Anna 2004).

**Precipitation process**

The saturation of water with calcium carbonate can result in either dissolution or precipitation, depending on the saturation degree (Hammer 2008). When dissolved carbonate and calcium ions become supersaturated in water, they will precipitate out as travertine, according to

the equation $Ca^{2+} + CO_3^{2-} = CaCO_3$ . These ions are usually dissolved into water by dissolved carbon dioxide interacting with limestone or other carbonates. The source of the carbon dioxide can either be the soil or atmosphere (the resulting is meteogene travertine) or hot rock or $CO_2$-rich fluid (thermal travertine) (Pentecost 1994). At this stage the solution is usually saturated to slightly supersaturated with respect to calcite and completely supersaturated with respect to carbon dioxide (Chavetz 1984). When the carbon dioxide leaves by degassing the solution then becomes supersaturated with calcite to the degree necessary to precipitate travertine. After degassing of $CO_2$, the degree of saturation of 5-10 times with respect to calcite is achieved, which is necessary to initiate carbonate precipitation. (Chen 2004).

Two stages exist in this process: 1) degassing, which is marked by an increase in the pH and 2) precipitation, where there is an increase in the conductivity of the water (Chen 2004). Carbon dioxide degassing can be visible to the eye as gas bubbles on the surface of the water or carbon dioxide vapor rising in hot water environments. The carbon dioxide degasses by multiple mechanisms: first, turbulent flow and mixing of the water promotes degassing. This is believed to be the dominant mechanism for precipitation, and can promote degassing by an order of magnitude (Buhmann 1984). Chen (2004) found that flowing water produced four times as much precipitation compared to stationary water in his experiments. Evaporation also will promote degassing and precipitation, however in many environments precipitation occurs on such short time scales that evaporation is not a major factor. Metabolic activity by microbes will uptake $CO_2$ and therefore also promote precipitation, but these are thought to have less of an effect than inorganic processes (Goldenfeld 2006).

After degassing, there are two phases of precipitation: nucleation of crystals and growth of crystals (Berner 1980). Chen's (2004) laboratory precipitation experiments estimate a calcite

supersaturation degree of approximately seven fold is necessary to initiate nucleation. After the nucleation barrier has been breached, precipitation can begin as the nucleated crystals grow in size and link together (Chen 2004).

**Rate of precipitation**

The precipitation of travertine depends on the interplay between many parameters, including water chemistry, physical processes, hydrology, biotic activity (Fouke 2000) and abiotic factors including temperature, pH, water discharge, and carbon dioxide degassing rate (Stelmach 2011). Colder water will favor dissolution of calcium carbonate (it can hold a great concentration of ions per volume), where warmer water will promote precipitation of dissolved ions out of solution (Stelmach 2011). A greater amount of dissolved ions will induce a lower, more acidic pH, and as precipitation of carbonate occurs the pH will steadily rise and become more basic. Flow rate has a direct relationship with growth rate: as the water velocity increases so does the precipitation rate (Hammer 2008). The cause is debated to be either because high velocity thins the diffusion-limiting boundary (Zaihua 1995), or because high velocity accelerates degassing of carbon dioxide due to greater agitation of the water (Hammer 2007).

Buhmann (1984) defines three points of the precipitation process which ultimately determine the precipitation rate: 1) dissolution kinetics between calcium carbonate, carbon dioxide and water 2) kinetics of carbon dioxide conversion to carbonic acid ($H_2CO_3$) and 3) mass transport of dissolved ions. The air-water interface, where carbon dioxide bubbling and degassing occurs, plays a much larger role in accelerating carbonate precipitation compared to the solid-water interface area (Chen 2004).

**Hot springs environments and Mammoth Hot Springs, Yellowstone**

In hot springs environments, precipitation of travertine occurs in the following way: geothermally heated water will be expelled from a vent at around 60-100 degrees Celsius. Once at the surface, the water will flow downhill over preexisting topography, carbon dioxide will degas and the dissolved calcite will precipitate as travertine (Goldenfeld 2006). Hot springs travertine is usually associated with faults: they provide the conduit for which the geothermal water can migrate to the surface (Chafetz 1984).

Mammoth Hot Springs (MHS) is the most active of three areas in Yellowstone National Park with travertine accumulation (Vescogni 2009). It spans an area of 4 square kilometers and has terraces up to 73 meters thick (Fouke 2000). The source of the geothermal water is from the Gallatin Mountain Range to the west of the Park (Sorey and Colvard 1997). The water then travels through the Mammoth and Swan Lake Faults where the surrounding rock is Paleozoic carbonates of Mississippi Madison Group Limestone. The heated water dissolves these carbonates at 2-3 kilometers depth (Sorey and Colvard 1997). This water erupts at vents at Mammoth Hot Springs at 71-73 degrees Celsius and with a pH of 6.1. By the time the flow runs its course over the surface of the springs and percolates back under ground the pH will have rose to 8 and it will be at ambient temperature (Fouke 2000). Travertine precipitates throughout the course of the springs, and Fouke (2000) outlines different mineral facies that exist based on their distance from the vent. Aragonite and calcite, the two mineral forms of travertine, both precipitate at MHS but will preferentially form based on facies' temperature (Fouke 2000). The springs are estimated to be 8,000 years old and 10% of the total discharge of 590 L/second for all Mammoth Hot Springs (Fouke 2000). Vents will seal, or reopen and flows will divert paths with the frequency of months to tens of years (Fouke 2000).

Microorganisms are present in each facies in Mammoth Hot Springs, though abiotic (chemical and physical) processes are responsible for the majority of precipitation (Fouke 2000). Vertical growth (aggradation) of the terraces averages about one to five millimeters per day when the springs are active, which is only during some seasons (Goldenfeld 2006). Three scales of terraces have been defined at MHS: terraces (area of tens of square meters), terracettes (few square meters) and microterraces (square centimeters) (Bargar 1978).

**Travertine terrace formation and growth processes**

Travertine terraces or dams will form only on gradual slopes. Slopes after threshold steepness will induce fast, chaotic flow and no dams will develop (Hammer 2007). Terrace steps form in preferential locations due to local obstructions, slope breaks, or disparities in topography. First growth of the terrace will begin here, and through difference in velocity and positive feedback the terraces will aggregate at a higher rate vertically here and the step morphology will be created (Pentecost 1994). Spacing between terraces depends on the steepness of the slope – terraces will be closer spaced on steep slopes because there will be less of an effect of inhibition of growth by upstream drowning, which is only prominent on shallow slopes (Hammer 2007).

Veysey (2008) noted several processes that occurred during terrace formation and growth by taking time-lapse photography at Canary Springs in MHS. Among these is pond inundation or upstream drowning, where downstream lips will grow at a faster rate than upstream lips and will produce rims that dam the flow, ponding water upstream of them. Also, pond merging, where two smaller ponds will aggregate to form on larger pond occurs at MHS, but this process is only applicable for two ponds and unlikely for three or more ponds. Also, at very high water flux, pond lips grow in the direction of the flow.

Hammer (2007) also noted the upstream drowning process at outcrops in Rapolano Terme, Italy. He further postulated that this ponding of water allows the upstream crests to coarsen to the height of the downstream crests. Crests then migrate down slope and grow up and outwards, due to alternating precipitating rate (Hammer 2007). Larger crests will grow faster and coarsen due to positive feedback, and will overtake smaller terraces downstream of their location (Hammer 2007). Another discrepancy along downstream profiles is thinning of outer walls in downstream crests (Hammer 2007). Crest distance is approximately constant and regularly spaced due to internal self-regulating mechanisms. Positive feedback crest growth will occur due to the positive flow rate relationship but crest growth is inhibited by upstream drowning (Hammer 2007). These processes are self-organized and regulate terrace spacing and crest size. Crests have also shown the ability to regenerate and reform with introduction to perturbations to their environment (Hammer 2007).

**Biological impact on travertine precipitation**

Microorganisms impact travertine precipitation during the initial nucleation of travertine and can accelerate the precipitation rate. Microbes act as a mechanical substrate on which the mineral precipitate can bind. Physical processes in which microbes assist in the positive feedback mechanism of precipitation include: encrustation, trapping, assimilation, and nucleation of travertine (Chen 2004). Also, photosynthetic and metabolic processes of the biota remove carbon dioxide from the system and further enhance supersaturation of calcite and travertine precipitation (Hammer 2007). Microbial metabolic activity locally influences the carbon dioxide distribution through the water column, thereby affecting the precipitation rate (Goldenfeld 2006).

Microbes also influence the mineralogy of the travertine. Aragonite will preferentially form in the presence of microbes (93% aragonite), and calcite will preferentially form in abiotic environments (95% calcite) (Folk 1994; Kandianis 2008; Vescogni 2009). This is from microbe lipids, proteins, and polysaccharides, which alter travertine precipitation rates (Mann 2001). Microorganisms also change the crystalline architecture of aragonite – aragonite will have ridges and "fuzz balls" with microbial influence (Stelmach 2011). On a whole, biologically induced mineralization tends to have poor crystallinity that is distinguishable from inorganic crystals (Frankel and Bazylinski 2003). Carbonate is also favorable for microbes, as they may grow at four times faster rate on a carbonate substrate compared to purely water.

The abiotic versus biotic impact on degassing of carbon dioxide and travertine precipitation is complicated, unknown, and highly debated among the scientific community (Goldenfeld 2006). Determining the dominant mechanism at a site is often difficult (Schlager 2003). Friedman (1970) insisted that inorganic degassing of carbon dioxide drives precipitation. Fouke (2000) proved through sulfur-isotope data that microbe metabolic processes are not occurring at MHS and that inorganic processes dominate. Chafetz (1984) also agreed that physically driven agitation of water results in a great loss of carbon dioxide, but stated that bacteria are responsible for a large percentage (>90%) of travertine accumulation at some sites. He designated these sites based on distance from the vent. Near vent where flow velocity is high and there is turbulence of flow, inorganic processes dominant. Down current, organic processes will play an increasingly important role. (Chavetz 1984).

**Previous studies**

Travertine has been studied in numerous different actively precipitating sites as well as stratigraphically in outcrop. Numerical models have also been constructed that capture aspects of terrace growth (Goldenfeld 2006; Hammer 2007; Veysey 2008). Only recently has travertine been successfully precipitated in a laboratory setting, both organically and inorganically (Vescogni 2009; Stelmach 2011). Vescogni (2009) studied mineralogy and crystal fabric of precipitated travertine in presence of microbes. Stelmach (2011) determined the total mass of precipitate and precipitation rate with biotic influence compared to an abiotic system. In my experiments, I precipitate travertine under similar conditions as Vescogni (2009) and Stelmach (2011), but with more focus on carbonate aggradation as a function of water temperature and flow agitation due to different terrace heights.

# Chapter 2: Experimental Design

**Precipitation Process in the laboratory**

Eight experiments were conducted in the morphodynamics carbonate flume lab at the University of Texas at Austin in spring 2012 (Figure 1.2 and 1.3). Travertine was precipitated from dissolved limestone of the Austin Chalk Formation. This limestone was obtained from outcrops overlying Waller Creek on the UT campus. The Austin Chalk limestone is known for its minimal chemical impurities and is suitable for precipitating travertine in our experiments. This limestone was pulverized into gravel sized grains, ranging from pebble to cobble sized, using a manual rock crusher. Smaller rock fragments increase the total surface area of rock immersed in the water, promoting a higher amount of carbonate dissolution. The limestone was then suspended using plastic netting in a 55-gallon polyethylene cylindrical tank. Bottled spring water was used to fill the reservoir tanks. $CO_2$ was injected into the tank at 3-5 psi to stimulate limestone dissolution. To promote adequate integration of the water with carbon dioxide, a mixing pump internally circulated water in the tank. An aquarium pump and bubble wands were also used, which distributed the $CO_2$ bubbles throughout the volume of the tank.

The solution at this point was supersaturated with $CO_2$ and slightly supersaturated with respect to the carbonate and calcium ions (Chafetz 1984); these dissolved ions in solution are then run through one-fourth inch polyethylene tubing that is coiled into two heating pots and was heated to temperatures replicating hot springs, ranging from fifty-five to sixty degrees Celsius. The inlet tube is positioned vertically over the surface of the flume channel. The temperature of the water was measured upstream out of the inlet tube and downstream end of the flume channel every thirty minutes using an electronic thermometer as well as an alcohol thermometer. The

water discharge was kept at 3.8-4 ml/s. The upstream discharge out of the inlet tube was measured every thirty minutes to guarantee consistency. As water releases onto the flume channel and flows downslope, the sudden expansion in surface area to the air drives the partial pressure of $CO_2$ down, and it degasses into the atmosphere. This causes a decrease in the solubility of the calcium and carbonate ions and they become supersaturated in the solution; precipitation of travertine is then favored and will occur over the area of the flume surface. Evidence of the precipitation process, such as bubbling and degassing of $CO_2$ vapor was visible over the surface of the water. As the water falls off the edge of the flume channel and into the tub below it is pumped and recirculated back to a second reservoir tank to cool to ambient temperature.

The target pH for the experiment ranged from 6.0-6.5 pH for the water coming out of the inlet tube onto the flume channel and from 6.5-7.0 for water leaving the channel to be recirculated. The pH was measured and documented every thirty minutes using a calibrated electronic pH meter. One source of $OH^-$ ions and one source of $H^+$ ions were used to buffer the ionized water to control pH: a solution of three grams CaOH powder (solvent) per liter of water (solute) was constantly added to the primary reservoir tank at a rate of 0.762 ml/s. It acted as a base to increase the pH of the solution as well as an added source of $Ca^{2+}$ ions in solution to increase the precipitation rate. Dry ice, the solid form of carbon dioxide, was added to the primary reservoir to increase dissolution of limestone. Five to six hundred cubic centimeters of dry ice pellets were added to the reservoir every thirty minutes. Its freezing temperature also further promoted dissolution. Time-lapse images of the aerial view of the flume channel were taken every five minutes over the course of the experiments. Slope was kept at 0.2 degrees for all

experiments, and was measured using the length of the separation of the wood planks below the channel and the difference in elevation.

**Design for experimental Set**

Two fifteen centimeter flume channels were constructed side-by-side so experimental runs could be conducted back to back. Artificial "steps" were placed down the length of the flume channel. Popsicle wooden sticks that covered the fifteen-centimeter width of the flume pathway were attached to the metal surface cross-stream wide, glued using silicone adhesive. The wooden sticks were placed every fifteen centimeters down the length of the flume. The sticks had a thickness of 0.16 cm and were placed at different descending heights downstream in the flume. The heights take into account total stick thickness plus adhesive thickness. The purpose of these steps is to provide an initial terrace-like surface perturbation for which the travertine can precipitate over and form terrace patterns. The total flume length includes five ponds and four steps separating each pond (Figure 1.4). Past field studies have shown that many active travertine terraces in natural settings are precipitating on top of previously deposited, solidified travertine steps (Pentecost 1994). By providing initial steps for the travertine to precipitate over, terrace development is likely to occur at an enhanced rate. A piece of wood was placed at the upstream end of the flume to act as a barrier to prevent water flowing upstream off of the flume and precipitating.

Four experiments were conducted using this experimental set-up. All experiments had the same base slope for the flume channel of 0.2 degrees. A topographic profiler was also placed at the downstream end of the flume and provided a straight laser line that marked the center of the flume (7.5 centimeters on each side of the laser line) through the entire flow path. Low-light images of the laser-sheet line were taken every thirty minutes to measure topography of the

deposit as the carbonate surface grew. The four experiments varied in temperature of the water and height of the artificial, wooden stick "steps". The influence of initial step height and temperature of the water on deposit morphology and growth rate was observed. In the first two experiments, the step heights are as follows: the most upstream step (step 1) had a height of 1.6 cm. The following step (step 2) had a height of 0.75 cm, step 3 had a height of 0.35 cm, and the most downstream step (step 4) had a height of 0.18 cm. In the final two experiments the stick heights were doubled, ranging from 0.32-3.2 centimeters in thickness. In the first and fourth experiments, $S_H$ and $L_H$, water was heated to hot springs temperatures of 55-60 degrees Celsius as it flowed over the flume. In the second and third experiments, designated $S_C$ and $L_C$ respectively, the same flume was used but the water circulated through the flume was at ambient temperature, 20-23 degrees Celsius. The tested parameters for each experiment are shown in Table 1. Measurements taken during each experiment, such as temperature, pH, and conductivity, are plotted for each experiment (Figures 2.1-2.12). Each experiment ran for forty hours.

# Chapter 3: Data Collection and Processing

Evolution of surface elevation and morphology over the course of an experiment were documented using time-lapse photography, with an image taken every five minutes (Figure 3.1). Elevation data was collected using a laser topographic profiler where the laser line was positioned at the center of the flume channel (7.5 centimeters from either side of the flume wall). Every thirty minutes the overhead utility light was shut off so that the laser line would be prominent on the image, improving the elevation data analysis (Figure 3.2). The contrast between the red laser line and near-black surroundings in the dark images was necessary to isolate the line using Adobe Photoshop. The images were corrected in Photoshop for lens distortion and camera angle, cropped to include only the flume channel and then resized. The threshold feature was applied to convert the images to black and white only, and the white color represented the laser line from the image (Figure 3.3). The images were then run through a MATLAB code that mapped the laser line to provide topographic elevation data. These values were then imported into Excel, which allowed for plotting of the elevation of the laser line through the cross section of the flume over experiment run time. Because of the reflection of the water on the images, corrections were made for the apparent versus actual water depth and applied to the elevation data. Elevation data was not obtained for pond 1 for all experiments and for pond 2 for the $L_C$ and $L_H$ runs. These represent the tallest dams of 3.2 and 1.6 centimeters respectively, and in these large water depths the laser line was not captured on the water surface.

Besides the laser elevation data, thickness of the deposit was also measured manually after experiments $S_H$, $L_C$, and $L_H$ by taking three measurements to cover the width of the flume, every five centimeters down the flume length. Manual measurements were the main source of data used in analysis and formulating conclusions. Elevation data from experiments $S_H$ and $S_C$

followed expected trends after water correction and calibration was applied. For experiments $L_C$ and $L_H$ the resulting data after calibration and water correction had large discrepancies compared to the manual measurements and was therefore not used for analysis. A unexpected shift of the imaging system during runs $L_C$ and $L_H$ caused the discrepancies in the manual and laser topographic data. However, the evolution of $L_C$ and $L_H$ system defined by the laser topographic data is still valid. In the following results, discussion, and conclusion sections, data provided will be from manual thickness measurements and elevation data for experiments $S_H$ and $S_C$ only. The exception to this is the thickness variance sections: to determine the overall evolution of carbonate deposition elevation, data from all four experiments was considered.

# Chapter 4: Results

## Deposit thickness

Using the manual measurements, thickness of the deposit decreased in the downstream direction in all experiments. The observed change in thickness with downstream distance is best represented by a second order polynomial, with $R^2$ values ranging from 0.90 to 0.99 (Figures 4.1-4.3). The thickest deposit measured was approximately ten millimeters and developed during the large stepped, hot water experiment in the most upstream pond (i.e. pond 1). Pond 1 generally had the thickest deposits ranging from 6-10 millimeters. Thickness measurements in pond 1 varied greatly if erosion of the deposit occurred from flow of water out of the inlet tube. Pond 2 thicknesses ranged from 1.5-4 millimeters, and pond 3 thicknesses ranged from 0.3-2 mm. A maximum thickness of 4 millimeters for pond 2 was reached in $L_H$ and $S_H$ and $L_H$ for pond 3. At the very downstream end in pond four, thickness measurements were a millimeter or less, with some areas of the flume having no precipitation at all.

Steps, the wooden sticks dividing the ponds, overall received less precipitation than ponds. Rather than step height, the route of the flowing water dictated the deposit thickness on the steps. In the small stepped and hot water experiment ($S_H$), the steps followed the same trend as the ponds, where the thickness decreased with downstream distance, from 0.5 millimeters upstream to 0.1 mm downstream (Figure 4.4-4.6). In the large stepped and ambient temperature experiment ($L_C$), water diverted so that flow occurred only over a small width of the first step, therefore the second step has the highest thickness values. The large stepped and hot water experiment, *($L_H$)*, shows no trend of step deposit thickness in the downstream direction. All measurements are 0.5 millimeters or less.

Thicknesses were obtained from the elevation data by taking the difference in elevation between the first and last time period. Comparing the two small stepped experiments, at ponds 2 and 3, $S_H$ shows slightly greater thickness than $S_C$ (Figures 5.1-5.5). For downstream ponds 4 and 5, thickness was approximately equally between $S_H$ and $S_C$.

Pond thicknesses decrease in the downstream direction according to the elevation data for all experiments (Figure 5.5). For example, pond 2 thicknesses in $S_H$ are from 6-10 millimeters, pond 3 thicknesses are 3.5-8 millimeters, 1 millimeter for pond 4, and 1-3 millimeters for pond 5. This thickness data is consistent with that from the manual measurements. For $S_C$, pond 2 and 3 thicknesses range from 2-6 millimeters, and 2 millimeters for pond 4 and 5.

**Temperature influence on pond aggradation**

Manual measurements of thickness for the two large stepped experiments, $L_C$ and $L_H$ show that the hot water temperature generally enhanced carbonate precipitation. Three out of four ponds showed thicker deposits for hot water temperatures (Table 2.1). Deposits associated with ambient water temperature were 66-92% thinner than in the corresponding hot water experiment.

In the elevation data (Figures 6.1-6.4) for experiments $S_H$ and $S_C$, ponds 2 and 3 show the greater increases in elevation over time compared to the downstream ponds 4 and 5. Experiment $S_H$ shows greater elevation increases compared to $S_C$ in all ponds. For pond 2, in $S_H$ the elevation increases about 9.44 millimeters, while for $S_C$ the elevation increases 7.15 millimeters. For pond 3, the elevation increase in $S_H$ is 7.91 millimeters compared to 4.32 millimeters in $S_C$. In downstream pond 4, the water correction method used is not able to resolve any change in surface elevation over time. Pond 5 also follows the same trend as the upstream ponds; $S_H$ shows a larger overall aggradation of 1.25 millimeters compared to 0.5 millimeters for experiment $S_C$.

Temperature influence applied equally to the results from the large step experiments. Both manual measurements and topographic data consistently show higher aggradation rates in the hot water experiments (Figures 6.1-6.4).

**Step height influence on pond aggradation**

In the current series of experiments we assembled two sets of step heights, smaller step heights ranged from 0.18-1.6 centimeters (downstream to upstream) in experiments $S_C$ and $S_H$, and larger step heights ranged from 0.32-3.2 centimeters in experiments $L_C$ and $L_H$. Generally the deposit thicknesses in the smaller stepped experiments are comparable to those in the large stepped experiments. The maximum thicknesses are still associated with $L_H$ but in comparing the spatial averages using the manual thickness measurements between $L_H$ and $S_H$, in three out of four ponds the smaller step heights yielded slightly higher thickness values, 106-167% greater than values for the same ponds of the corresponding large stepped runs (Table 2.2).

Unfortunately the elevation evolution data for $S_C$ and $L_C$ cannot be accurately compared because there are no manual measurements for $S_C$.

**Step aggradation**

All four experiments show slight increase in elevation on the steps over time (Figures 6.5-6.8). Regardless of upstream or downstream location, the growth trend and thus positive slope of the elevation line is similar for all four steps. $S_H$ shows higher aggradation in upstream steps: an elevation increase of 3 millimeters for step 1 and step 2, and a 1.5 millimeter increase for steps 3 and 4. There is some offset from the manual measurements but these show the same downstream trend. $S_C$ shows an increase in elevation with time for steps 2, 3, and 4, but step 1 stays at a constant elevation value. Experiment $S_C$ shows no change in elevation towards the

downstream direction. This error in the elevation data was from a shift in camera location during this run. We will cover this in more detail in the discussion section.

**Deposit thickness variance in a single pond**

The process of downstream coarsening within a pond, where the thickness of the deposit increases in the downstream direction, was observable using manual measurements and elevation data. Manual thickness measurements show a slight increase, up to two millimeters, in thicknesses towards the downstream direction within a single pond. For example, in pond 1 of experiment $L_H$, the deposit coarsens from 2 millimeters at the very upstream end to 5 millimeters at the downstream edge of the pond.

This downstream coarsening is confirmed in the elevation data in all four experiments for at least one of the ponds (Tables 3.1-3.4). In experiment $S_H$, pond 2 showed the greatest amount of coarsening, 3 millimeters, over a single fifteen-centimeter pond (Figure 5.1). Between all four runs, the downstream coarsening trend is also observed for ponds 3 and 4, but is less dramatic. In pond 5, the thickness measurements across the pond are approximately constant. Precipitation did not occur at the downstream termination of pond 5 in some runs so the reverse relationship (downstream thinning) was seen and produced negative values in Table 3.4.

**Aggradation rate**

Time and space averaged aggradation rates were measured for each pond and step for each of the four experiments. These represent rates of deposition in units of millimeters per minute. In general, aggradation rates were positive but fluctuated with time. There is no strong trend of the rate increasing or decreasing over time. For experiments $S_H$ and $S_C$, aggradation in the upstream ponds generally was at slightly higher rates compared to downstream ponds

(Figures 8.1-8.4 and Table 4.1 and 4.2). The majority of rates fall within an order of magnitude of each other, the greatest magnitude difference being the increase in aggradation rate from 8.99 x $10^{-4}$ 4 mm/min to 2.47 x $10^{-3}$ mm/min from pond 5 to pond 2 in experiment $S_C$, under ambient water temperature and small stepped conditions. All of the other experiments showed a similar trend, with pond 5 having the smallest aggradation rate and pond 2, the most upstream pond measured, having the highest aggradation rate.

Comparing hot versus ambient water temperature runs, hot water runs had higher aggradation rates. For the small stepped experiments $S_H$ and $S_C$, the hot water experiment had rates from 7.71 x $10^{-3}$ mm/min to 1.01 x $10^{-3}$ mm/min, where as the ambient temperature experiment had lower rates from 2.47 x $10^{-3}$ mm/min to 8.89 x $10^{-4}$ mm/min (Table 4.1). The magnitude of the fluctuation rate was higher for the hot water experiments compared to the consistent growth shown in the ambient temperature experiments.

Comparing the aggradation rate between steps within each experiment, a similar trend was found. Steps 1 or 2 had the highest rate of aggradation all experimental runs, and the aggradation rate decreased towards the downstream direction in steps 3 and 4 (Table 4.2). Hot water experiment $S_H$ also displayed higher aggradation rates on the steps compared to ambient temperature experiments.

Comparing between ponds and steps most aggradation rates occur within the same orders of magnitude (Table 4.1 and 4.2). Overall, the pond aggradations are slightly higher than those on the steps. The most noticeable disparity is the rates between pond 3 and step 3, which divides ponds 3 and 4. In experiment $S_C$ the aggradation rate in pond 3 is ten times greater than that on step 3.

# Chapter 5: Discussion

## Temperature influence on bed aggradation

Higher temperatures are expected to result in increased precipitation rate of travertine. At higher temperatures the dissolved carbonate ions in solution become supersaturated and favor precipitation. This relationship was confirmed by the manual measurements of deposit thickness. In experiments $L_C$ and $L_H$, the influence in more pronounced further downstream in ponds 4 and 5. We believe temperature to be the dominant control on amount of degassing in these downstream ponds because the step heights are small enough to isolate the temperature control. Thicknesses in ponds 2 and 3 between these two experiments are generally more or less the same. An explanation for this attenuation of the temperature control is that hydraulic processes, such as mixing and turbulence of the water are the dominant influence on degassing as the water comes out of the inlet tube or over the tallest step from ponds 1 to 2. Chen (2004) concludes that hydrological changes at waterfalls are the main mechanism by which tufa deposits form at those sites, and similar reasoning applies here. In contrast, for the smaller step heights between ponds 3 and 4 and 4 and 5, hydraulic processes are less prominent and therefore temperature becomes the main control of precipitation rate.

## Step height influence on thickness

In ponds 2, 3, and 4, the thickness of the travertine for the smaller step heights of experimental run $S_{H.}$ are fairly comparable to those for the large stepped run $L_H$. We expected the large steps to enhance precipitation by hydraulic processes e.g., water mixing and turbulence over the structures. However, a higher temperature is maintained through the length of the flume with smaller steps, while with large dams the circulation of the water through the flume system takes longer, especially through the first and second pond. This allows the water to further cool

by the time the water arrives at the downstream ponds, which causes less precipitation in these ponds. The average temperatures measured at the downstream end of the flume during experiments show that the water was in fact cooler for experiment $L_H$. The average water temperature was 46.8 degrees Celsius for experiment $L_H$, compared to an average water temperature of 51.1 degrees Celsius for experiment $S_H$ with the smaller steps. At the most upstream pond (pond 1), the thickness measurements were similar between the two experiments. Since the tube is discharging directly into the ponded water, we conclude that consistent temperature is maintained between these experiments in this pond regardless of step height. Local erosion by flow out the inlet tube water also affects thickness of the deposit in pond 1, but it has been excluded from this analysis.

**Control of flow path on step thicknesses**

A slight decrease in step deposit thickness was found in experiment $S_H$, while no clear trend presented itself with the manual measurements of step thicknesses in experiments $L_C$ and $L_H$. The location of precipitation of carbonate on steps is due to water flow. The route that the water flowed was different in each step and in each experiment and also shifted laterally, thus resulting in randomly arranged thicknesses. In some experiments, such as $L_C$, saw small increases and decreases in thickness towards the downstream, which might be caused by change in the lateral location of major flow over the steps. Since the overall thicknesses are small on the $L_C$ steps, 0-0.5 millimeters, these small increases may also reflect instrument measurement errors.

**Overall downstream trend in precipitation**

Aggradation occurs at a greater amount in upstream ponds than in downstream ponds. As water is discharged from the source and flows over the flume surface, the water is supersaturated

with carbonate and calcite ions, so precipitation of travertine is highly favorable. But as degassing of $CO_2$ and precipitation of travertine initiates, the ion concentration falls below the saturation point, and degassing and precipitation become less favorable and will decrease downstream. With our experimental setup, small step heights were placed downstream and higher step heights were upstream. Since turbulence and mixing of water promotes precipitation of travertine, our experimental set up also favors higher precipitation at the upstream end, where higher dam height drops promote these hydraulic processes occurring.

Aggradation for steps was less than that in ponds and was steady over time. Experiment $S_H$ shows a higher overall amount of aggradation for upstream steps compared to downstream steps, which follows the same trend as the ponds.

The lack of increase in elevation for step 1 for experiment $S_C$ is confirmed looking at experimental images – no precipitation occurs on the second step of this experiment, water is routed into the left corner of the flume and flows over about a centimeter of the step. For experiment $S_C$ aggradation increases towards the downstream direction, opposite of the trend for $S_H$. This is because of a significant jump in elevation around hour 31 for ponds 4 and 5. Looking at original and corrected images and notes from the experiment run, this is when batteries were changed for the laser scanner. It is most likely that this sharp jump in elevation corresponds to a slight shift in the position of the laser line after the batteries were replaced and the position of the scanner was realigned to the transect down the center of the flume. Therefore we conclude that steps follow the same trend as ponds and overall aggradation decreases in steps toward the downstream direction.

**Downstream coarsening in a single pond**

The downstream coarsening trend was observable especially in upstream ponds (e.g., ponds 1, 2, and 3) for all four experiments. Pond 4 also shows comparably smaller, but still positive values for downstream coarsening (Table 3.3). The mechanism for downstream coarsening can be attributed to two processes. 1) Erosion can take place immediately after the vertical drop of a step at the immediate upstream of a pond; at these locations turbulence of the water can erode the existing fragile travertine precipitate from the bottom of the pond. 2) As water travels through the length of a pond and approaches the step downstream, flow accelerates until it reaches the downstream termination of a pond. Since the velocity of the water increases over the length of the pond, and travertine precipitation rate increases with increasing agitation of water, more aggradation occurs as the water travels downstream.

**Fluctuations in aggradation rate with time**

The pattern shown in the plots of aggradation rate in a single pond over time include small fluctuations and large fluctuations (Figures 8.1-8.4). The small fluctuations in aggradation rate of 0.1 millimeters are most likely resulting from instrument error of the laser scanner, discharge inconsistencies due to tubing leaks or clogging or other complications experienced during experimental runs, and/or image analysis. The thickness of the laser line is approximately one millimeter, giving an instrument error of 1 mm/30 minutes or 0.03 mm/minute, so most small fluctuations from one time period to the next fall within this error range.

For the large changes in aggradation rate, whether these are natural processes or experimental error are unknown. However, the time variability of the aggradation rates shown is systematically higher in the hot water experiments. $L_H$ and $S_H$ had a temperature decrease of 10-20 degrees Celsius from the upstream to the downstream. The temperature reduction through the

flume channel would vary in time and space due to changes in the flow path and air mixing over the path. The current research cannot thoroughly explain but suggests that there may be internal processes in travertine precipitation and $CO_2$ degassing due to changes in temperature along the path of the flume that results in pulses of precipitation followed by little or no deposition.

**Future experimental goals**

In my experiments carbonate was successfully precipitated in a laboratory setting. Carbonate was precipitated both replicating hot springs temperature and pH conditions as well as at ambient water temperature. However, step terrace morphology did not develop as the deposit grew, even with initial steps in place, constructed using wooden sticks. In fact, deposit thickness was less on steps compared to ponds, the opposite of what should occur to recreate the terrace step morphology. In future experiments, the focus will be on reproducing this travertine terrace morphology seen at Mammoth and other hot springs environments. In these experiments, temperature and step height were varied to try and induce step formation. Parameters to alter in further experiments to obtain terrace morphology include varying the base slope, constructing a longer flume channel, or introducing mud and sand particles into the system. Once terrace morphology is accomplished, time lapse photography can be used to observe if processes occurring in natural terrace systems arise in artificial terraces, such as upstream drowning and pond merging.

# Chapter 6: Conclusions

While temperature and step height can influence precipitation rate, upstream versus downstream position and vicinity to a step edge equally play a factor in how much precipitation will occur. Water hydraulics can drastically change based on location within a terrace. Directly after a step, with the change in height, turbulence, and mixing of the water cause erosion of the deposited travertine substrate. As the water travels downstream within a single pond, velocity increases until the next step "waterfall" and enhances precipitation. These hydrological properties can dominate if step heights are large or if the inlet source of water is nearby. If locations are far from the source, with lower velocities and calmer flow, or if step heights are small, temperature can have a more dominate role on precipitation. Higher temperatures induce more precipitation, so for the hot water experiments, $S_H$ and $L_H$, more precipitation would occur compared to the ambient temperature experiments. The conclusions are summarized as follows:

1. Carbonate thickness and overall precipitation rate in ponds are greatest upstream and decrease downstream.
2. Aggradation rates on the top of steps are overall lower compared to adjacent ponds.
3. Temperature is a more dominant control in downstream ponds compared to upstream ponds, where hydraulic processes play a greater role.
4. Small steps in $S_H$ induce a higher precipitation rate comparable to ones in $L_H$, due to loss of heat in the large stepped experiments towards the downstream. Larger steps may have just as high of a precipitation rate as small steps in ponds right by the inlet source of hot water.

5. There is no trend in aggradation rate over time. However, the magnitude of fluctuations is higher in the hot water experiments due to a wider range of temperature decrease over the flow through the flume.

Tables

Table 1:Experimental matrix. Values for step heights and temperatures show range from downstream to upstream end of flume.

| Experiment | Step heights (cm) | Water temperature (C) |
|---|---|---|
| 5, $S_H$ | 0.18-1.6 | 55-60 |
| 6, $S_C$ | 0.18-1.6 | 20-23 |
| 7, $L_C$ | 0.32-3.2 | 20-23 |
| 8, $L_H$ | 0.32-3.2 | 55-60 |

Table 2.1: Ratio of thickness of ambient temperature water deposit to hot water deposit using manual measurements. An average value below 100% indicates a thicker deposit for the hot water experiment.

$\% = T_C / T_H$

*$T_C$ = thickness of ambient temperature water deposit ($L_C$)*

*$T_H$ - thickness of hot water deposit ($L_H$)*

| **Pond Number** | ***$T_C / T_H$ (%)*** |
|---|---|
| 1 | 92 |
| 2 | 109 |
| 3 | 76 |
| 4 | 66 |
| **Average** | **86** |

Table 2.2: Ratio of thickness of small stepped experiment to large stepped experiment using manual measurements. An average value above 100% indicates a thicker deposit for the small stepped experiment.

$\% = T_S / T_L$

$T_S$ = *thickness of small steps deposit* ($S_H$)

$T_L$ - *thickness of large steps deposit* ($L_H$)

| **Pond Number** | $T_S / T_L$ **(%)** |
|---|---|
| 1 | 85 |
| 2 | 131 |
| 3 | 106 |
| 4 | 167 |
| **Average** | **122** |

Tables 3.1: Elevation differences for pond 2, calculated using last and first topographic scans captured. Positive values represent downstream coarsening in a pond, negative values represent downstream thinning of deposit. High dam height in pond 2 of experiments 7 and 8 was unable to be processed into elevation data.

| **Pond 2** | **Elevation difference (mm)** | **Slope gradient (%)** |
|---|---|---|
| Expt 5, $S_H$ | 6.91 | 4.60 |
| Expt 6, $S_C$ | 13.82 | 9.21 |
| Expt 7, $L_C$ | N/A | N/A |
| Expt 8, $L_H$ | N/A | N/A |
| **Average** | **10.37** | **6.91** |

Tables 3.2: Elevation differences for pond 3, calculated using last and first topographic scans captured.

| **Pond 3** | **Elevation difference (mm)** | **Slope gradient (%)** |
|---|---|---|
| Expt 5, $S_H$ | 4.95 | 3.30 |
| Expt 6, $S_C$ | 12.14 | 8.10 |
| Expt 7, $L_C$ | 3.15 | 2.10 |
| Expt 8, $L_H$ | 3.00 | 2.00 |
| **Average** | **5.81** | **3.88** |

Tables 3.3: Elevation differences for pond 4, calculated using last and first topographic scans captured.

| **Pond 4** | **Elevation difference (mm)** | **Slope gradient (%)** |
|---|---|---|
| Expt 5, $S_H$ | 0.045 | .03 |
| Expt 6, $S_C$ | 0.02 | .01 |
| Expt 7, $L_C$ | 2.00 | 1.33 |
| Expt 8, $L_H$ | 0.25 | 0.17 |
| **Average** | **0.58** | **0.39** |

Tables 3.4: Elevation differences for pond 5, calculated using last and first topographic scans captured.

| **Pond 5** | **Elevation difference (mm)** | **Slope gradient (%)** |
|---|---|---|
| Expt 5, $S_H$ | -3.75 | -2.50 |
| Expt 6, $S_C$ | -0.25 | -0.17 |
| Expt 7, $L_C$ | 0.75 | 0.50 |
| Expt 8, $L_H$ | -1.25 | -0.83 |
| **Average** | **-1.13** | **-0.75** |

Tables 4.1: Pond time and spatially averaged aggradation rates in millimeters per minute, from the elevation data.

| **Experiment** | **Pond 1** | **Pond 2** | **Pond 3** | **Pond 4** | **Pond 5** |
|---|---|---|---|---|---|
| **5,** $S_H$ | N/A | 7.71E-03 | 4.67E-03 | 1.01E-03 | 2.36E-03 |
| **6,** $S_C$ | N/A | 2.47E-03 | 1.13E-03 | 8.17E-04 | 8.89E-04 |
| **7,** $L_C$ | N/A | N/A | 2.81E-03 | 1.12E-03 | 6.62E-04 |
| **8,** $L_H$ | N/A | N/A | 4.23E-03 | 5.38E-03 | 3.52E-03 |

Tables 4.2: Step time and spatially averaged aggradation rates in millimeters per minute, from the elevation data. The negative value for experiment 7, step 4 is because no travertine precipitation exists on the corresponding image.

| **Experiment** | **Step 1** | **Step 2** | **Step 3** | **Step 4** |
|---|---|---|---|---|
| **5,** $S_H$ | 2.09E-03 | 2.71E-03 | 1.57E-03 | 1.52E-03 |
| **6,** $S_C$ | 5.68E-04 | 1.85E-03 | 1.07E-04 | 5.22E-04 |
| **7,** $L_C$ | 2.55E-03 | 1.70E-03 | 6.95E-04 | -3.84325E-05* |
| **8,** $L_H$ | 2.51E-03 | 4.95E-03 | 5.53E-03 | 4.17E-03 |

Figures

Figure 1.1 Travertine terrace morphology at Mammoth Hot Springs, Yellowstone National Park (Goldenfeld 2006). This morphology was recreated in the experimental set-up.

Figures 1.2: Lab facility and experimental set-up for carbonate experiments, conducted at University of Texas at Austin.

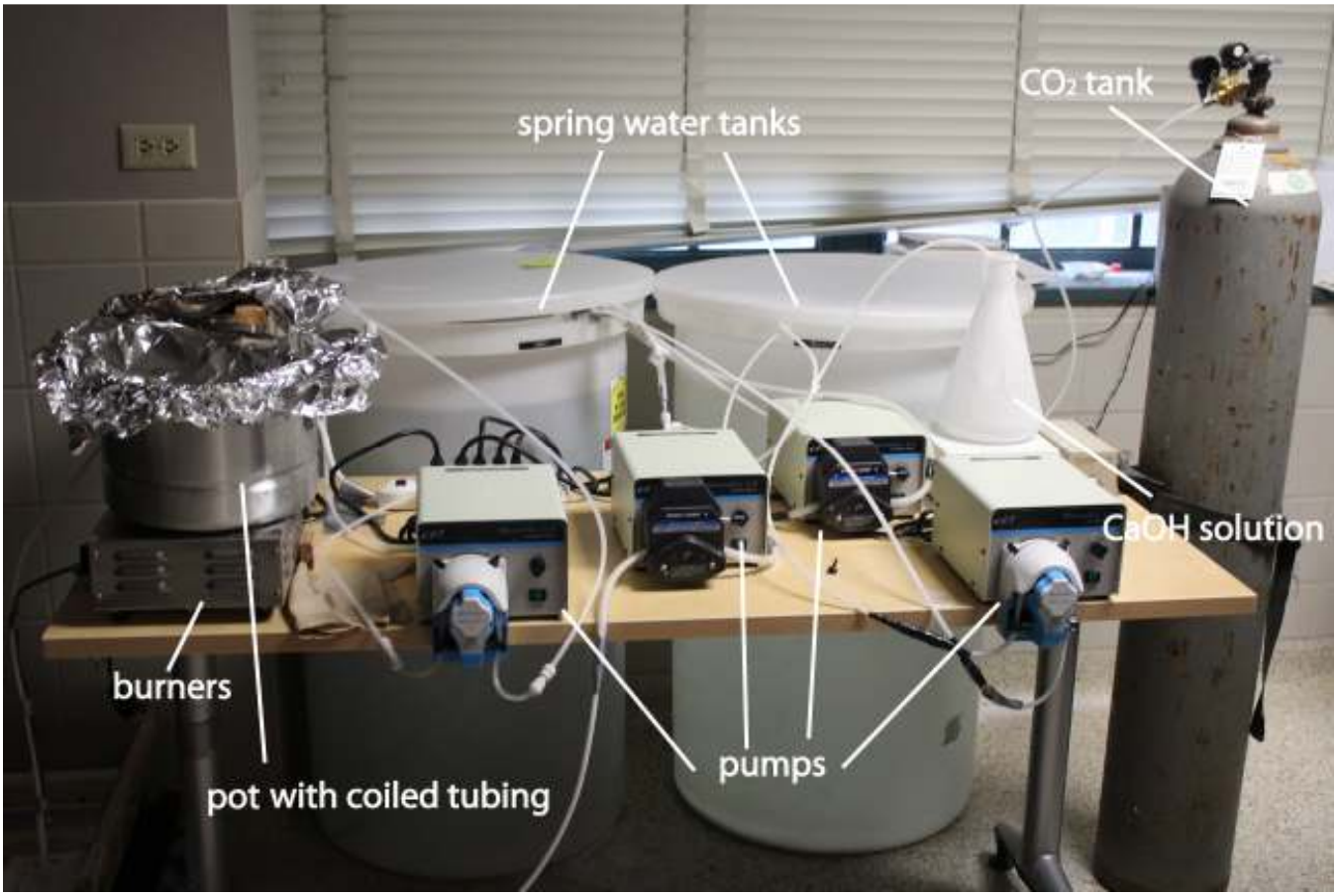

Figures 1.3: Lab facility and experimental set-up for carbonate experiments, conducted at University of Texas at Austin.

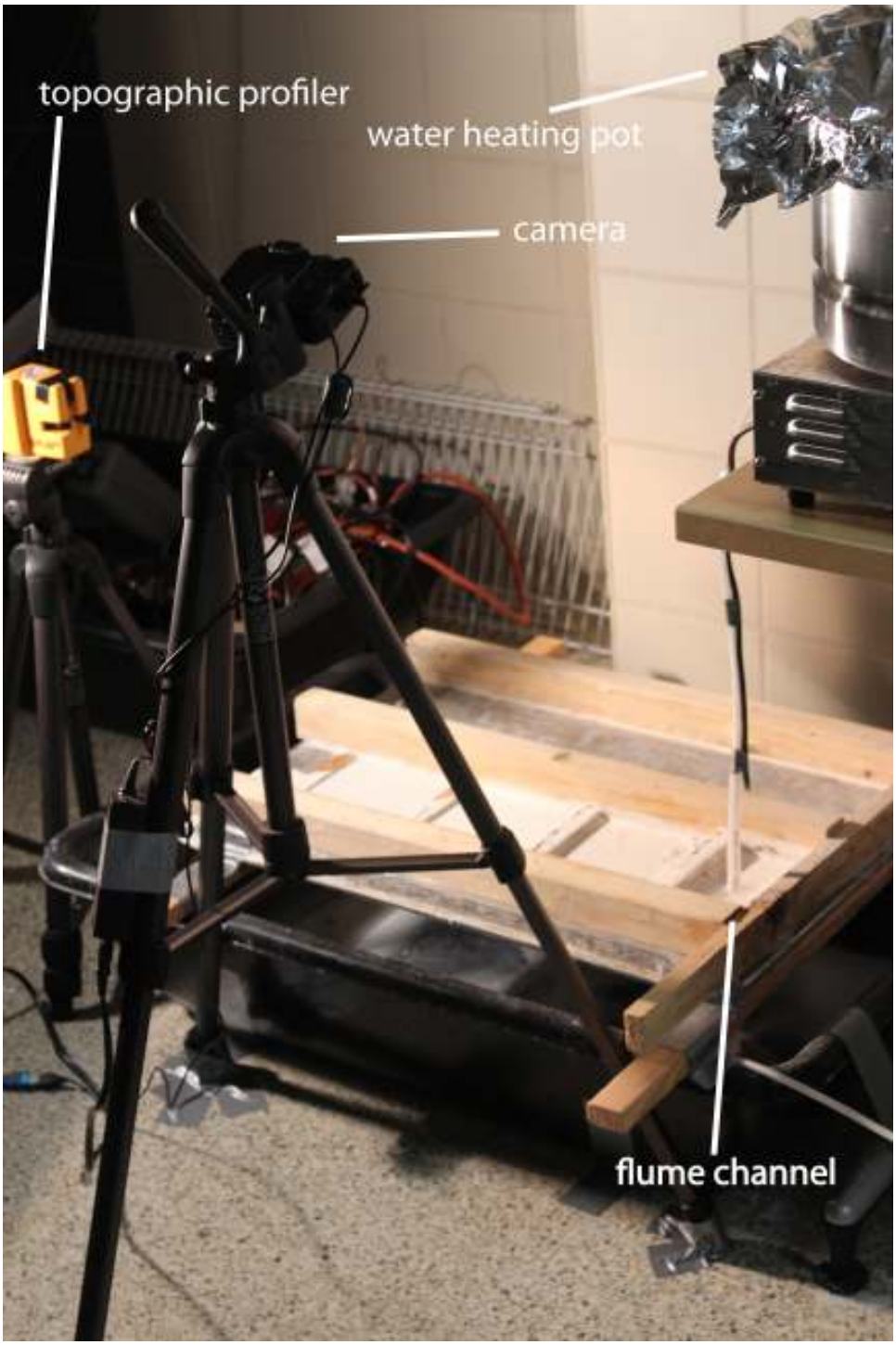

Figure 1.4: Flume design and dimensions. The flume was composed of five ponds (P) and four steps (S).

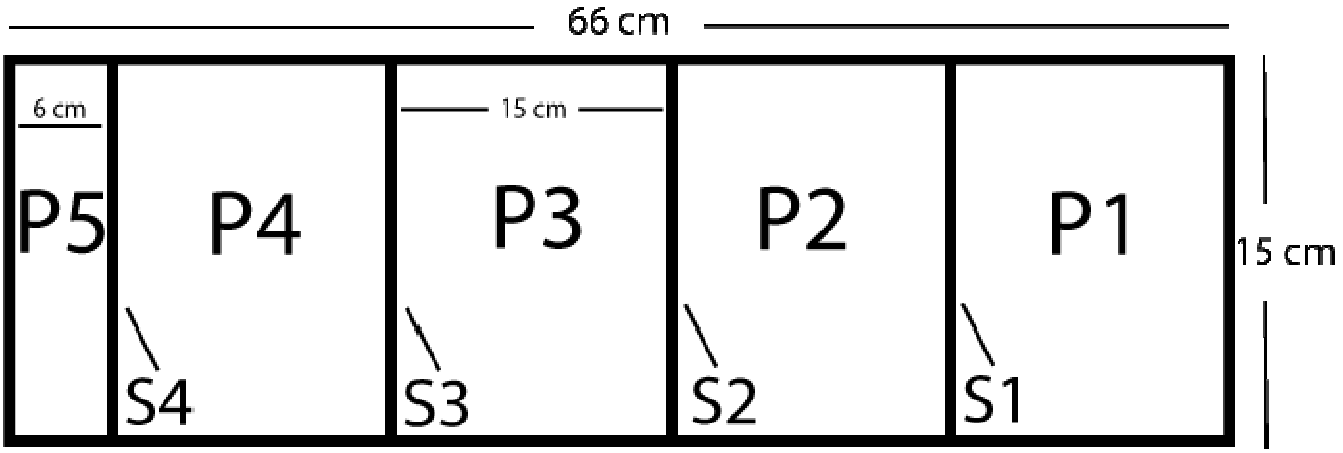

Figures 2.1: $S_H$ temperature at the upstream and downstream ends measured every thirty minutes over the experimental run.

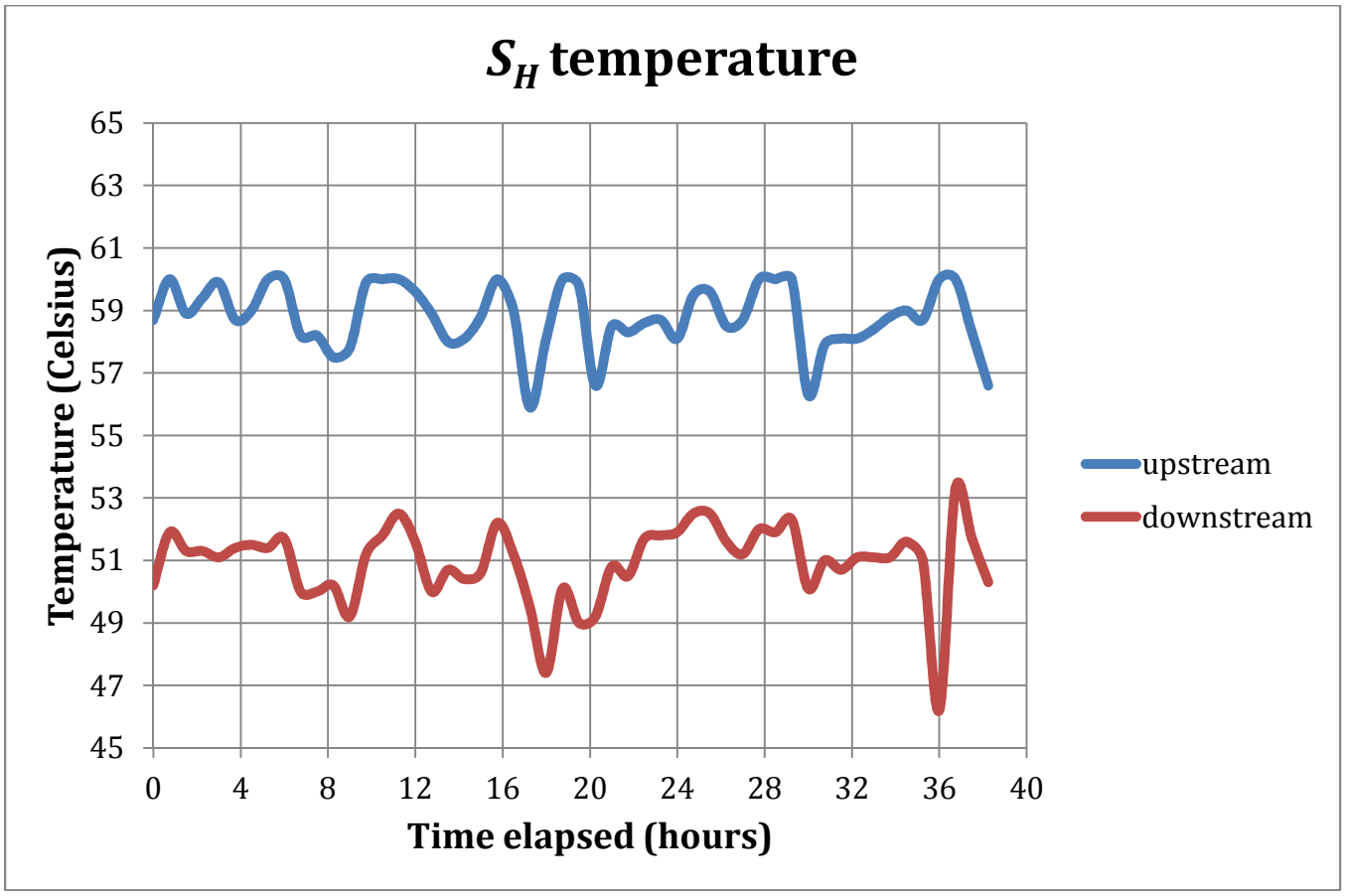

Figures 2.2: $S_H$ pH at the upstream and downstream ends measured every thirty minutes over the experimental run.

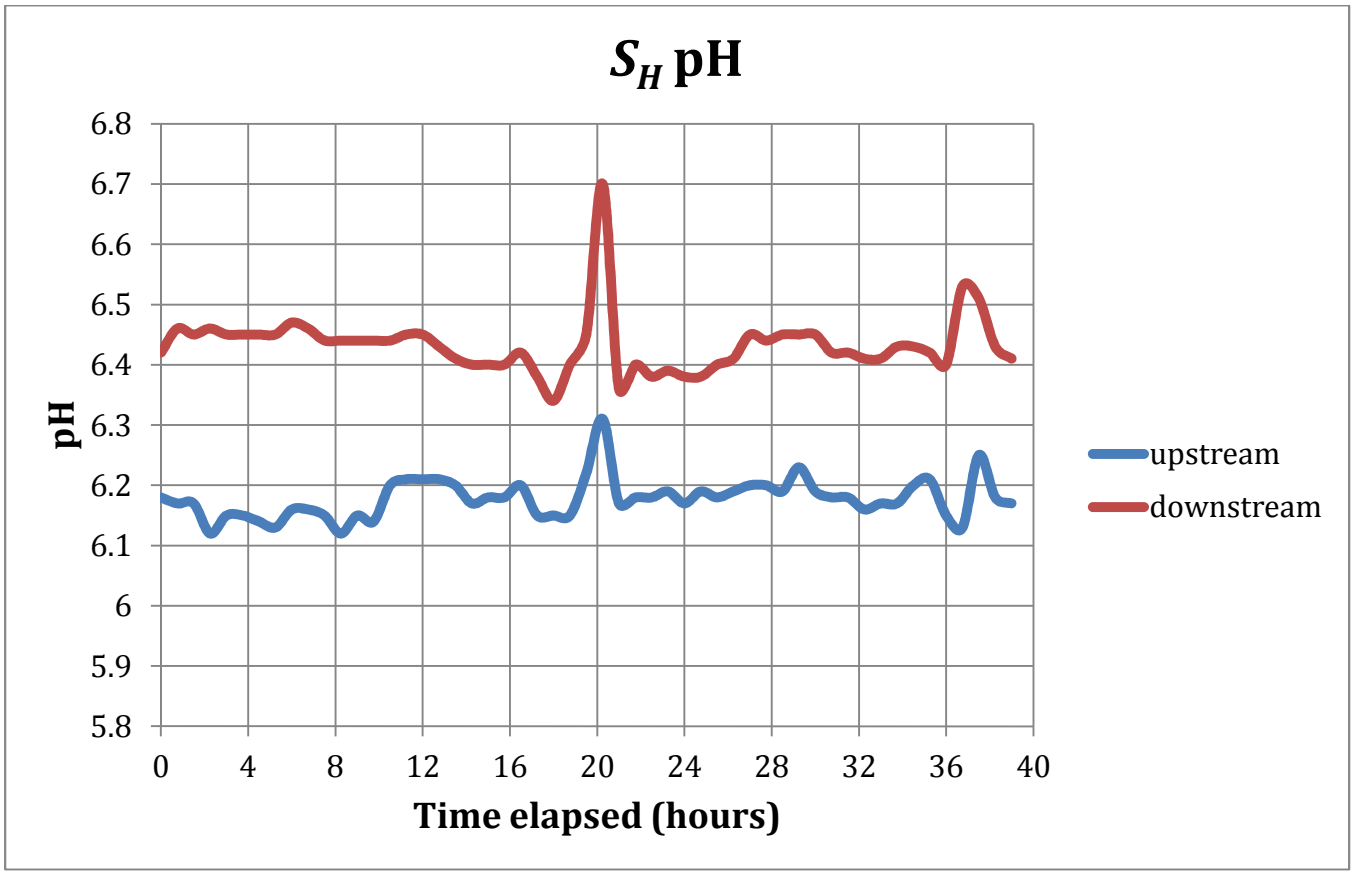

Figures 2.3: $S_H$ conductivity at the upstream and downstream ends measured every thirty minutes over the experimental run. Conductivity started being measured at hour 24.

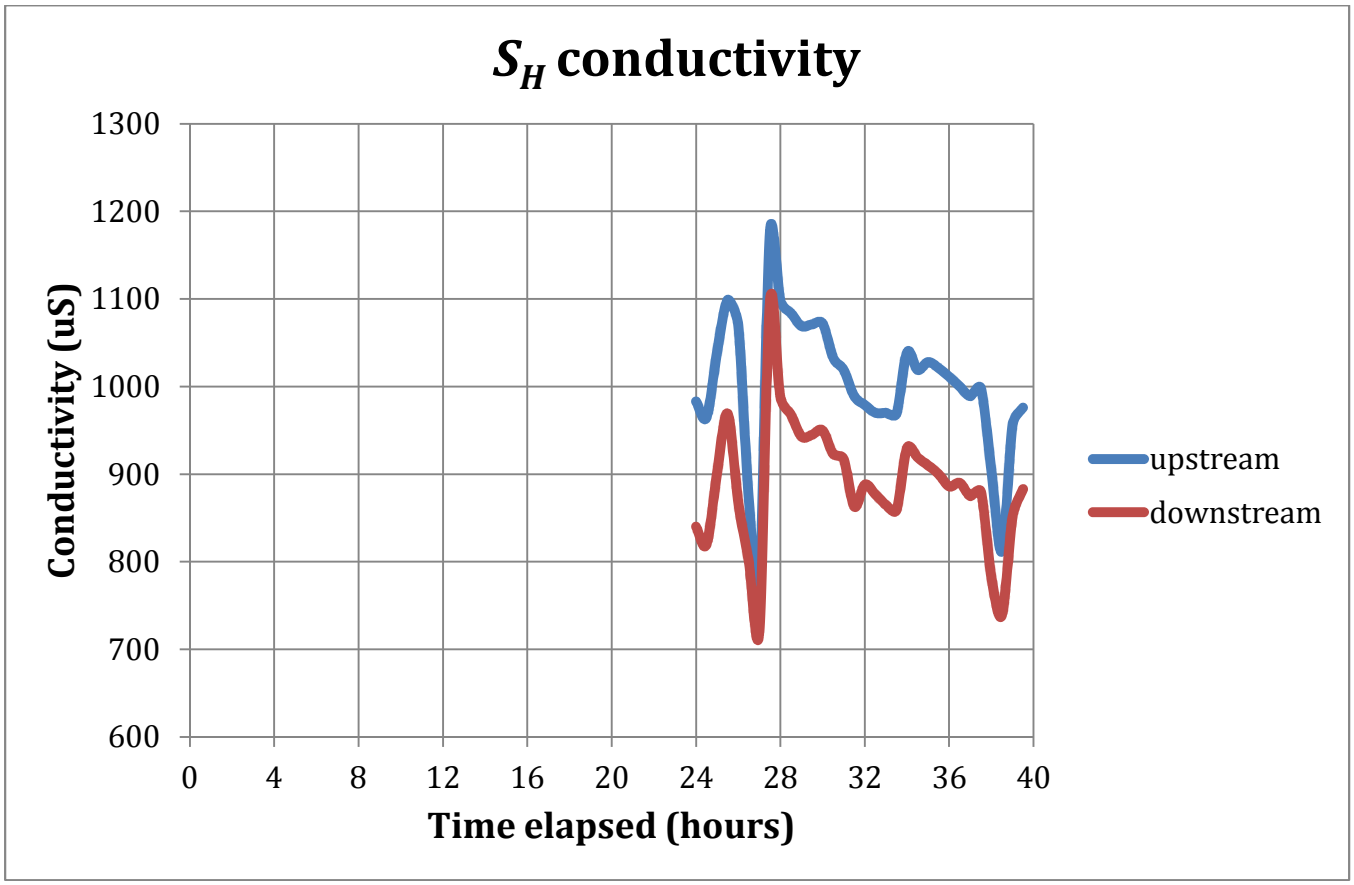

Figures 2.4: $S_C$ temperature at the upstream and downstream ends measured every thirty minutes over the experimental run

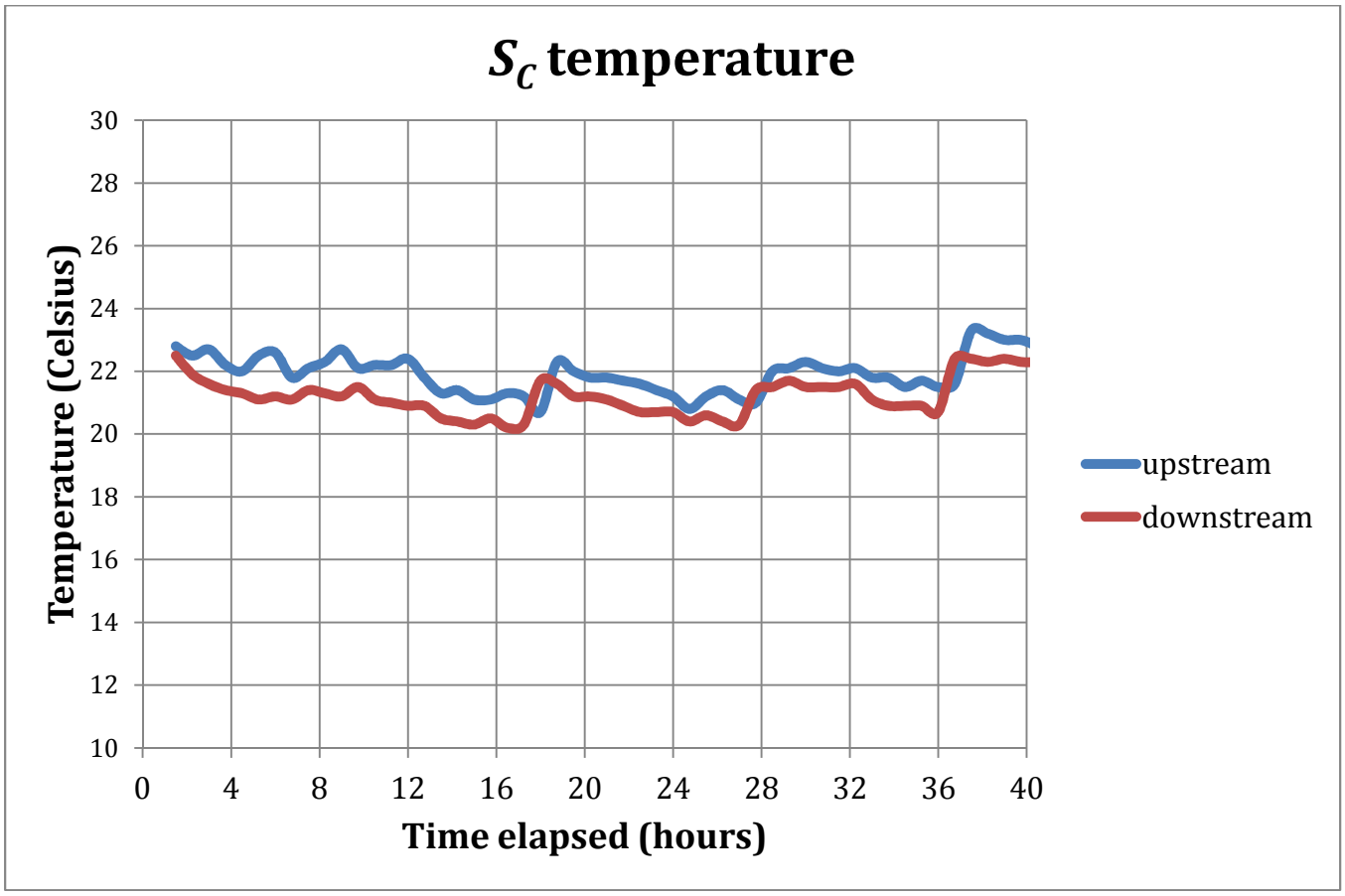

Figures 2.5: $S_C$ pH at the upstream and downstream ends measured every thirty minutes over the experimental run

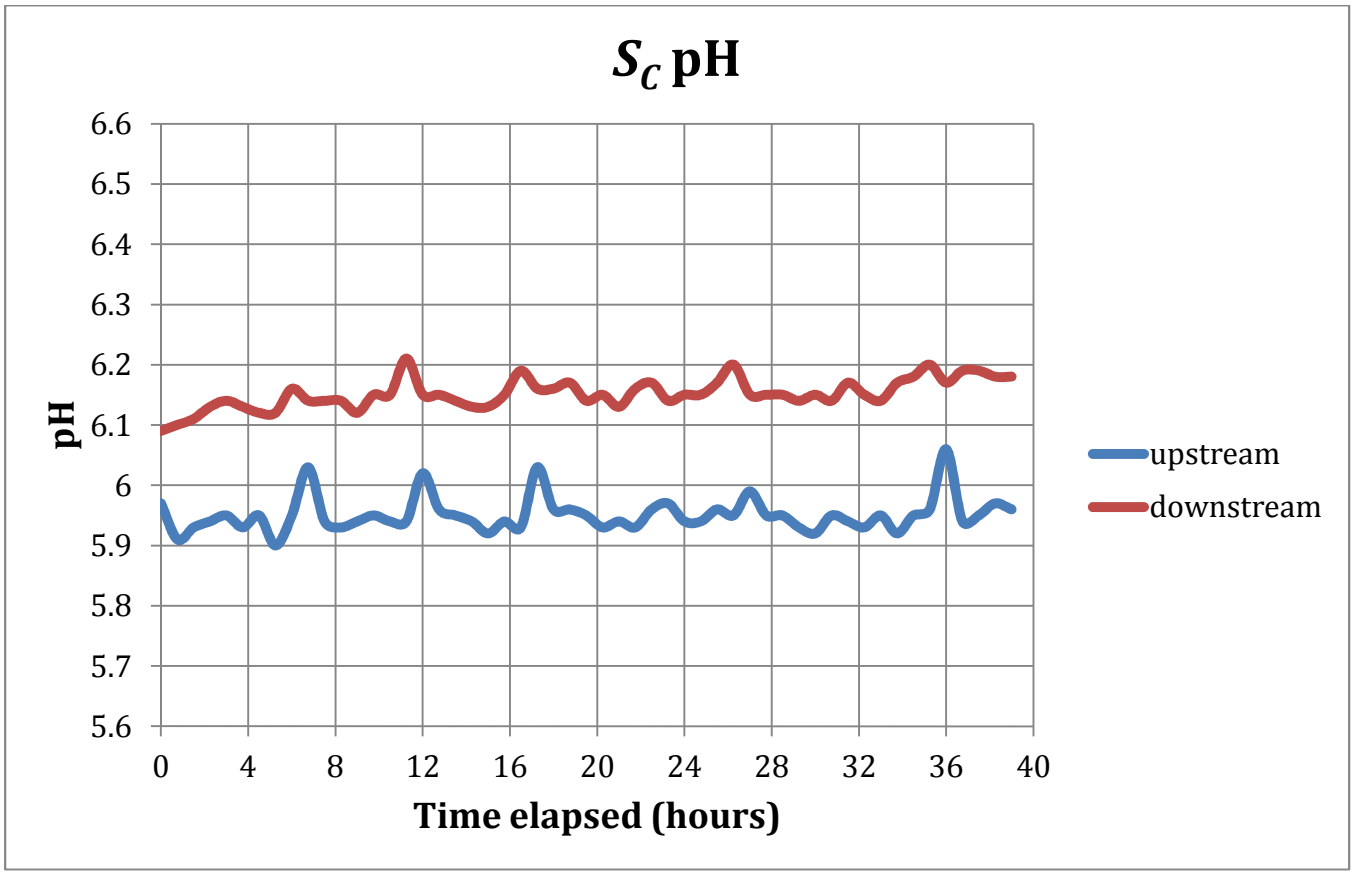

Figures 2.6: $S_C$ conductivity at the upstream and downstream ends measured every thirty minutes over the experimental run

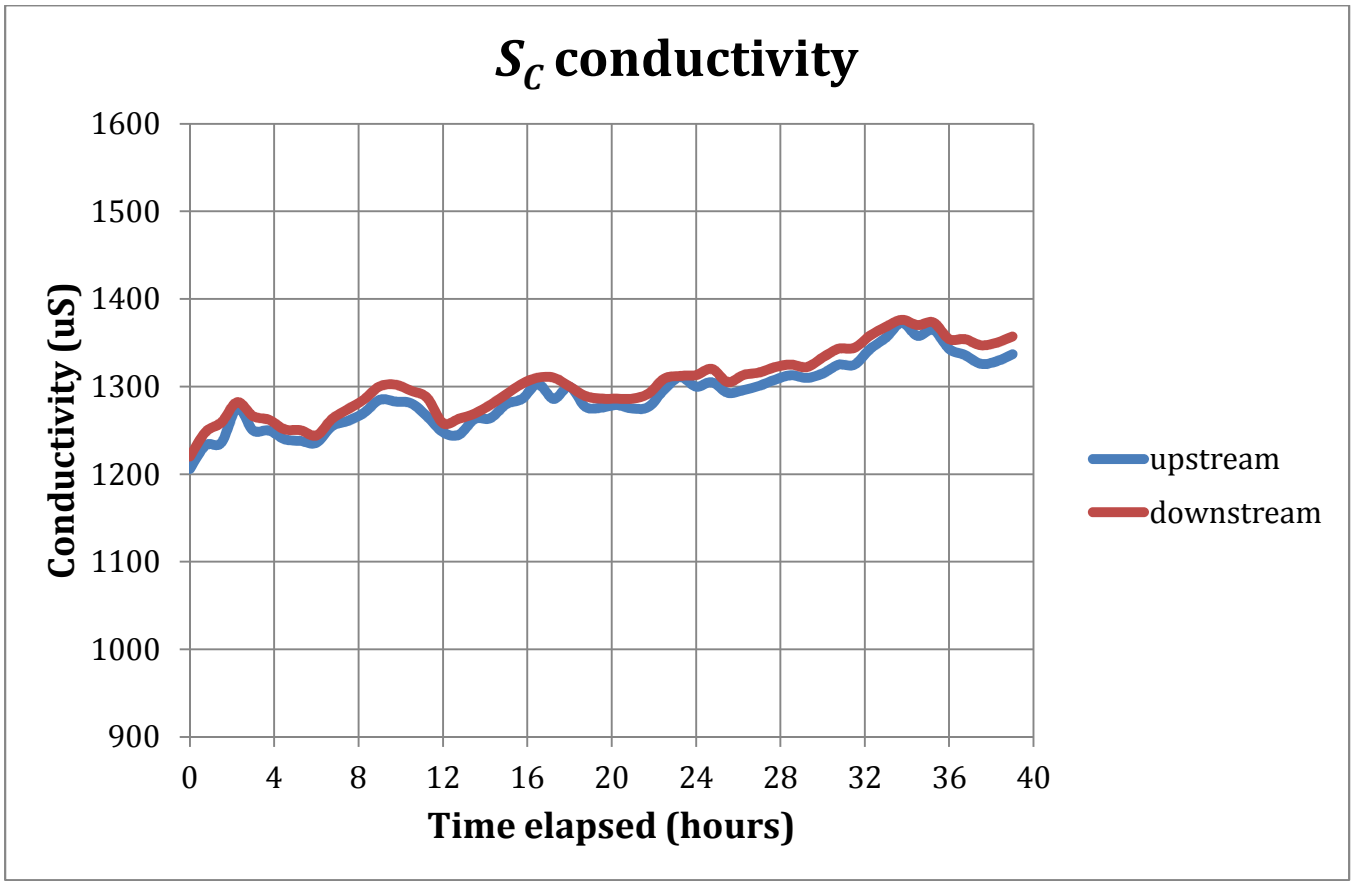

Figures 2.7: $L_C$ temperature at the upstream and downstream ends measured every thirty minutes over the experimental run

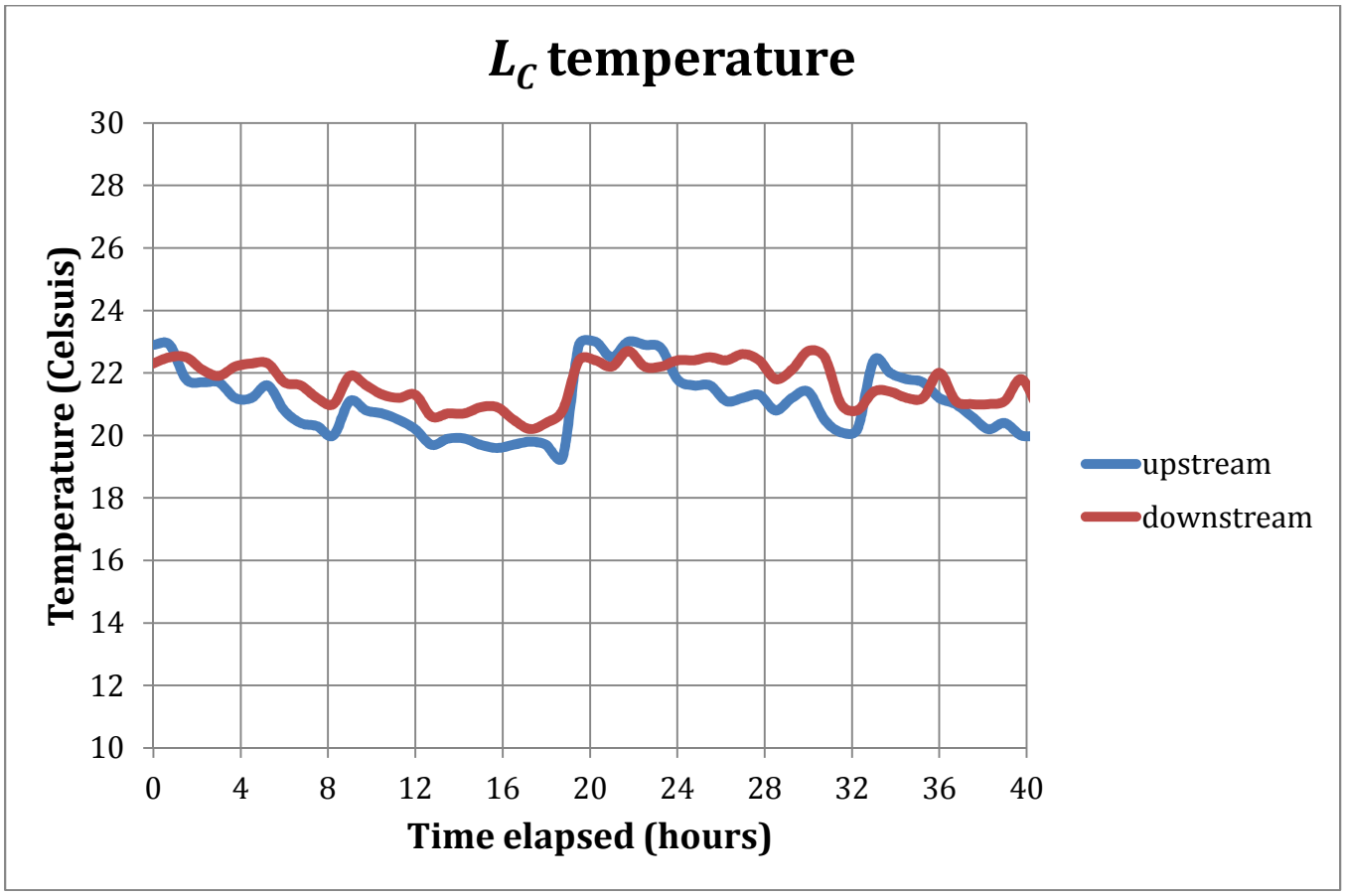

Figures 2.8: $L_C$ pH at the upstream and downstream ends measured every thirty minutes over the experimental run

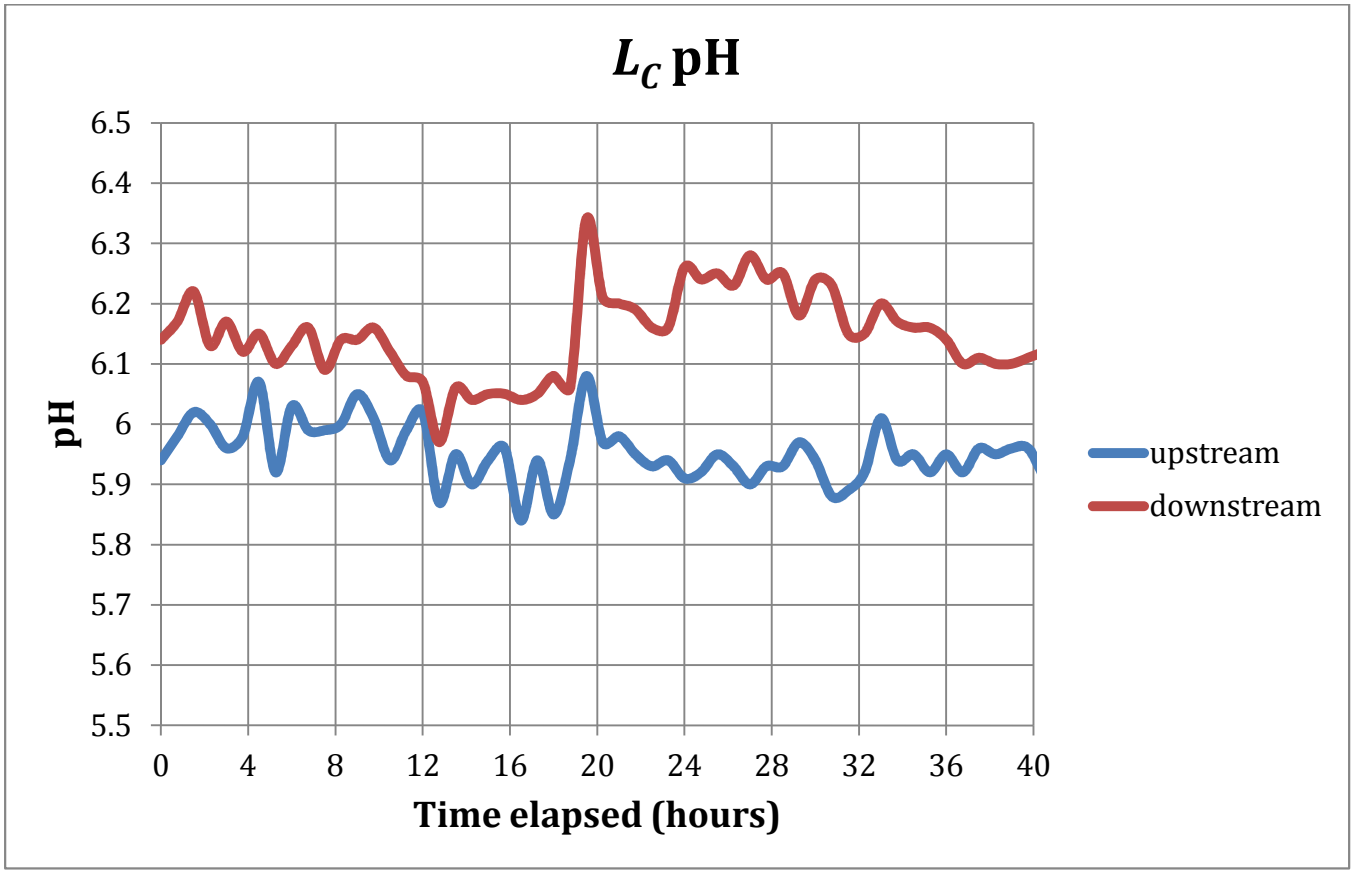

Figures 2.9: $L_C$ conductivity at the upstream and downstream ends measured every thirty minutes over the experimental run

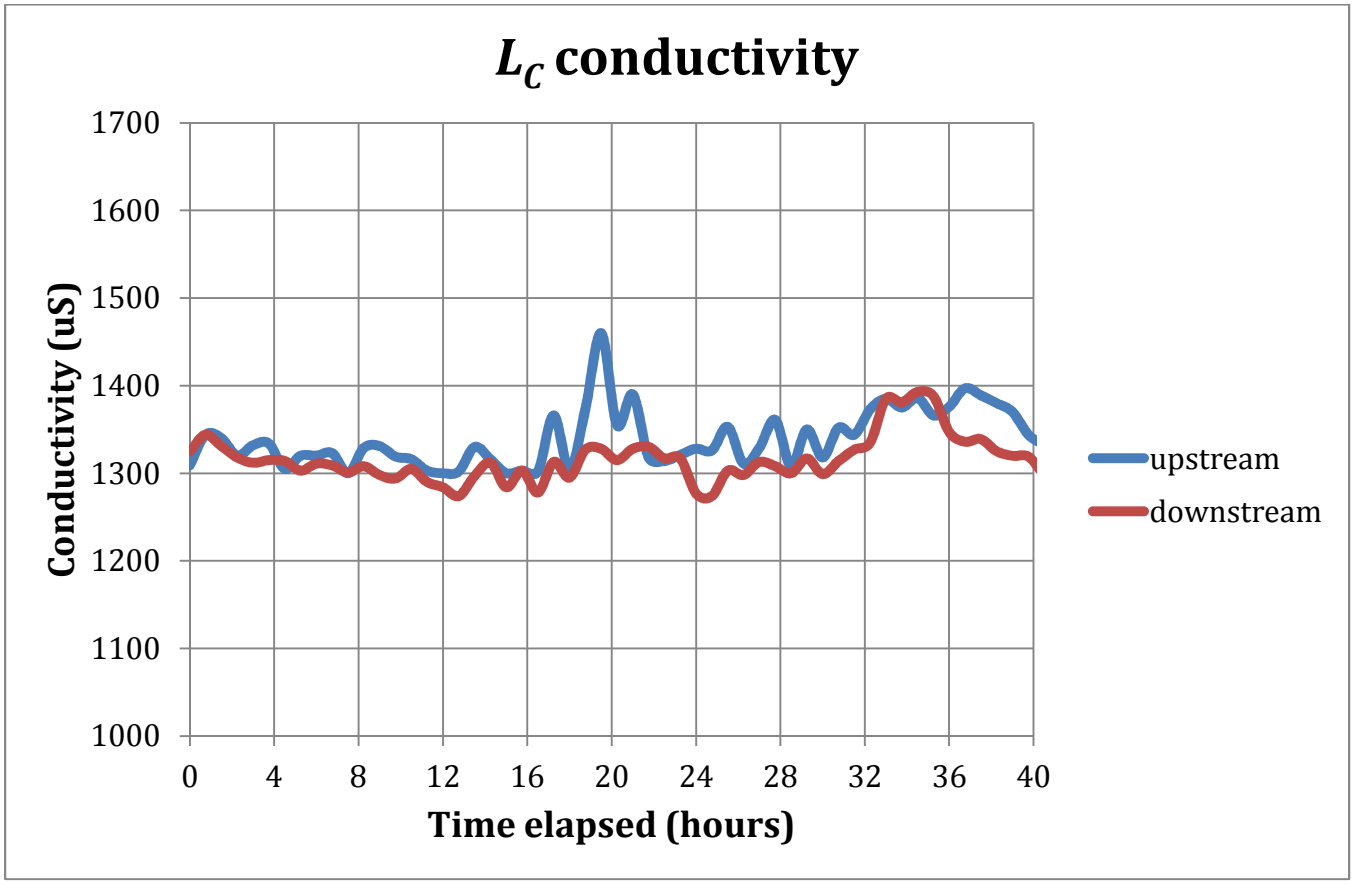

Figures 2.10: $L_H$ temperature at the upstream and downstream ends measured every thirty minutes over the experimental run

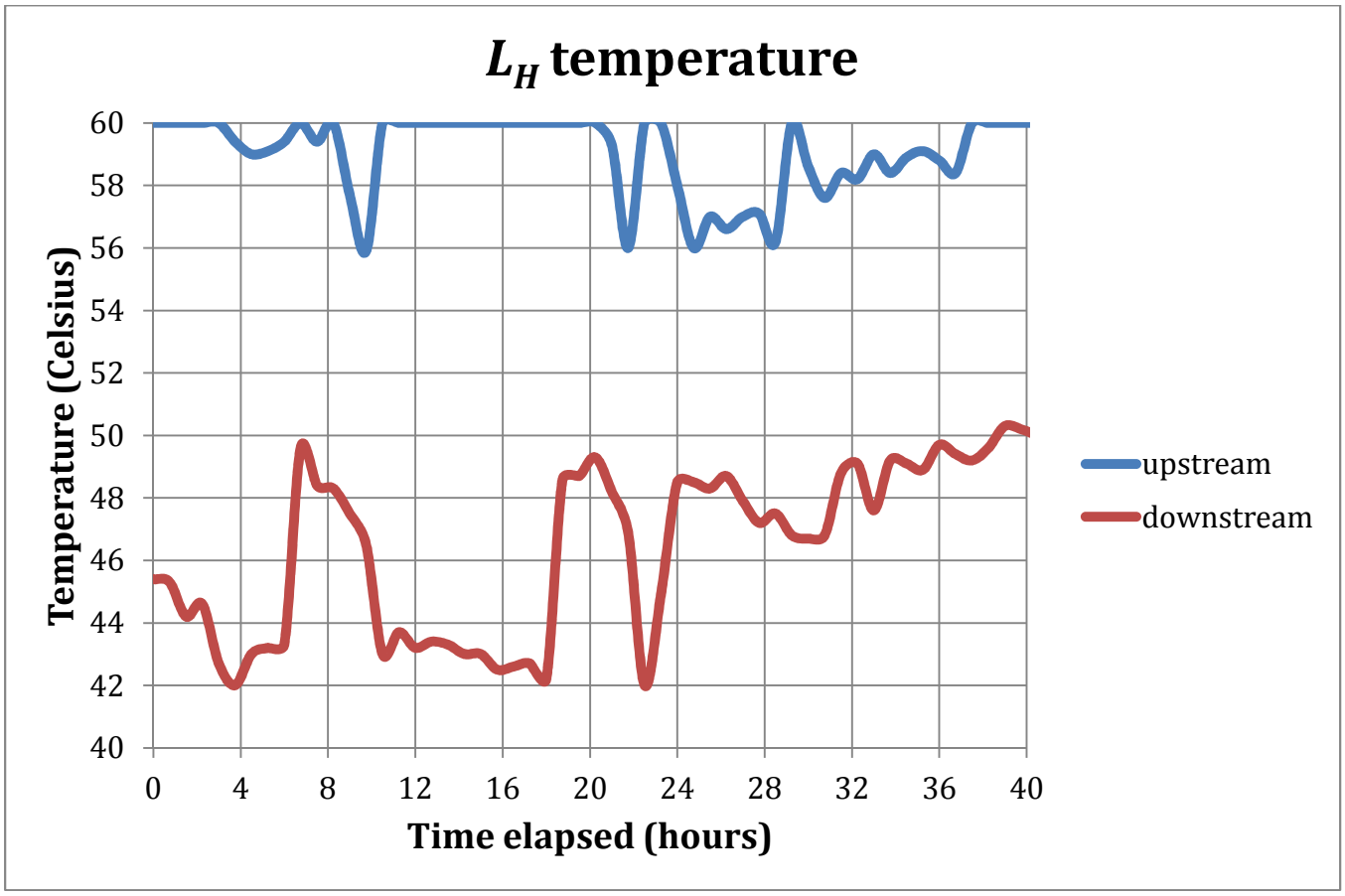

Figures 2.11: $L_H$ pH at the upstream and downstream ends measured every thirty minutes over the experimental run

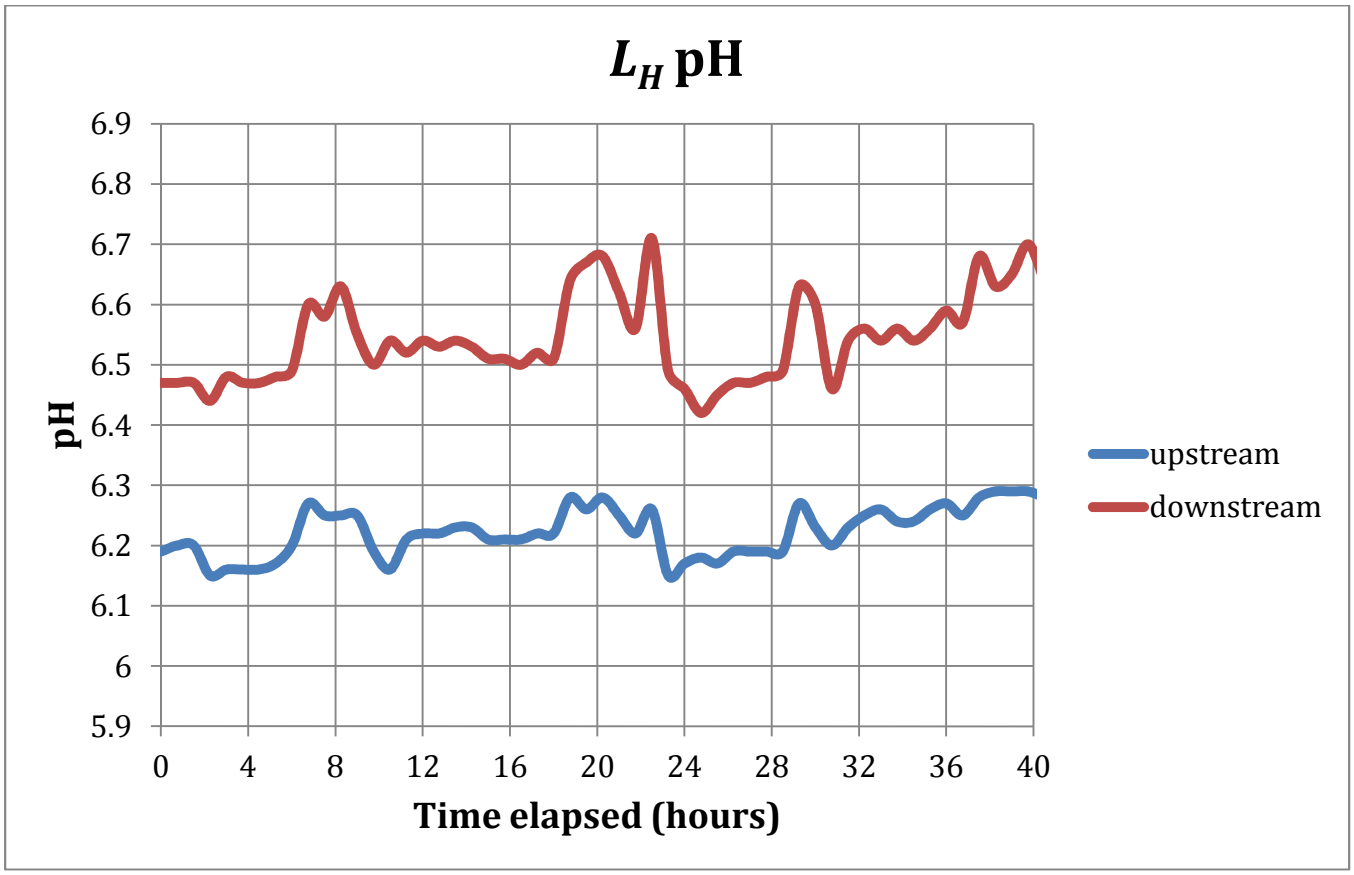

Figures 2.12: $L_H$ conductivity at the upstream and downstream ends measured every thirty minutes over the experimental run

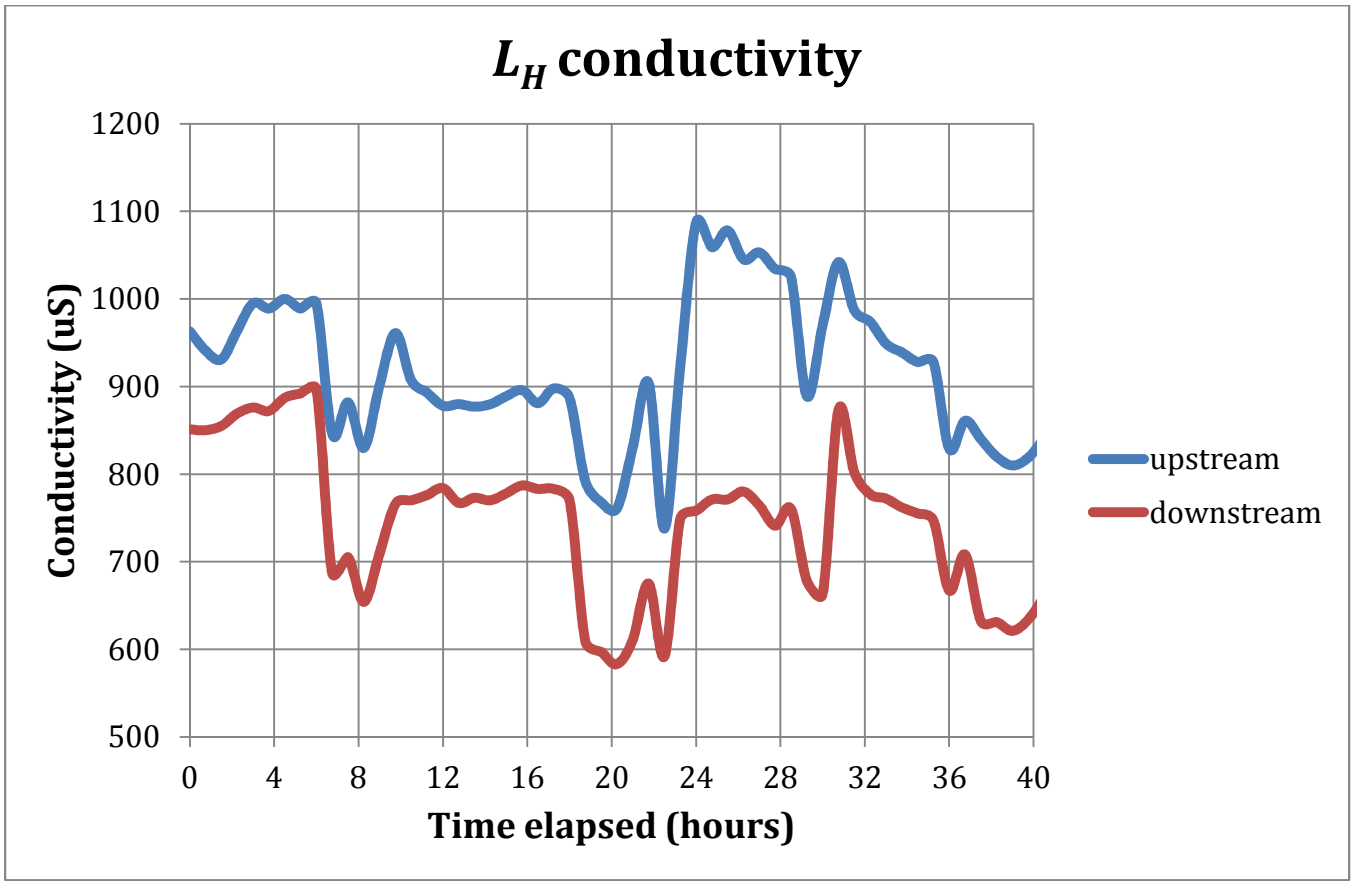

Figure 3.1: Original captured time-lapse image from experiment $S_C$ after 28.5 hours of run time.

Figure 3.2: Dark image from experiment $S_C$ after 29 hours of run time. Image is taken without artificial light to better capture laser line. Laser is more faint for tall upstream ponds.

Figure 3.3: Same dark image after Photoshop corrections and processing. Taller ponds not captured by laser line.

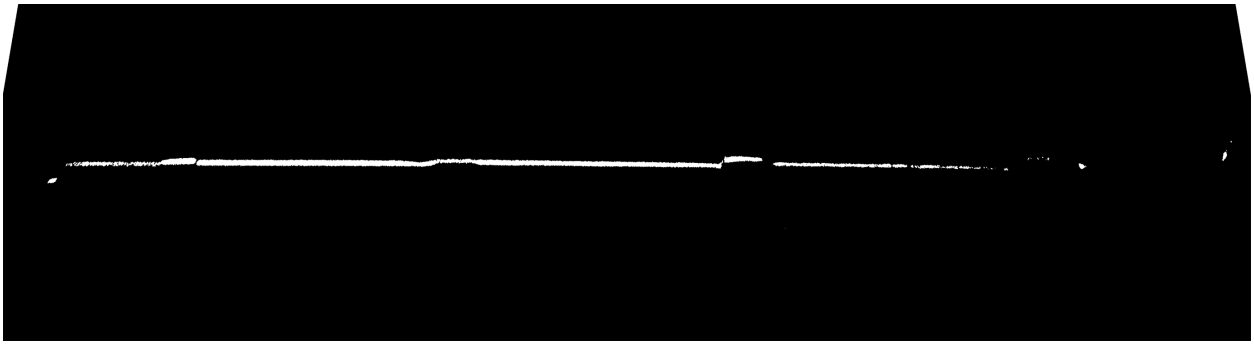

Figures 4.1: Manual thickness measurements of ponds for experiment $S_H$ with second order polynomial best-fit line. Three measurements were made in each pond. Thickness decreased in the downstream direction.

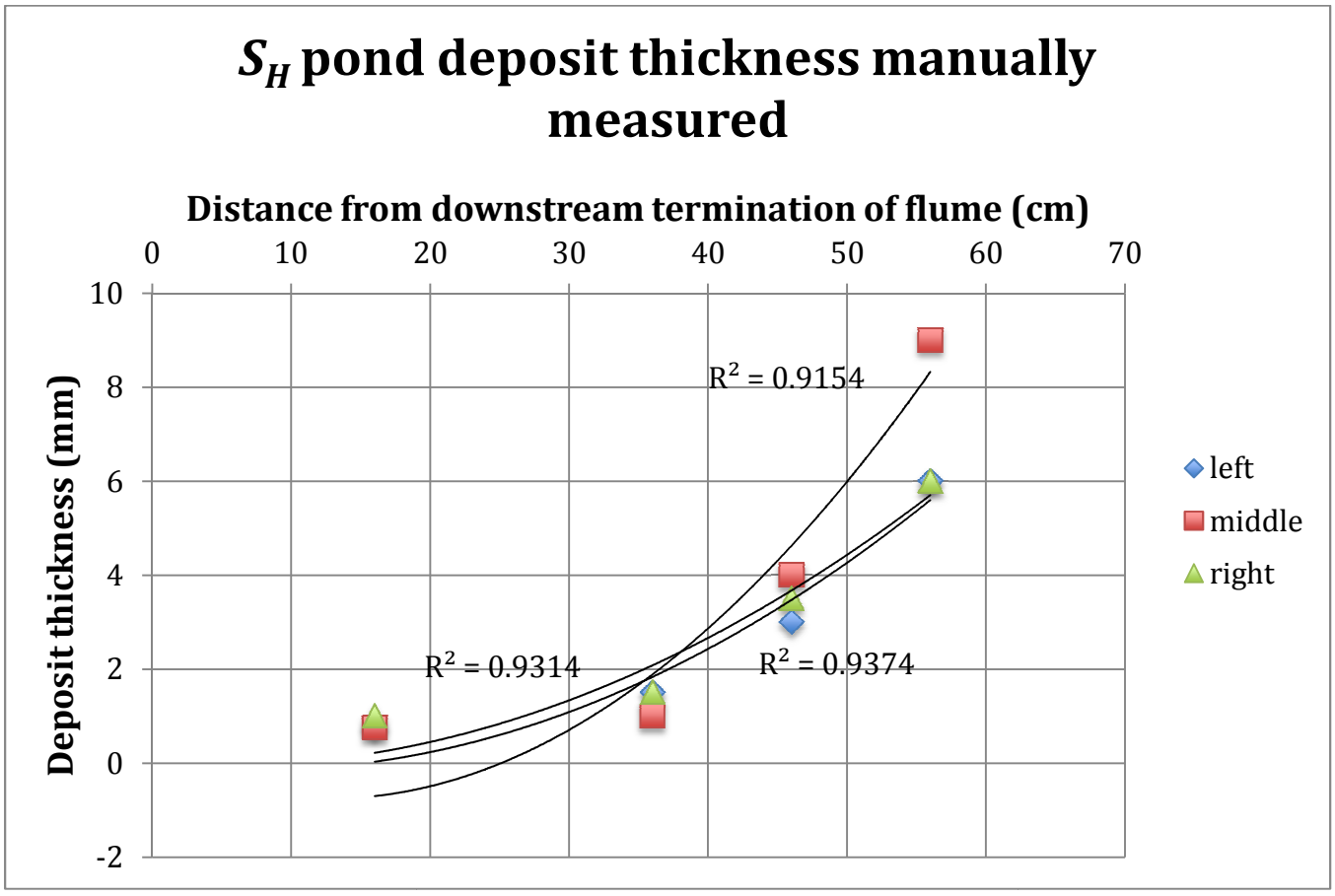

Figures 4.2: Manual thickness measurements of ponds for experiment $L_C$ with second order polynomial best-fit line. Six measurements were made in each pond. Thickness decreased in the downstream direction.

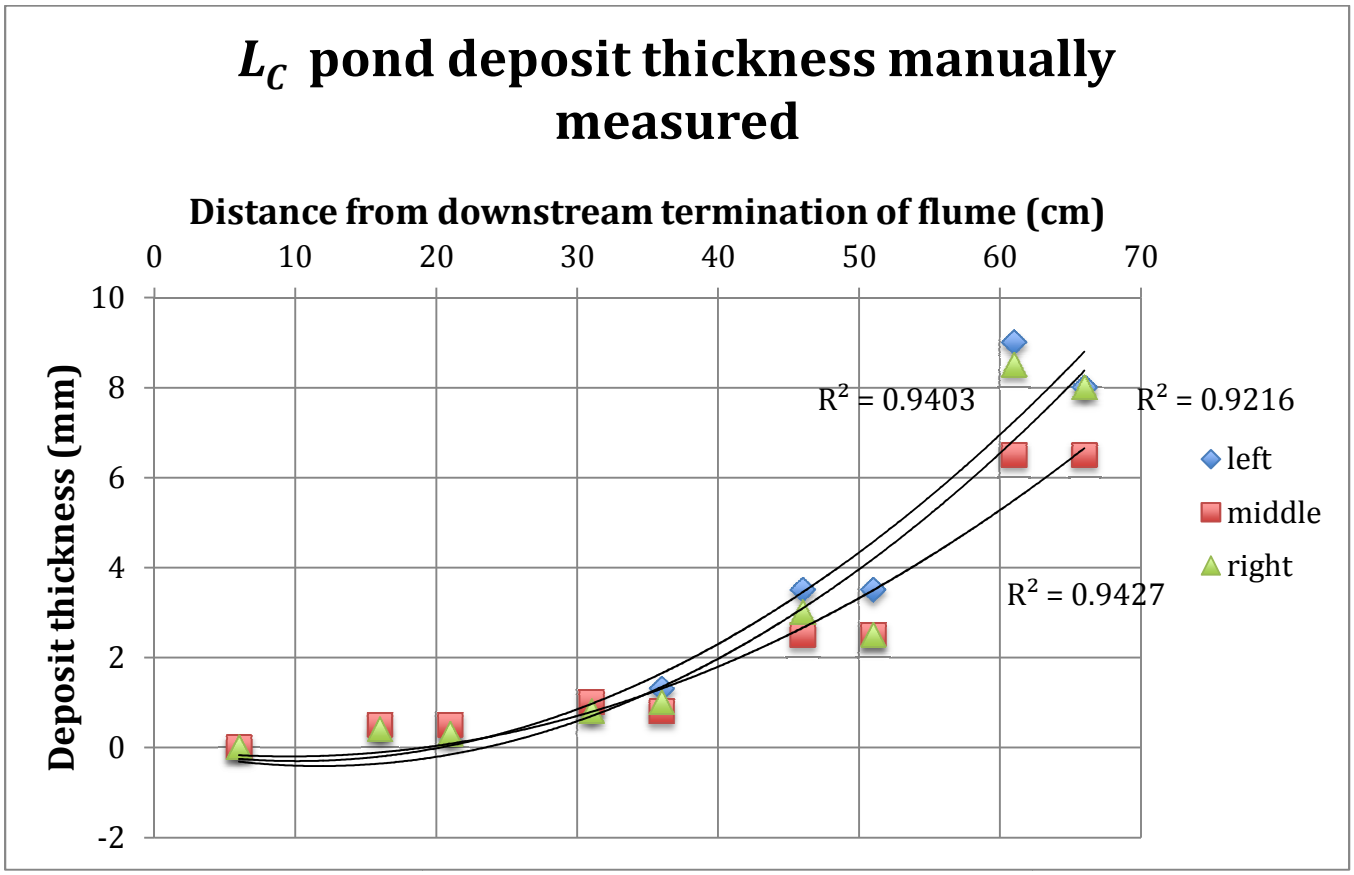

Figures 4.3: Manual thickness measurements of ponds for experiment $L_H$ with second order polynomial best-fit line. Six measurements were made in each pond. Thickness decreased in the downstream direction.

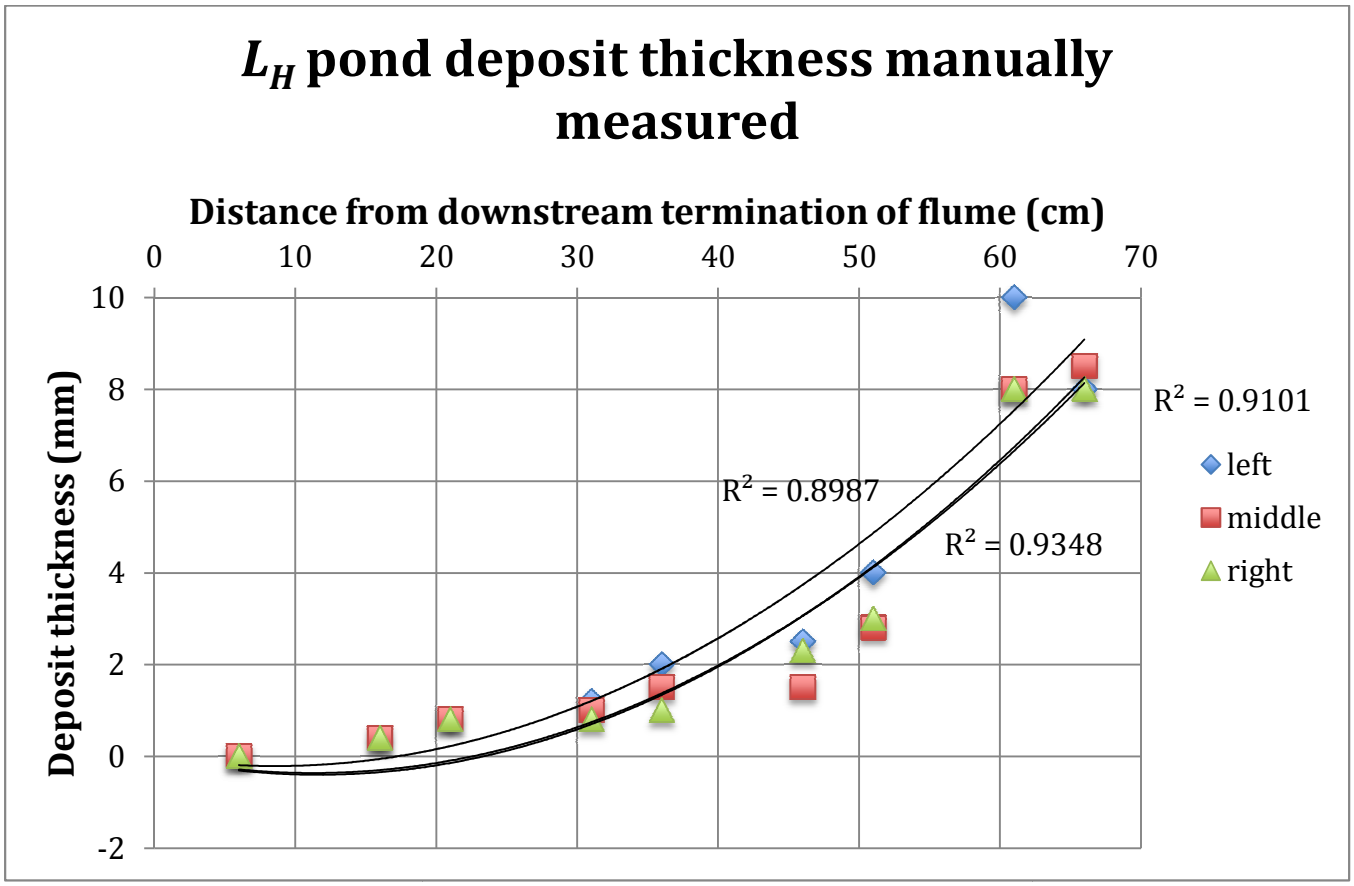

Figures 4.4: Manually measured deposit thickness on the wooden steps for experiment $S_H$. Three measurements were made in each step. Thicknesses were less than 0.5 millimeters and followed no trend.

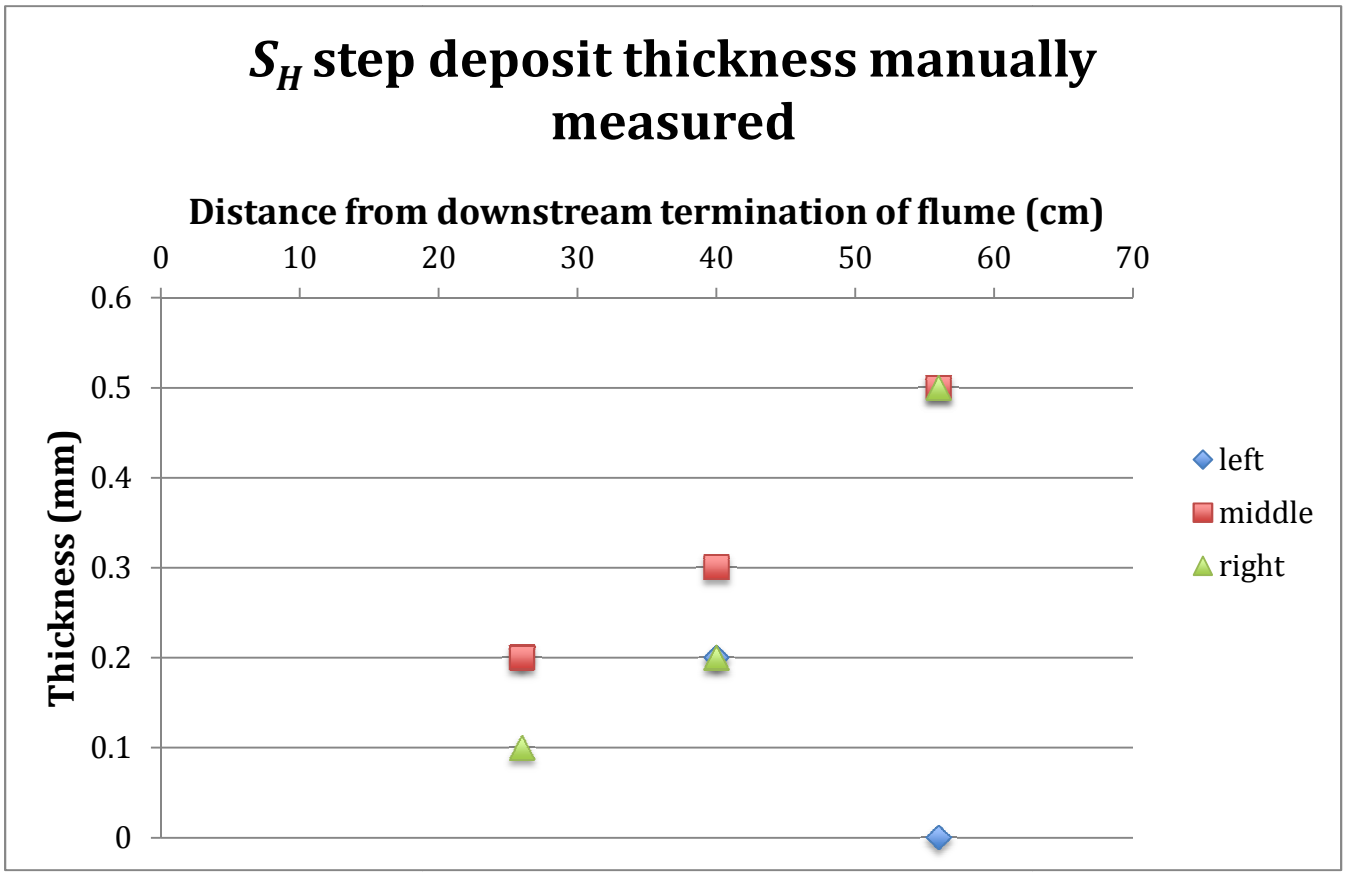

Figures 4.5: Manually measured deposit thickness on the wooden steps for experiment $L_C$.

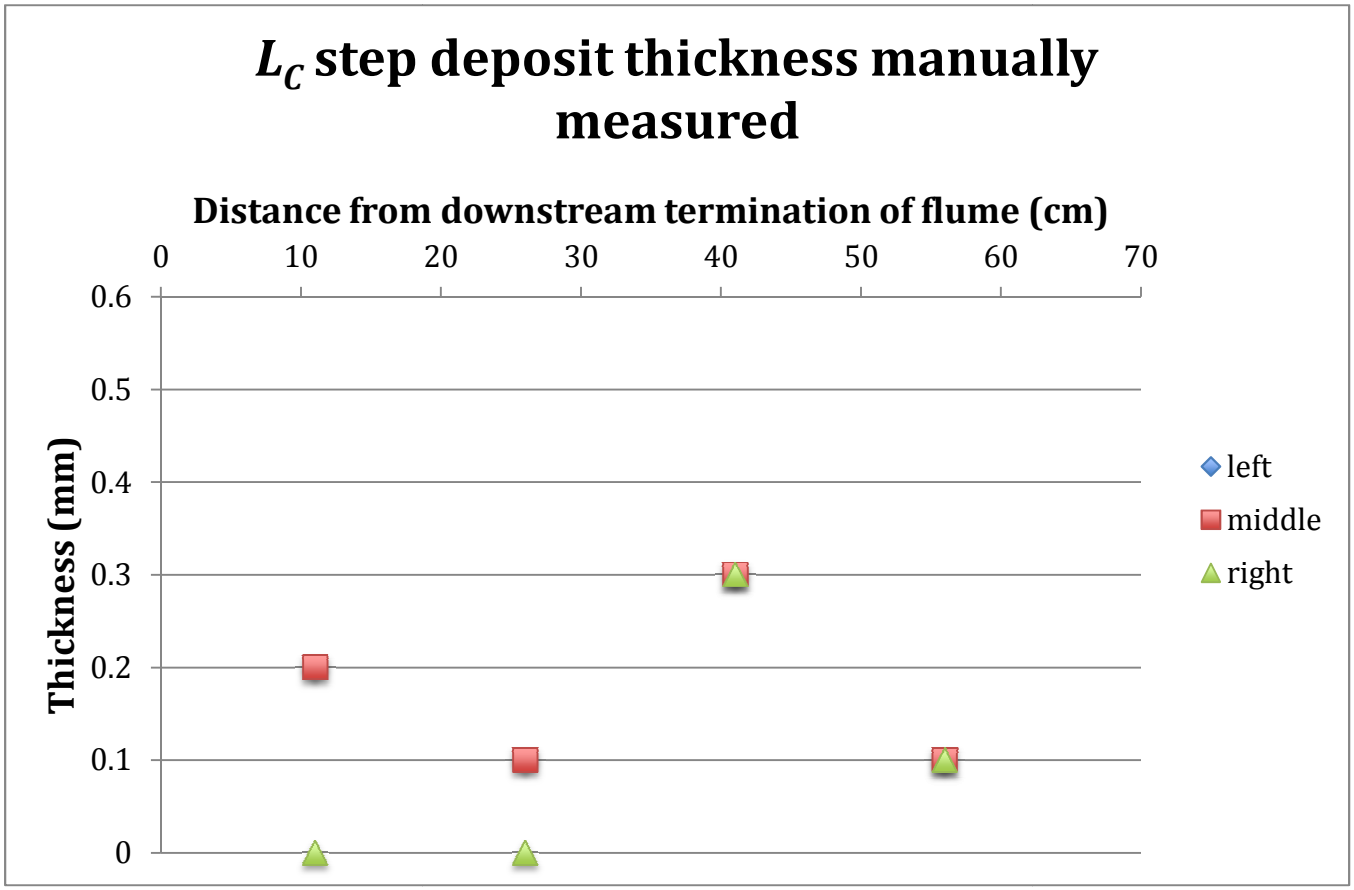

Figures 4.6: Manually measured deposit thickness on the wooden steps for experiment $L_H$.

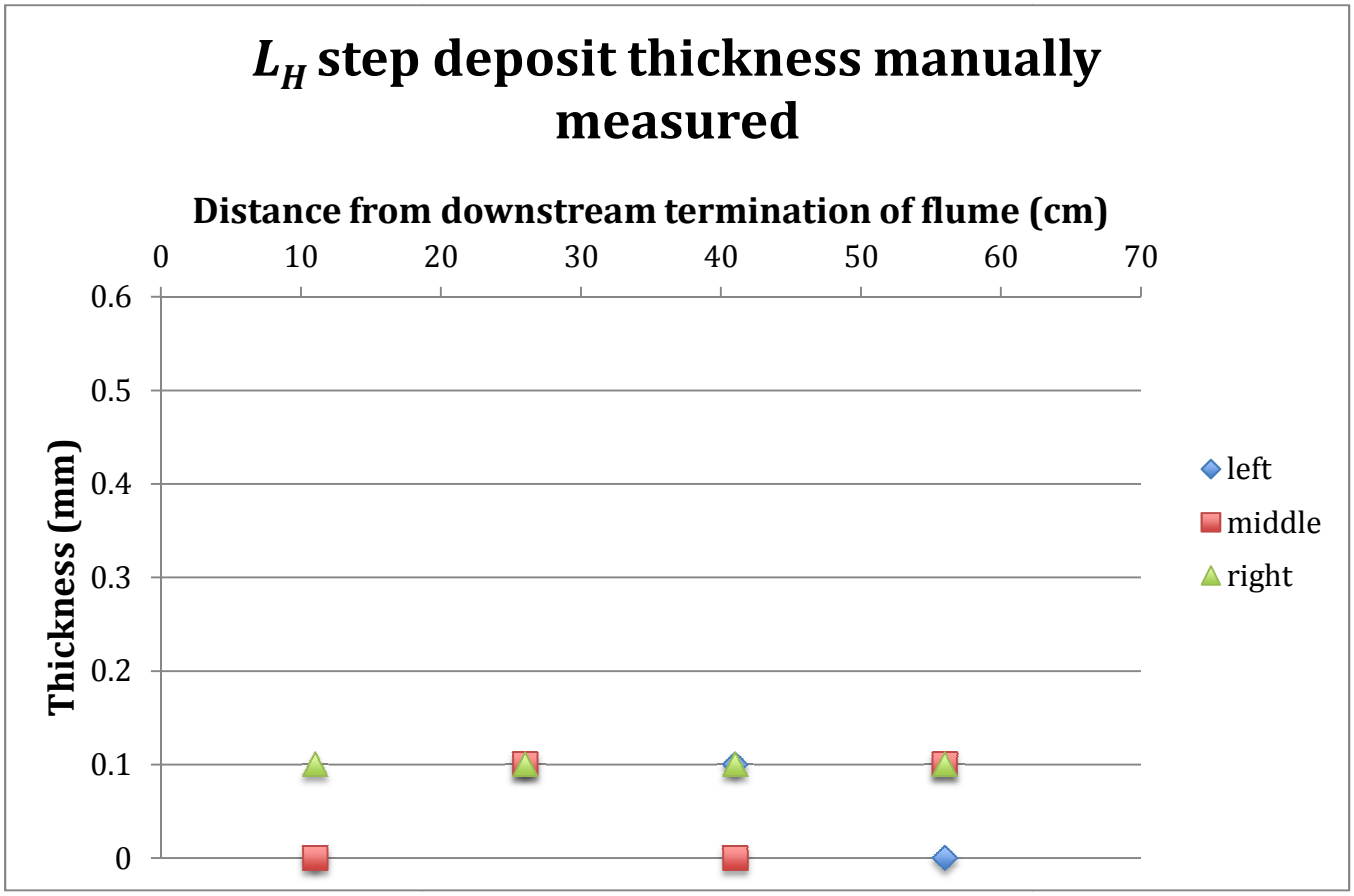

Figures 5.1: Thickness values for pond 2 from elevation data. Pond thicknesses decreases towards the downstream direction. $S_H$ generally shows greater thicknesses than $S_C$.

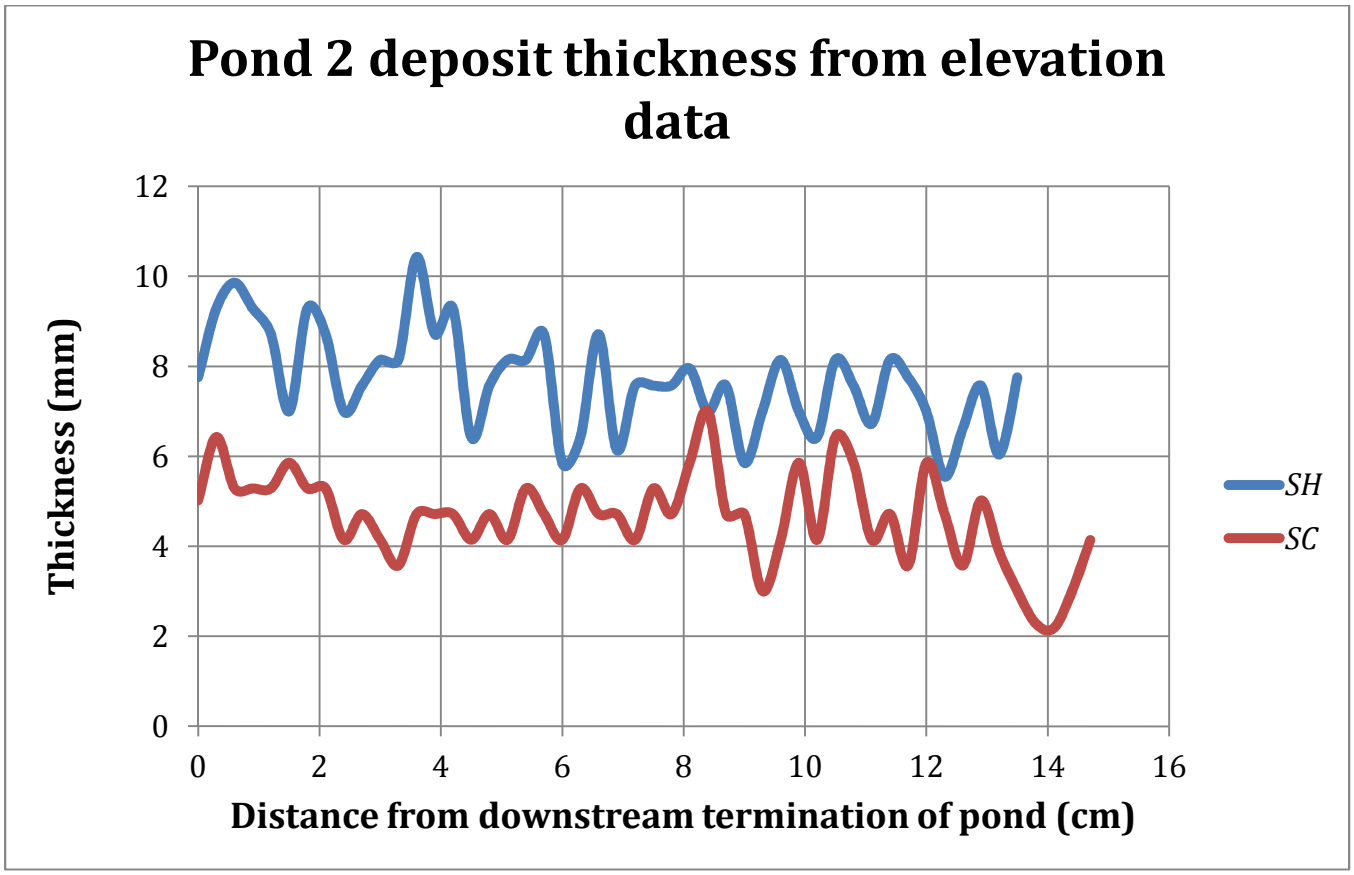

Figures 5.2: Thickness values for pond 3 from elevation data.

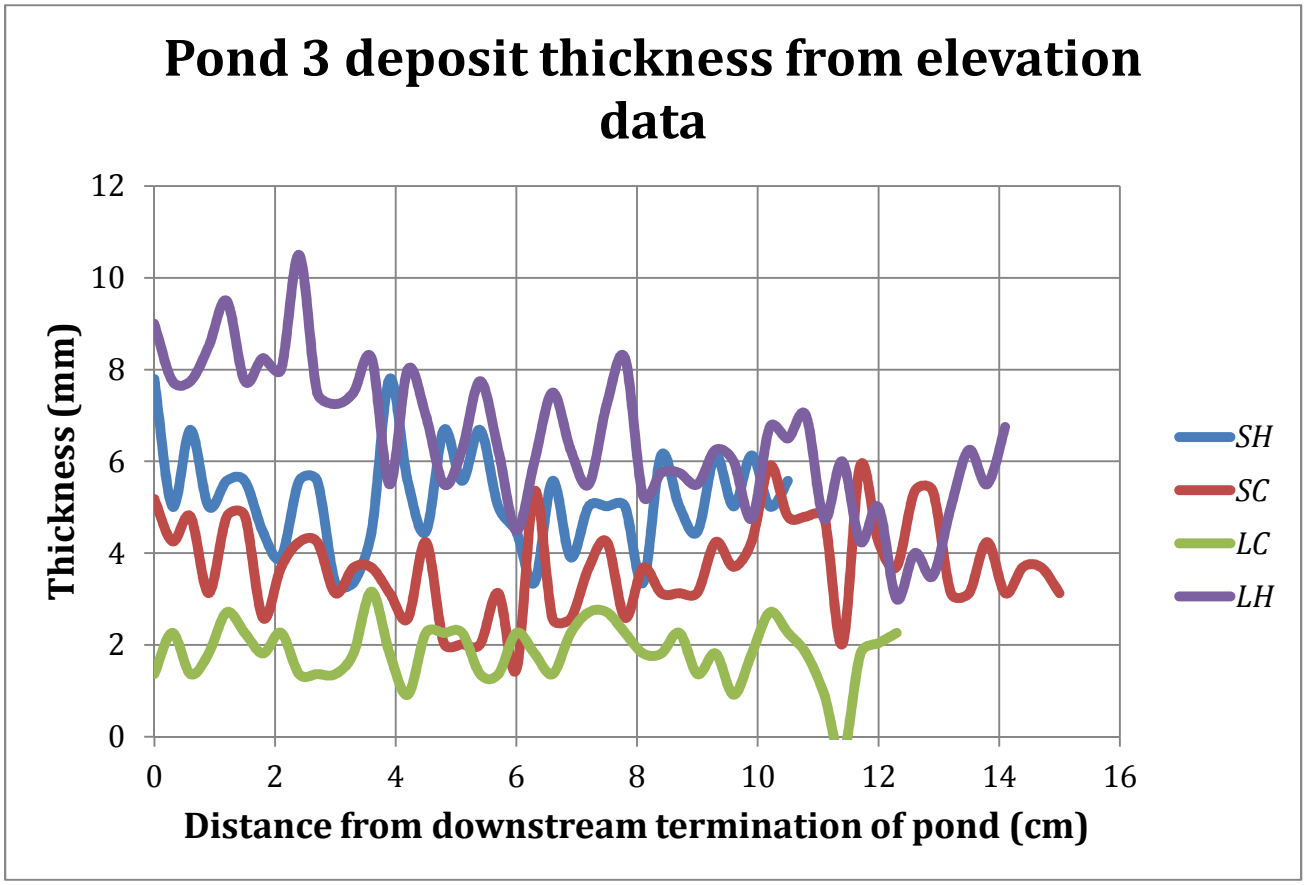

Figures 5.3: Thickness values for pond 4 from elevation data.

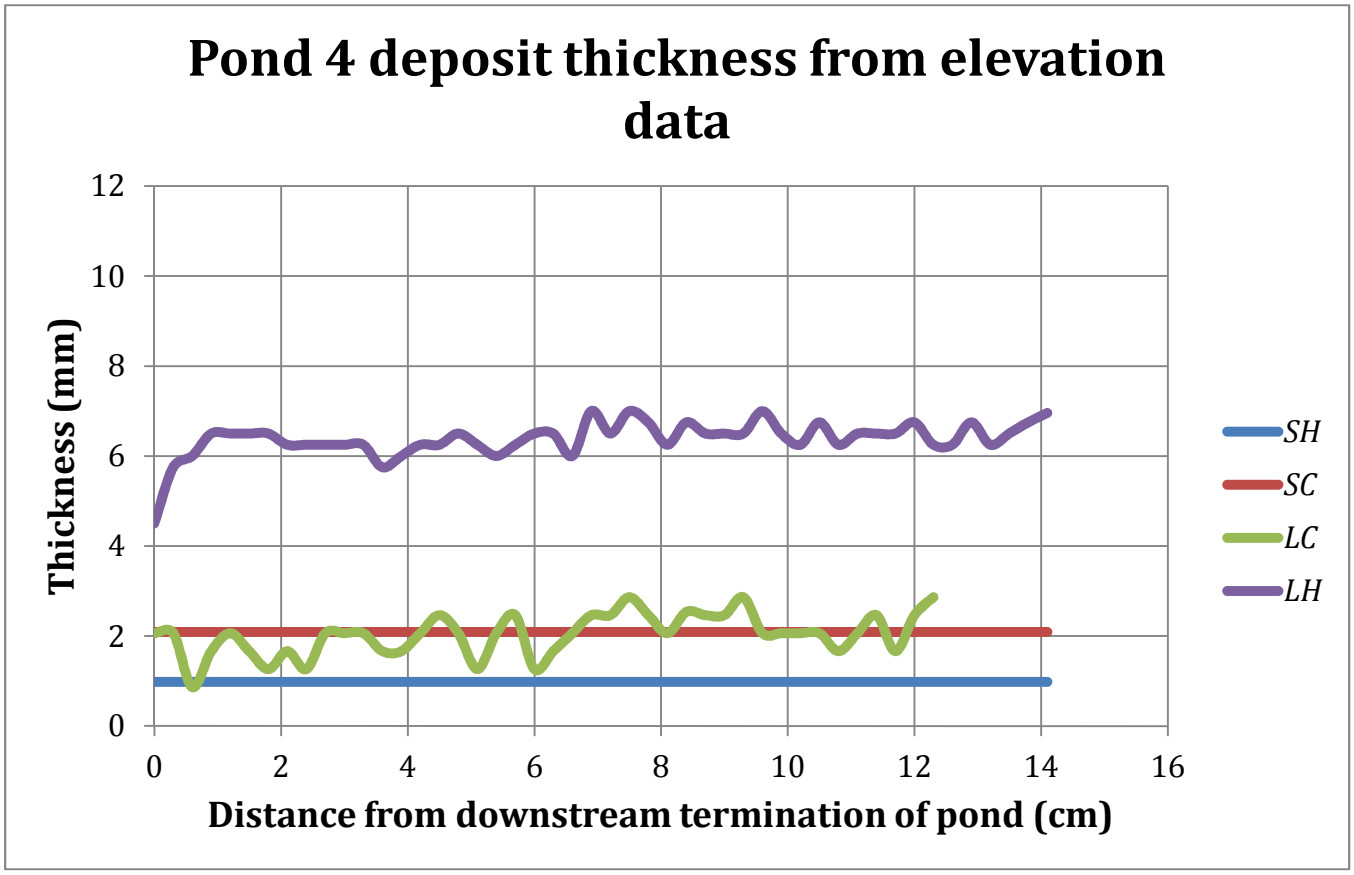

Figures 5.4: Thickness values for pond 5 from elevation data.

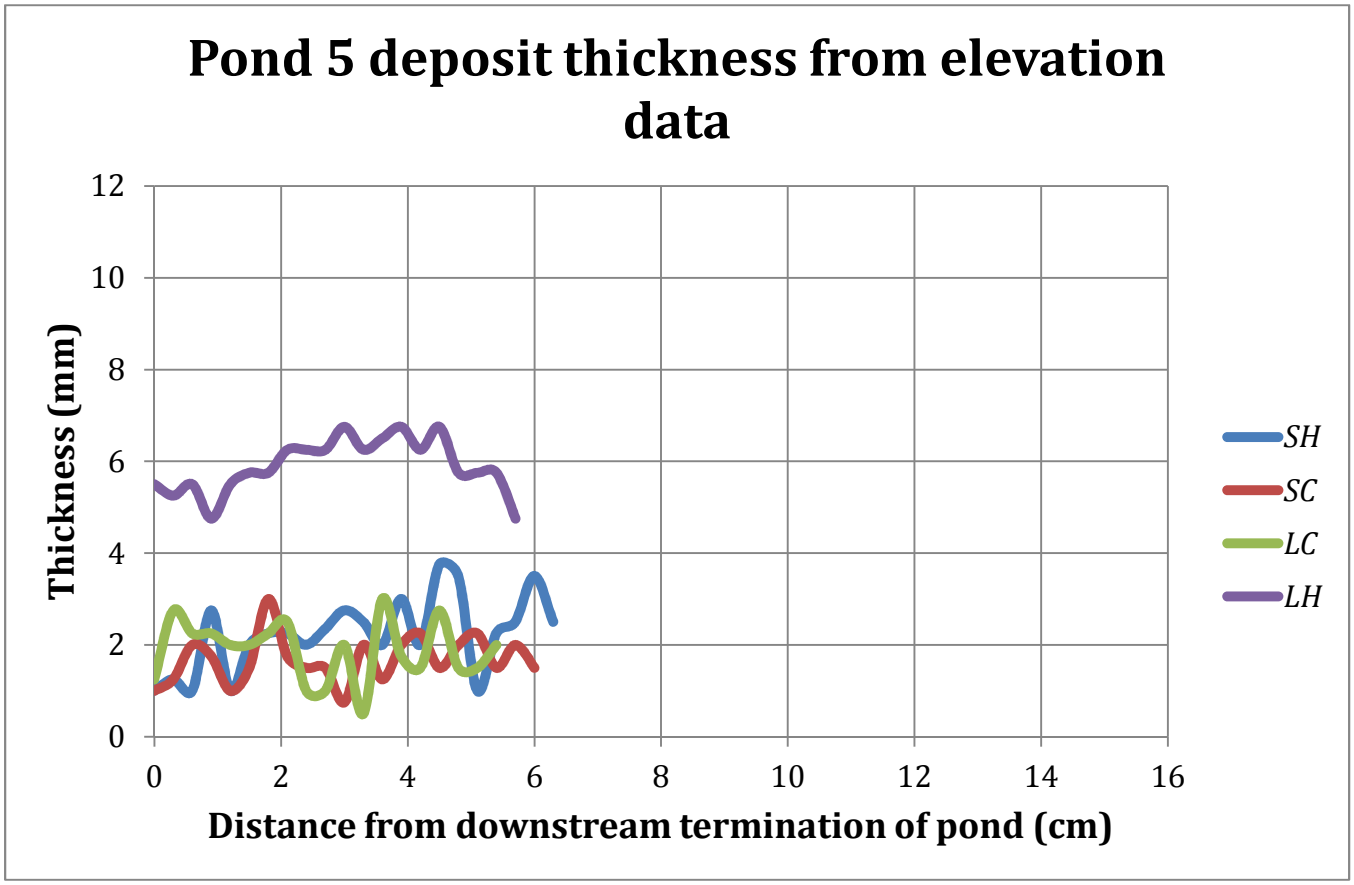

Figures 5.5: Average thickness values for all ponds from elevation data.

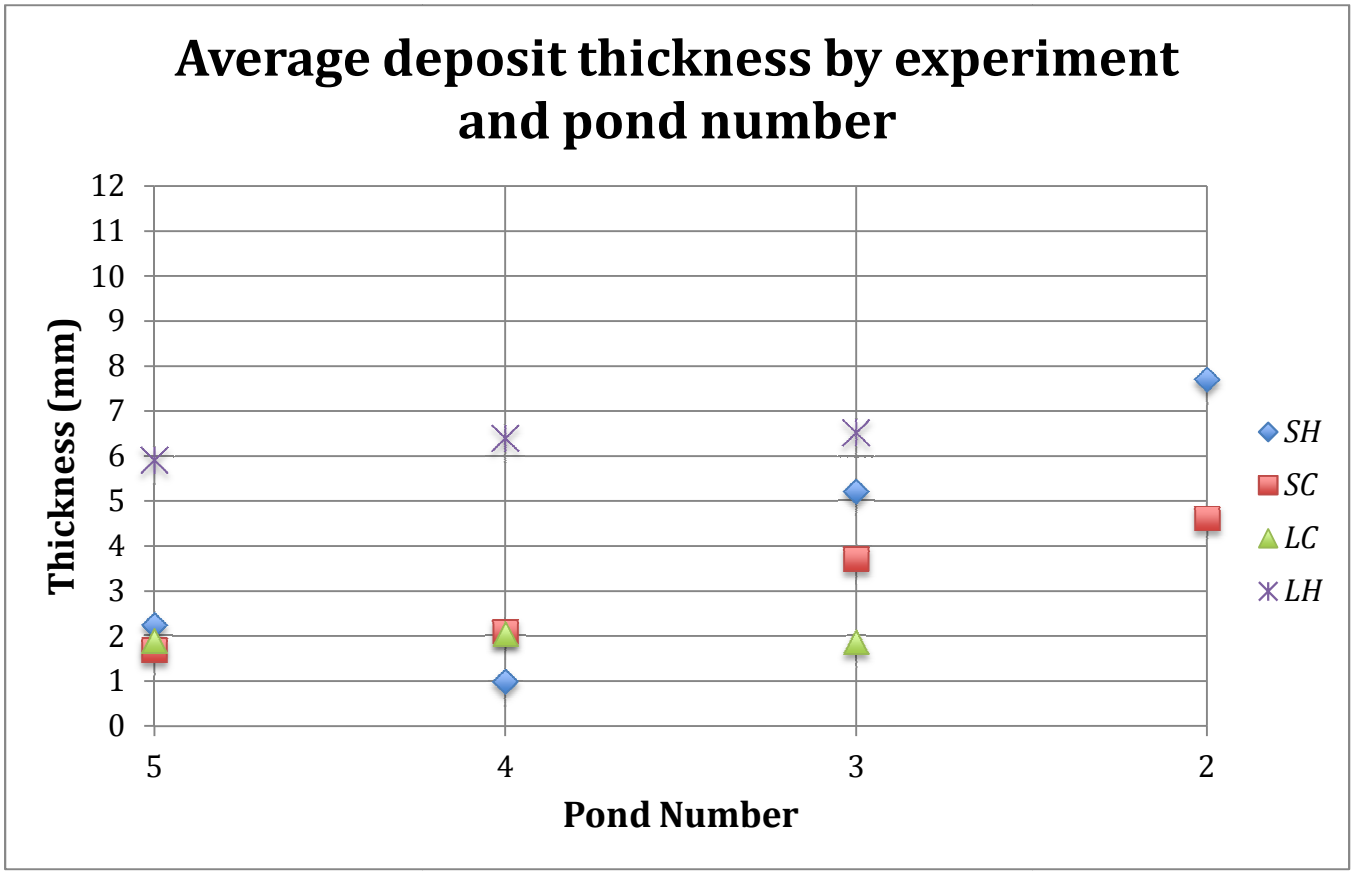

Figures 6.1: Pond aggradation over time for $S_H$. Ponds 2 and 3 show greater aggradation compared to ponds 4 and 5. The elevations are not referenced to the basement elevation but lines are separated to show the overall growing trends.

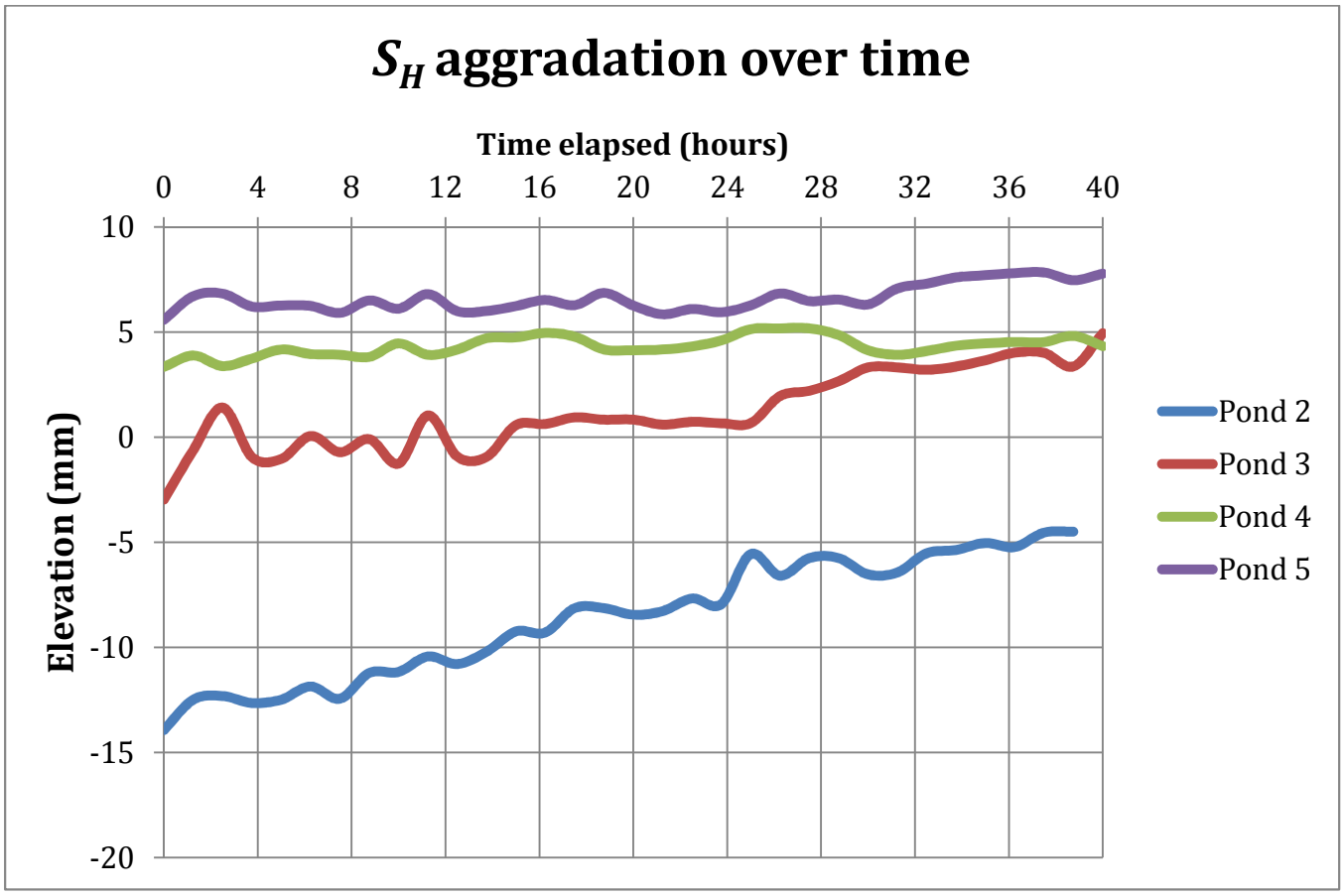

Figures 6.2: Pond aggradation over time for $S_C$.

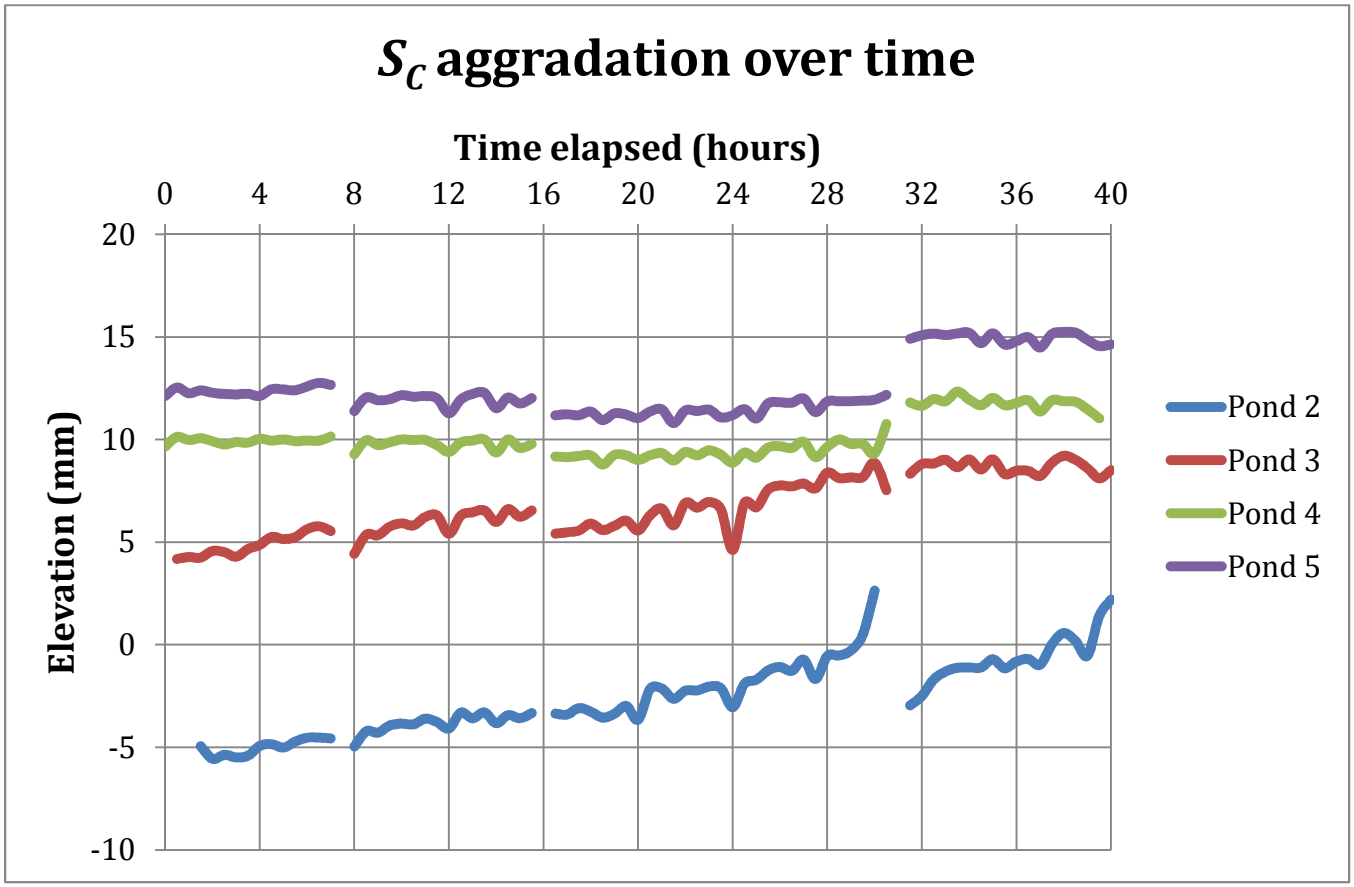

Figures 6.3: Pond aggradation over time for $L_C$.

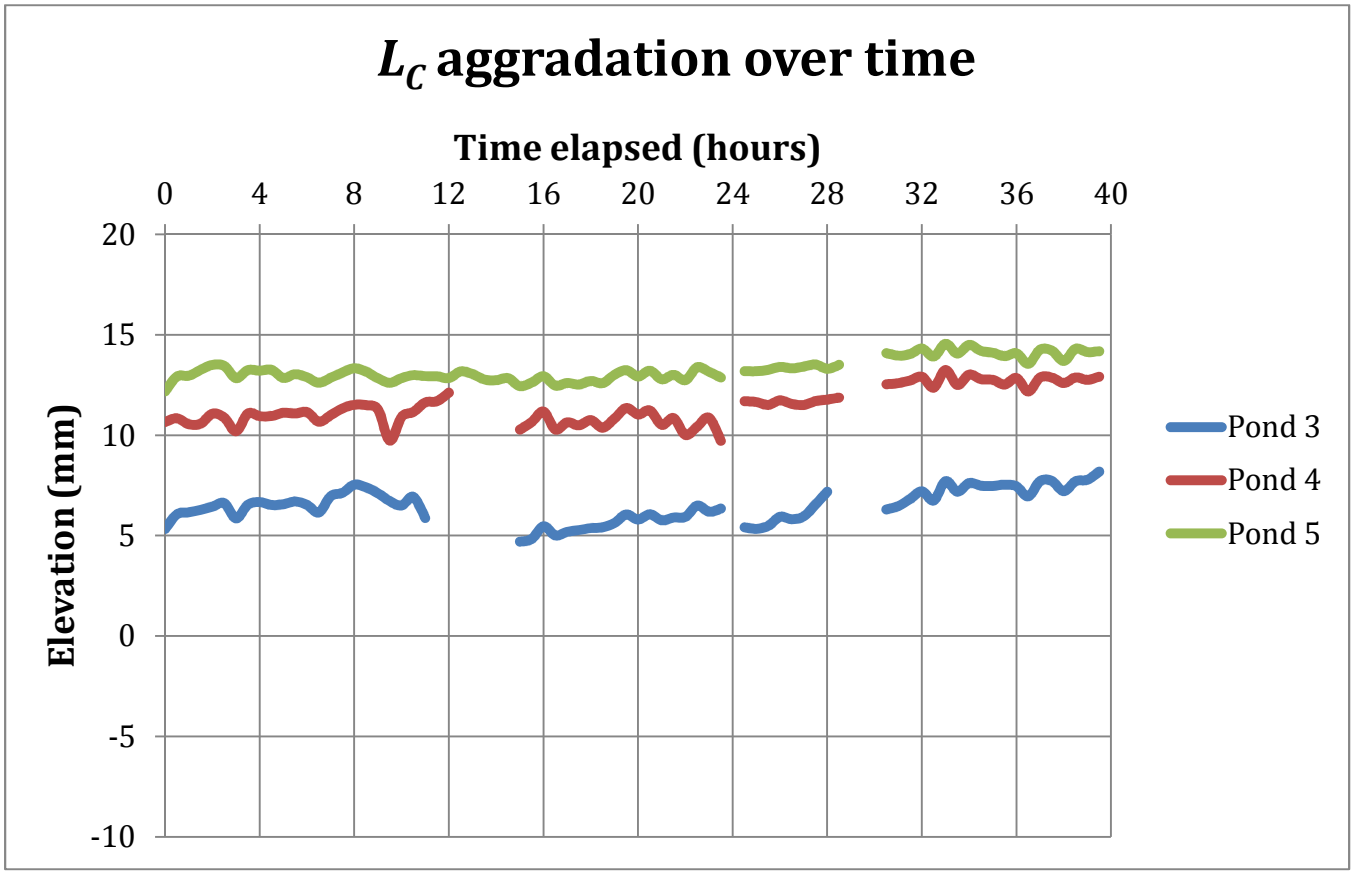

Figures 6.4: Pond aggradation over time for $L_H$.

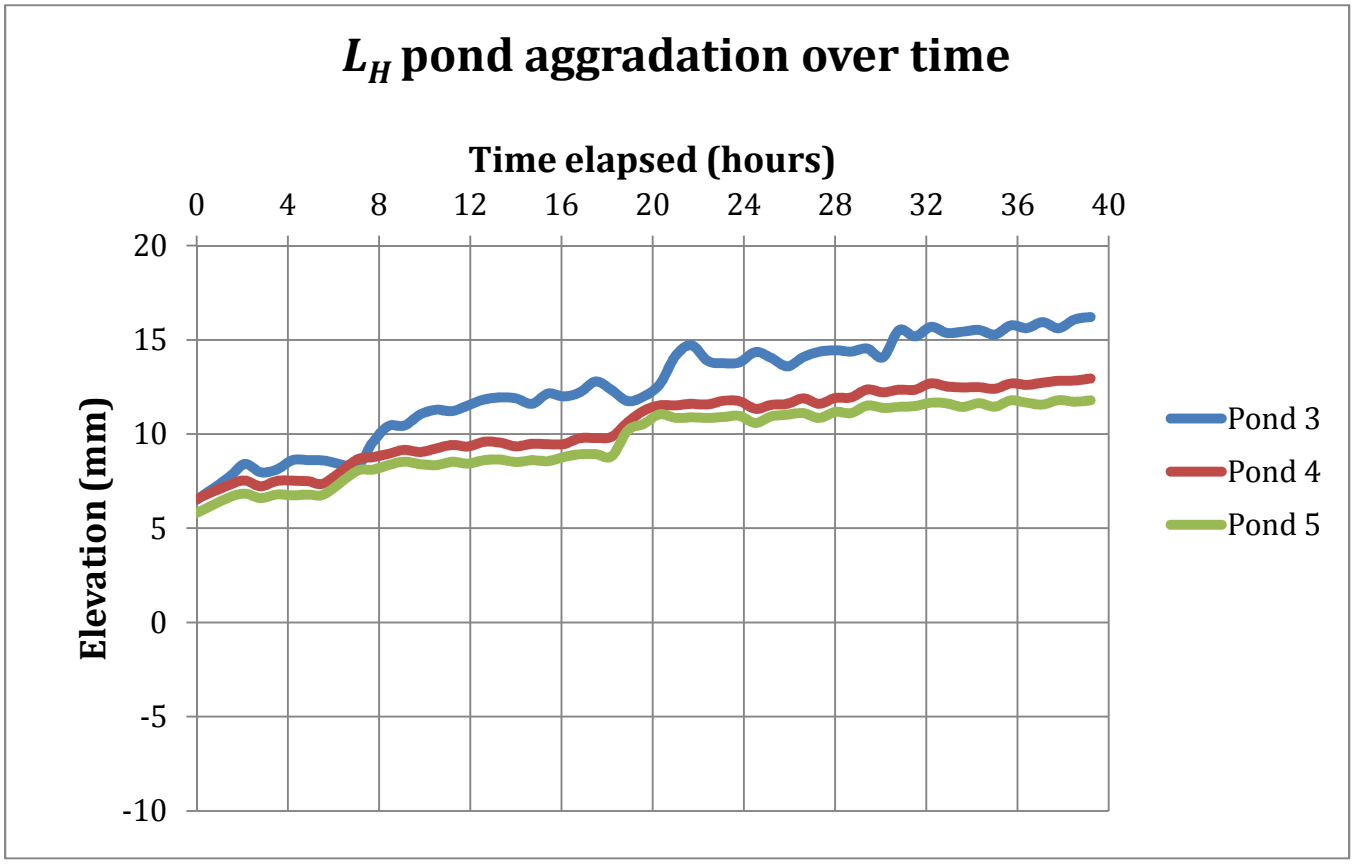

Figures 6.5: Step aggradation over time for $S_H$. Steps show slight elevation increase over time. The elevations are not referenced to the basement elevation but lines are separated to show the overall growing trends.

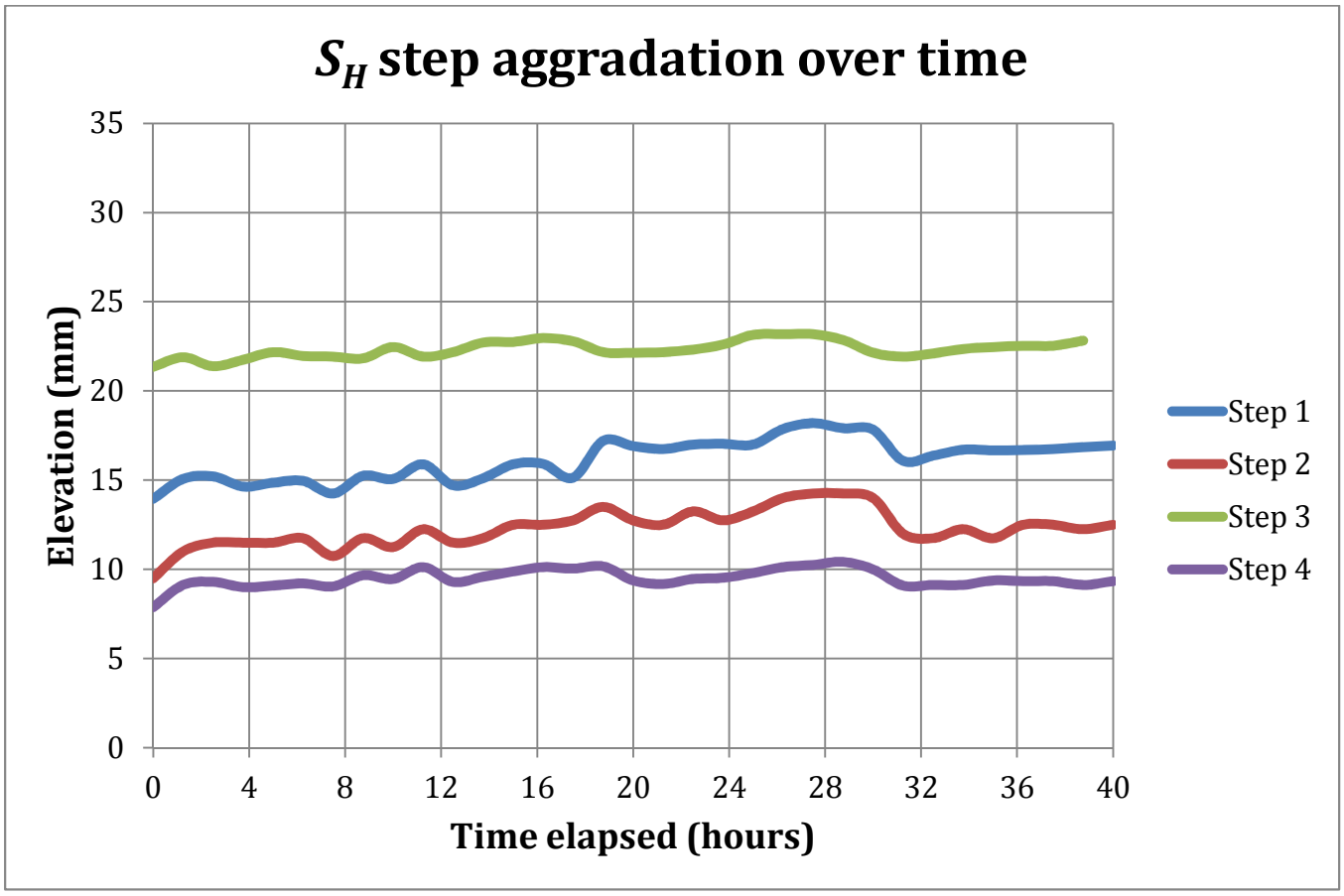

Figures 6.6: Step aggradation over time for $S_C$.

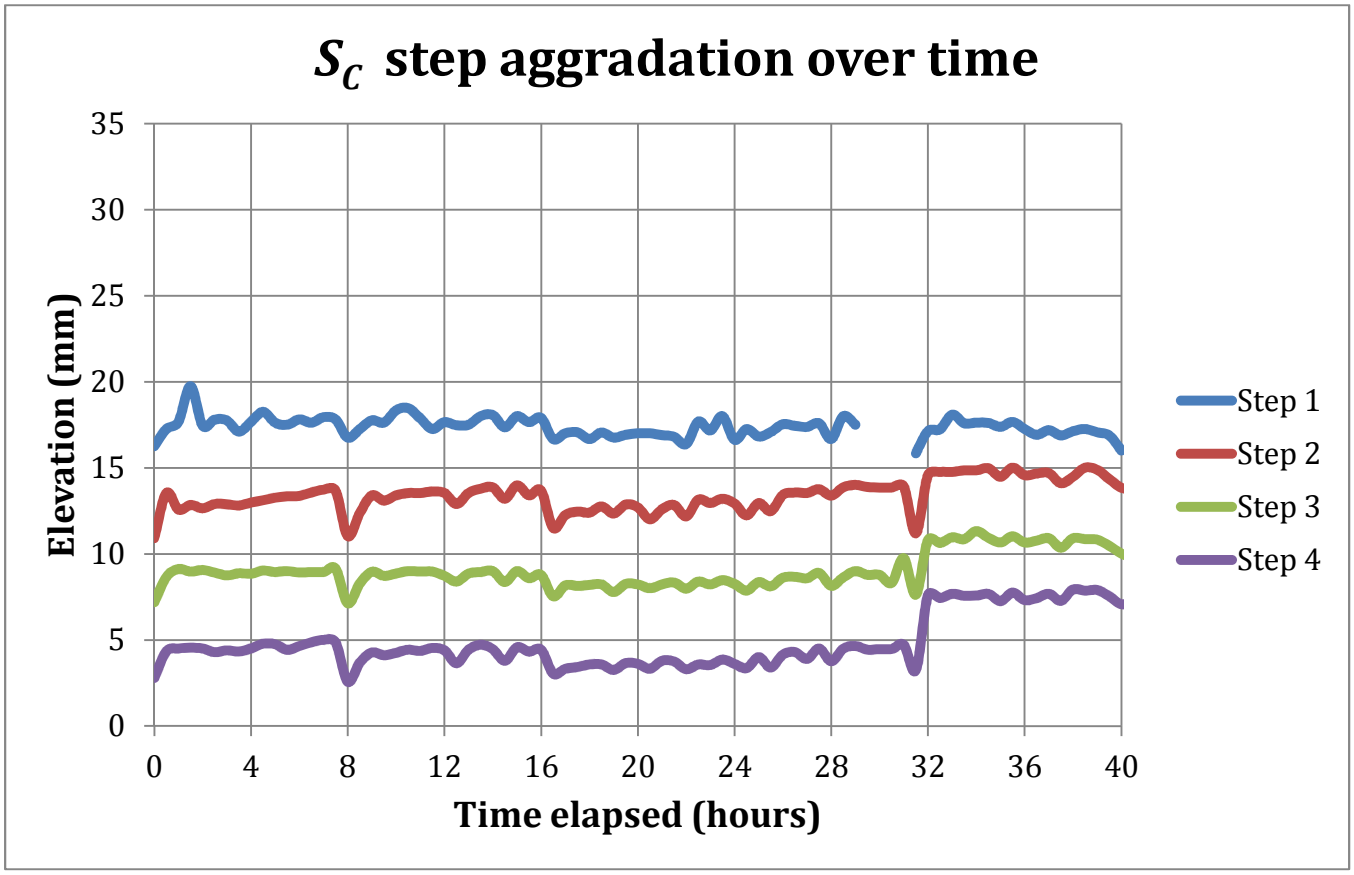

Figures 6.7: Step aggradation over time for $L_C$.

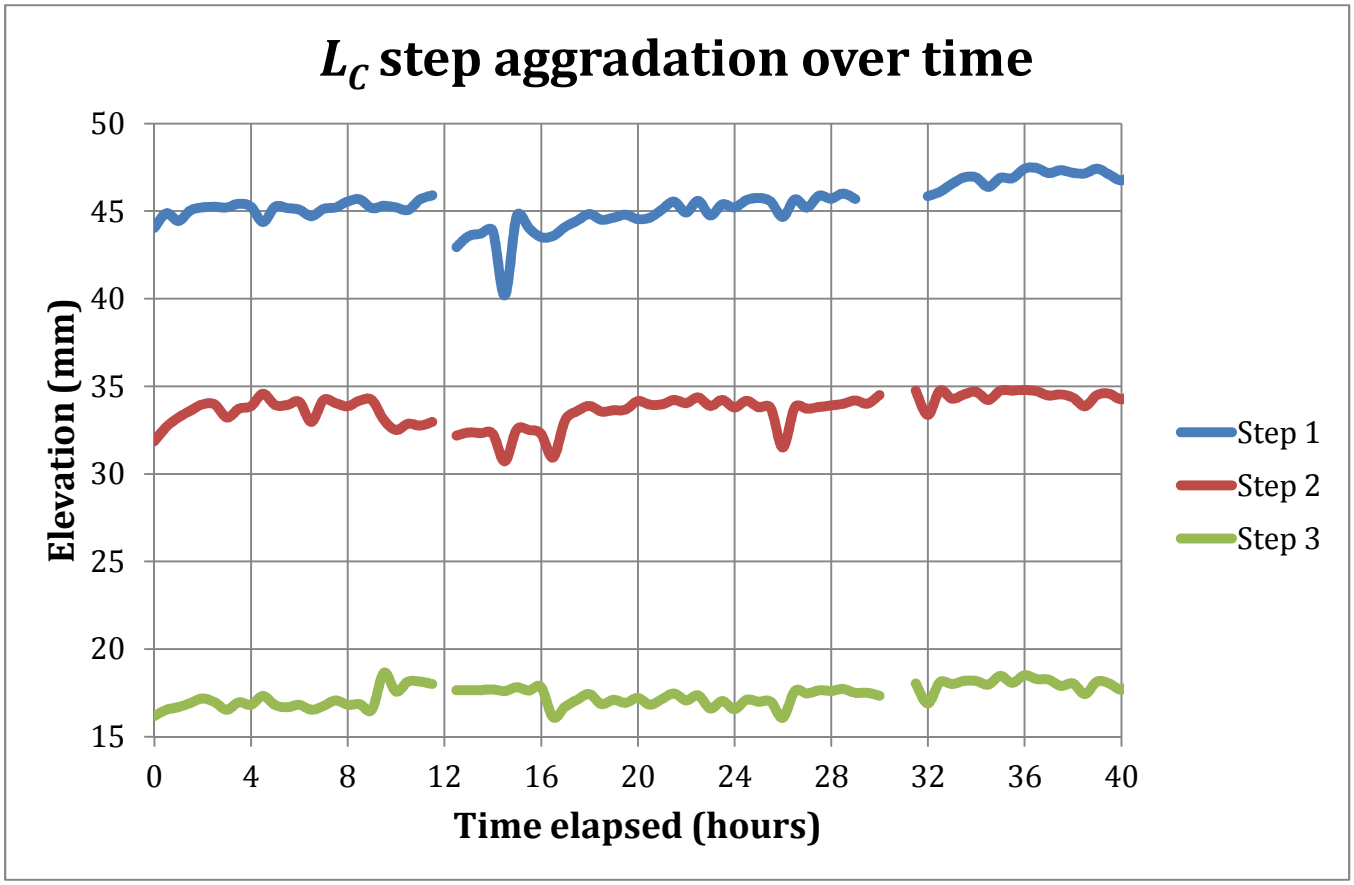

Figures 6.8: Step aggradation over time for $L_H$.

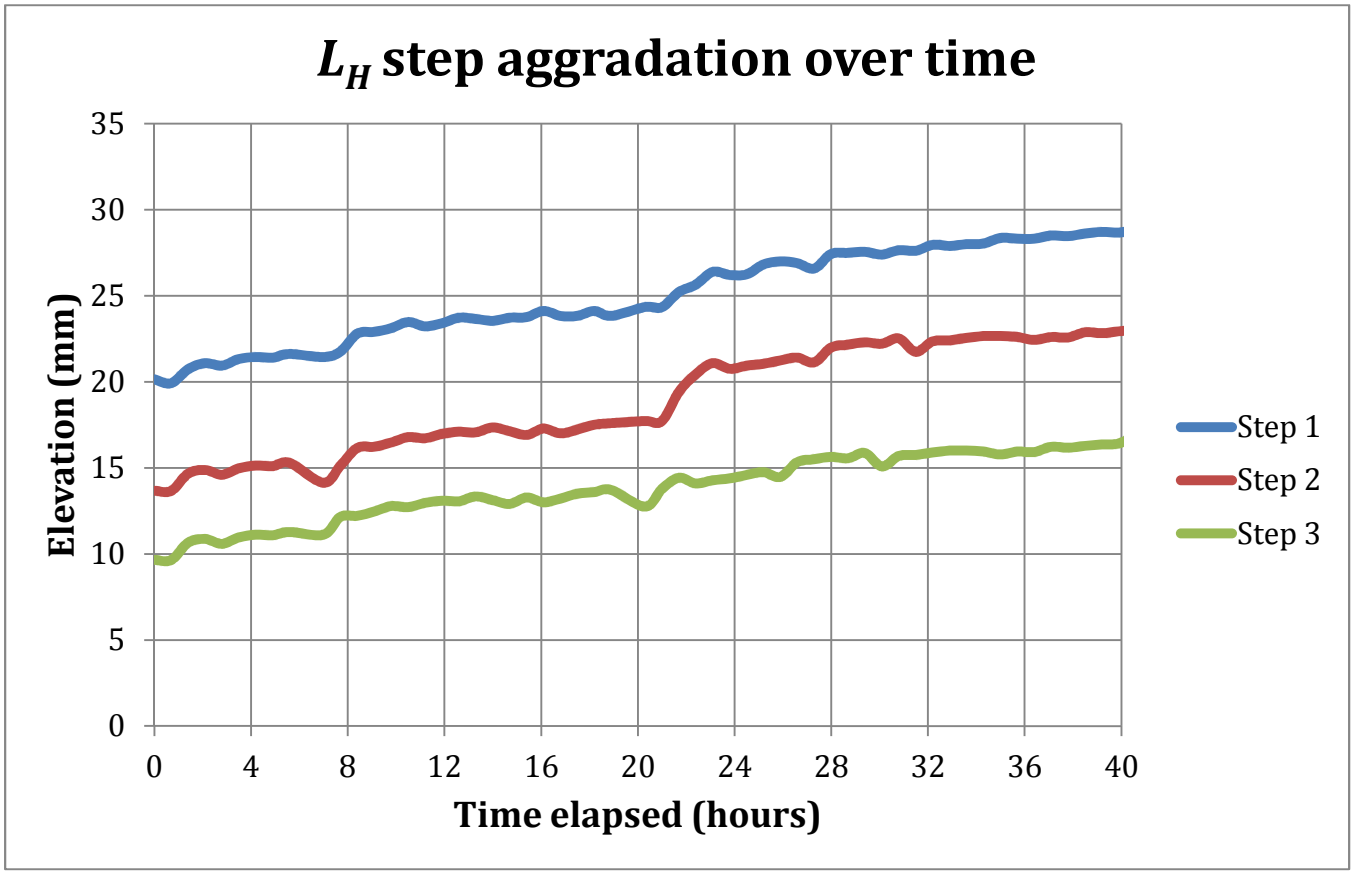

Figures 7.1: Initial and final elevation lines for $S_H$. Ponds 2-5 are displayed. Greater difference between initial and final elevation values before a step indicates downstream coarsening, which is most observable in ponds 2 and 3. The elevations are not referenced to the basement elevation but lines are separated to show the overall growing trends.

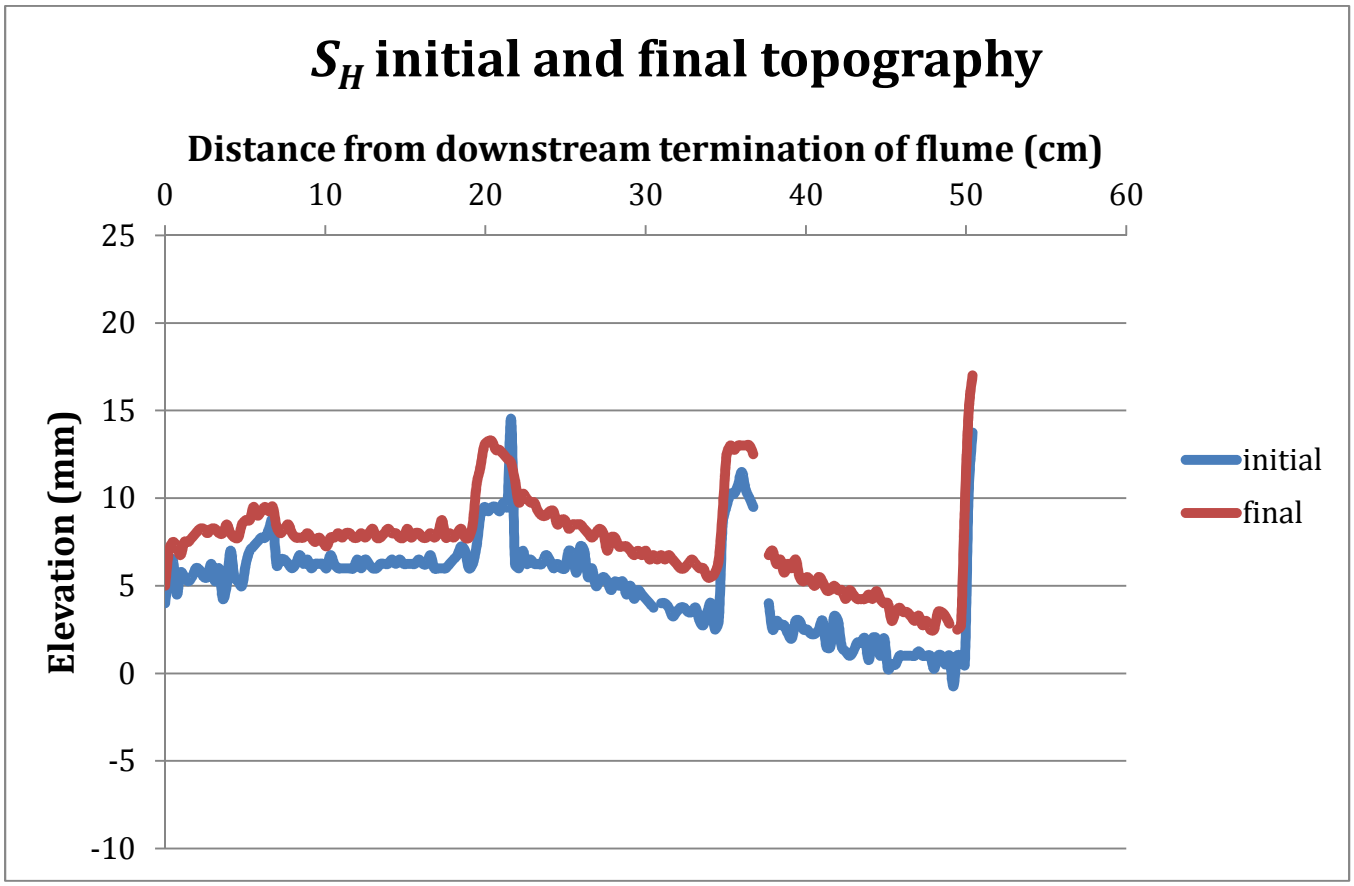

Figures 7.2: Initial and final elevation lines for $S_C$. Ponds 2-5 are displayed.

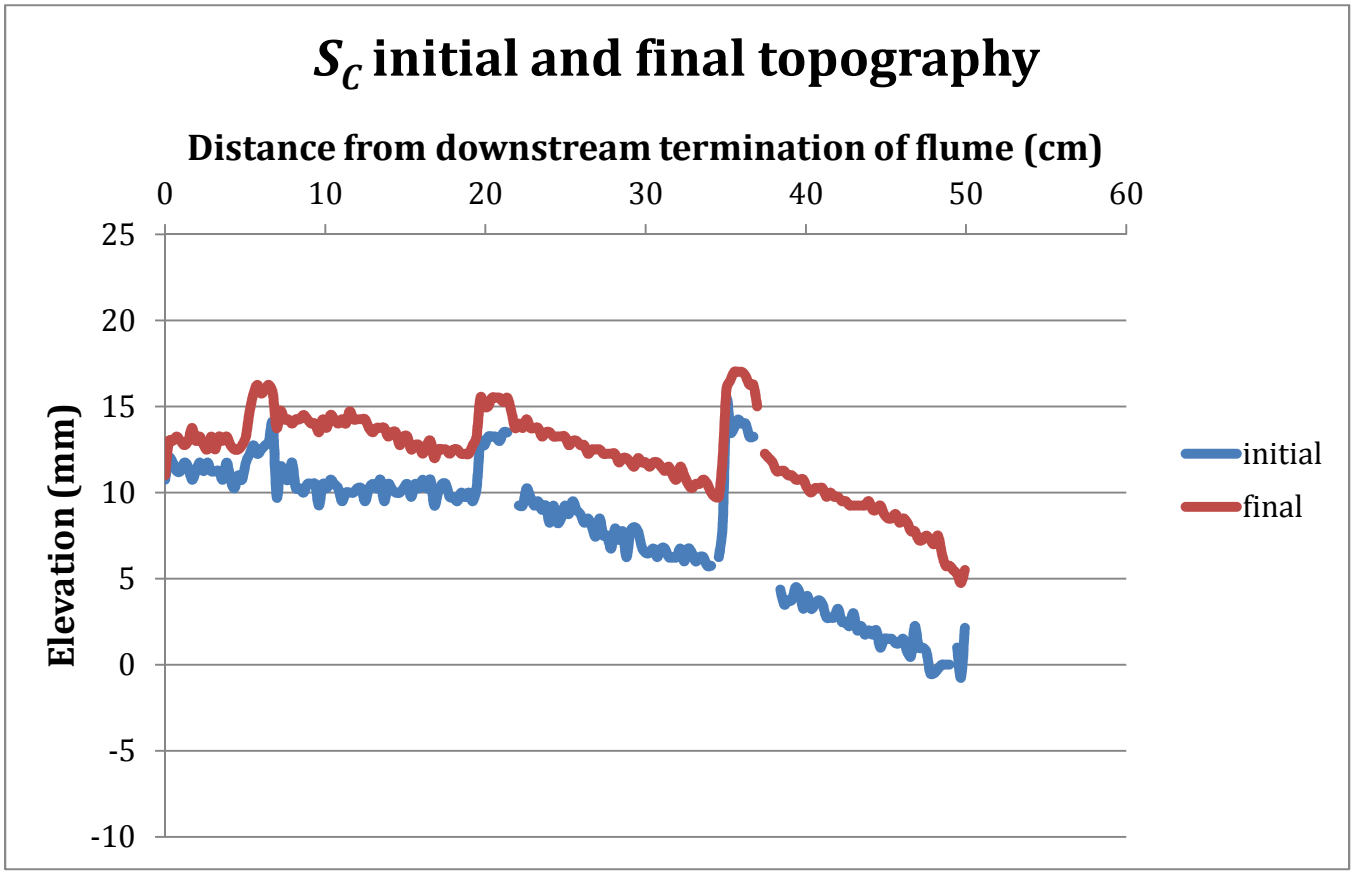

Figures 7.3: Initial and final elevation lines for $L_C$. Ponds 3-5 are displayed.

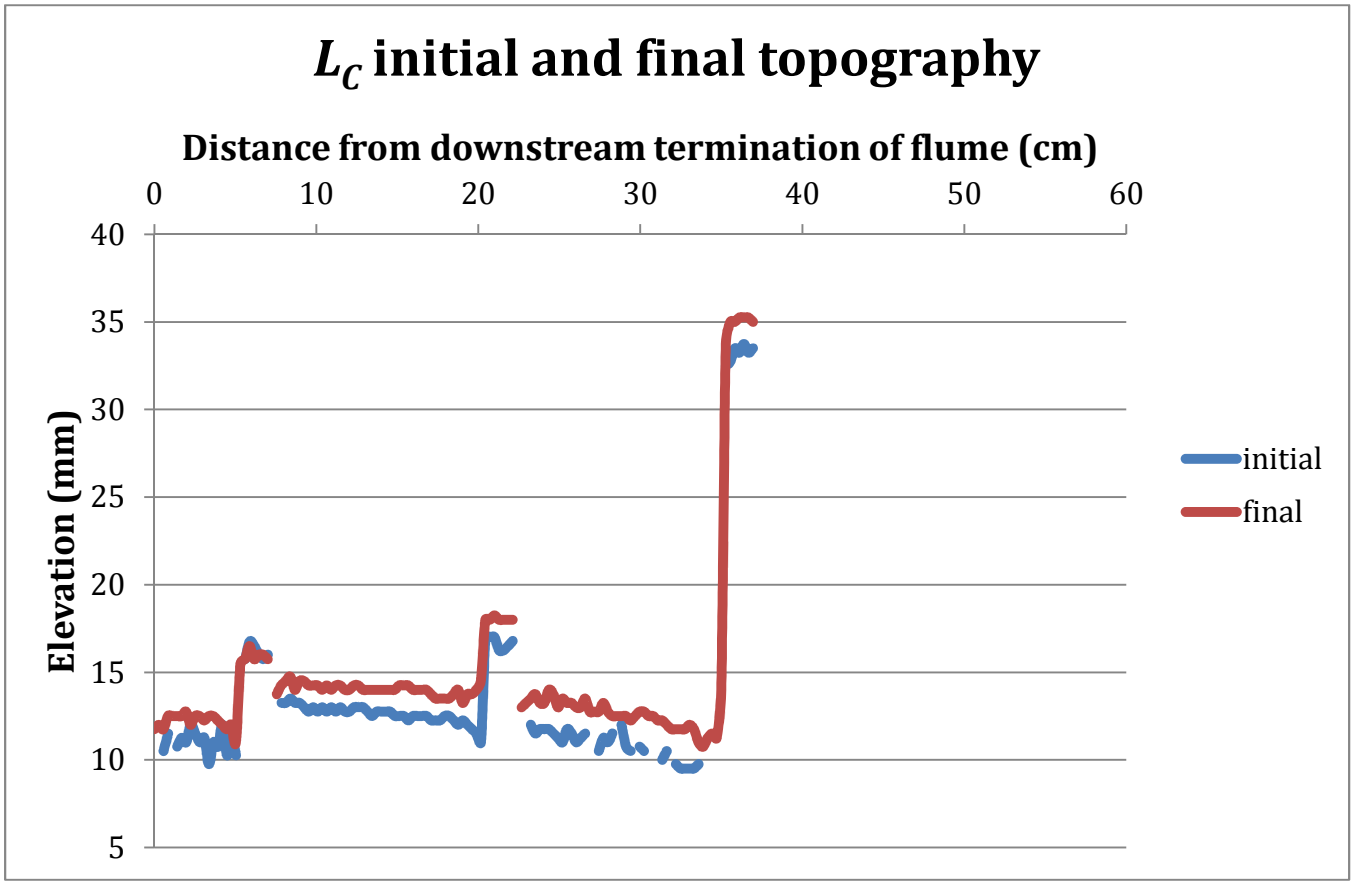

Figures 7.4: Initial and final elevation lines for $L_H$. Ponds 3-5 are displayed.

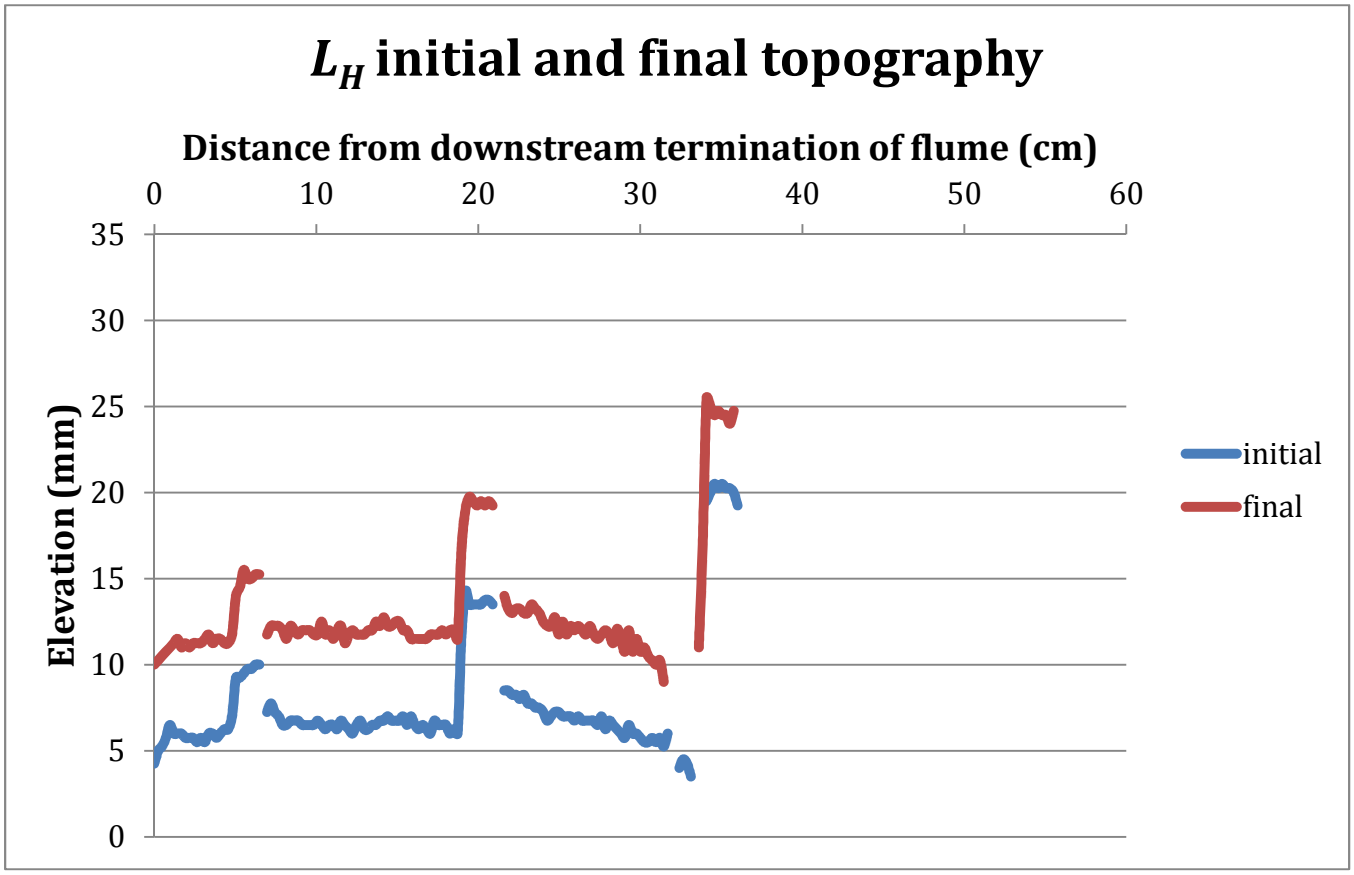

Figures 8.1: Pond aggradation rate for $S_H$. No trend in aggradation rate is seen over the course of the experiment. Aggradation rates show fluctuation in the range of less than 0.1 mm/min.

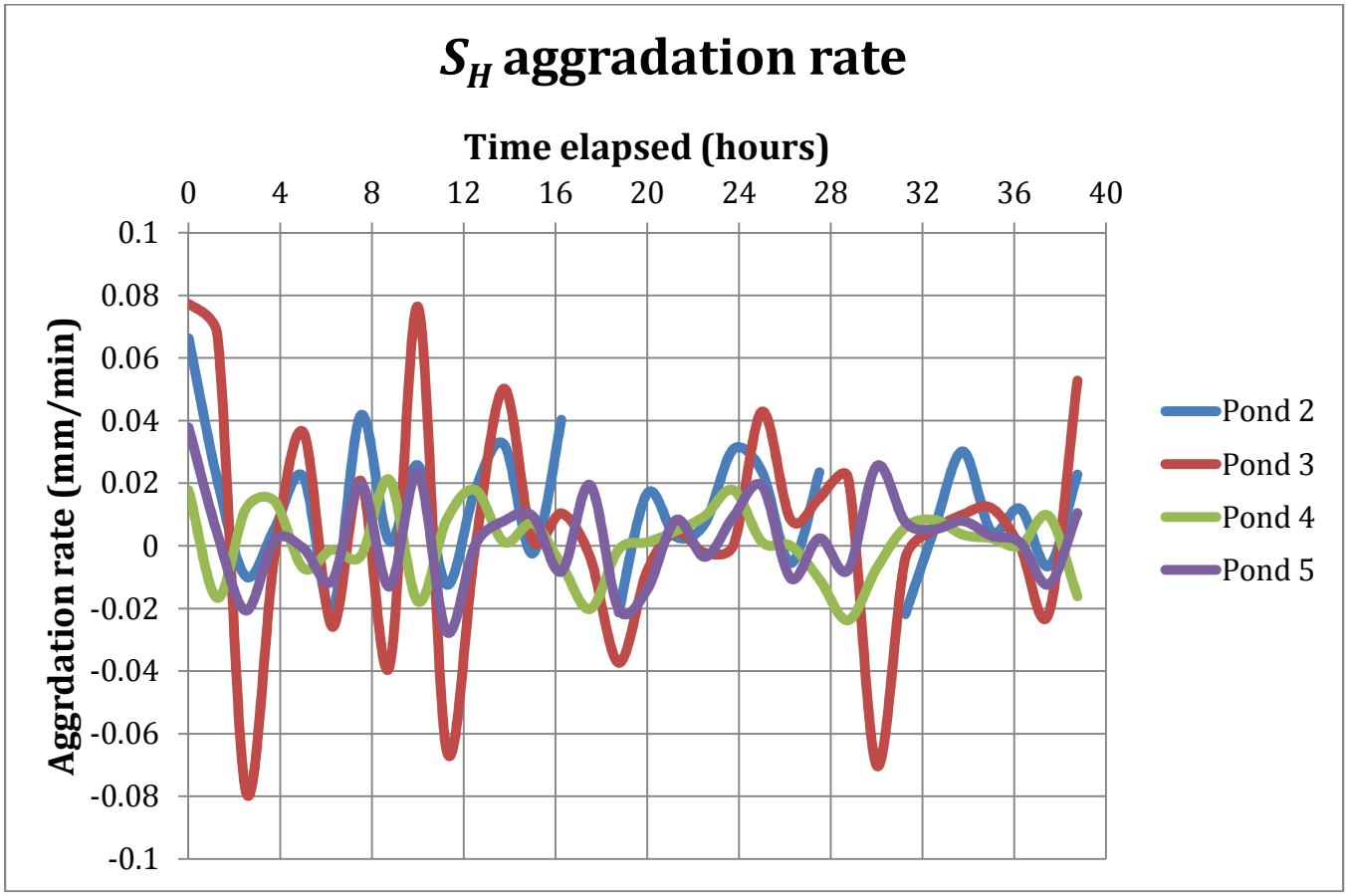

Figures 8.2: Pond aggradation rate for $S_C$.

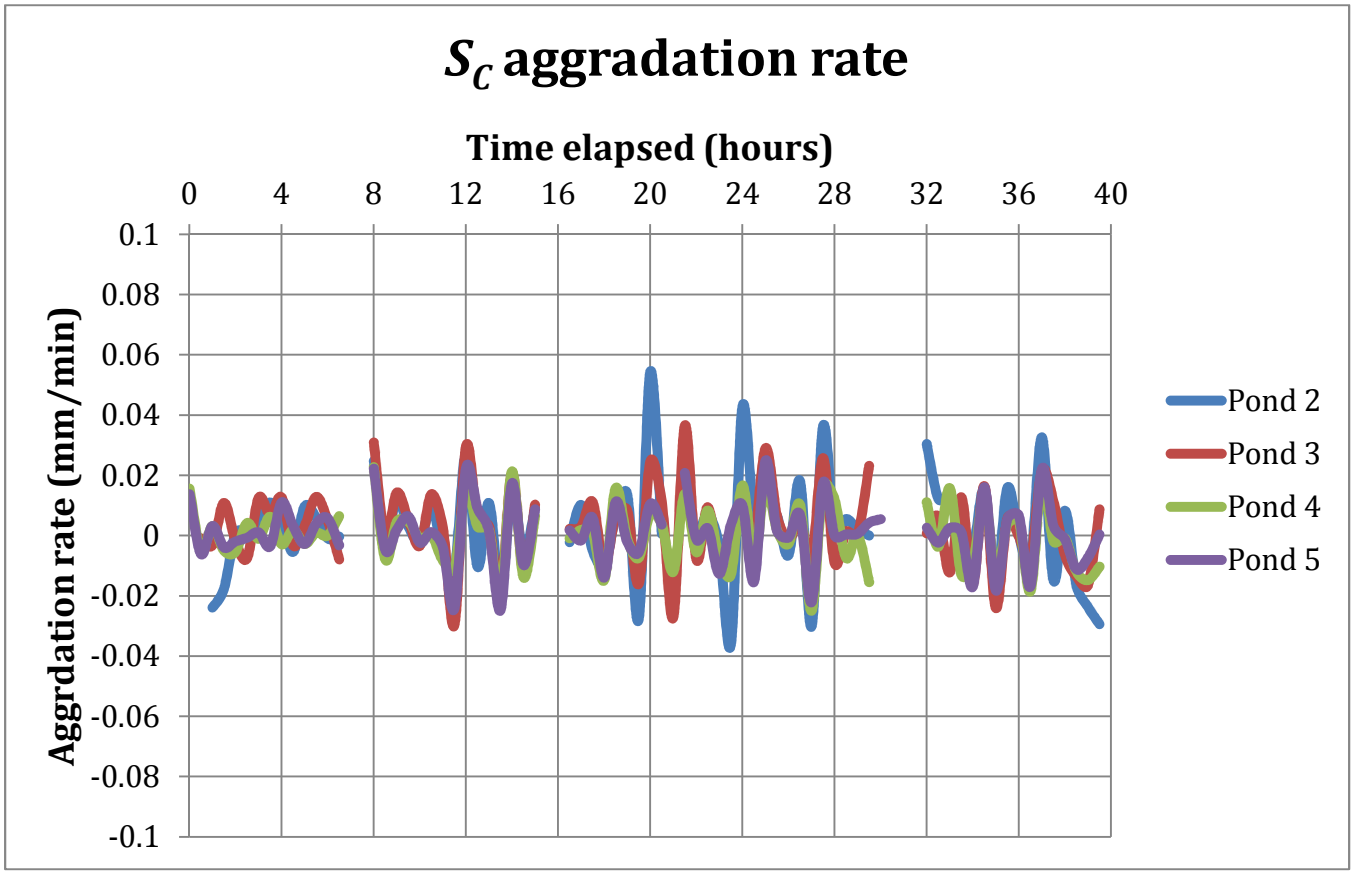

Figures 8.3: Pond aggradation rate for $L_C$.

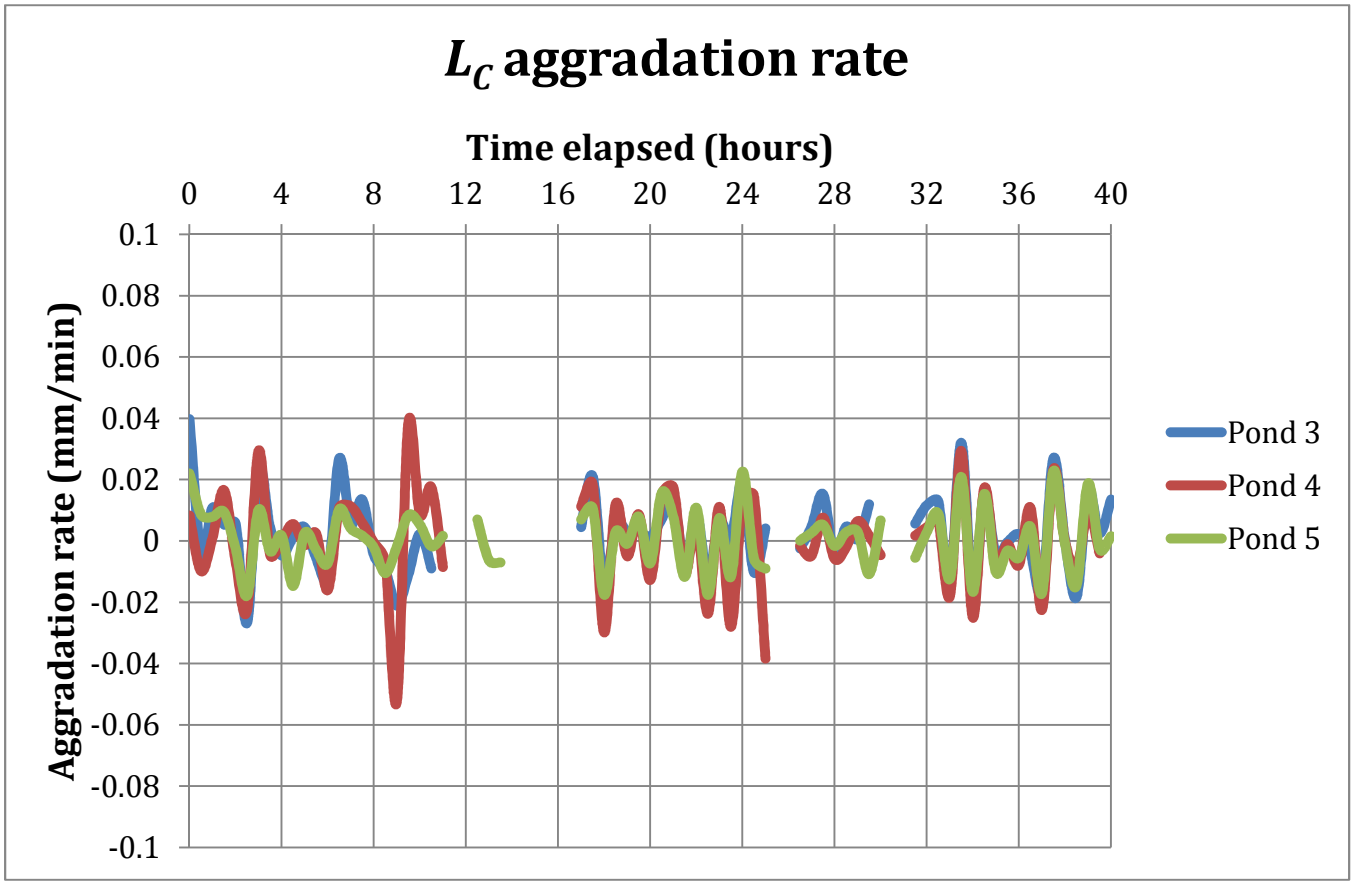

Figures 8.4: Pond aggradation rate for $L_H$.

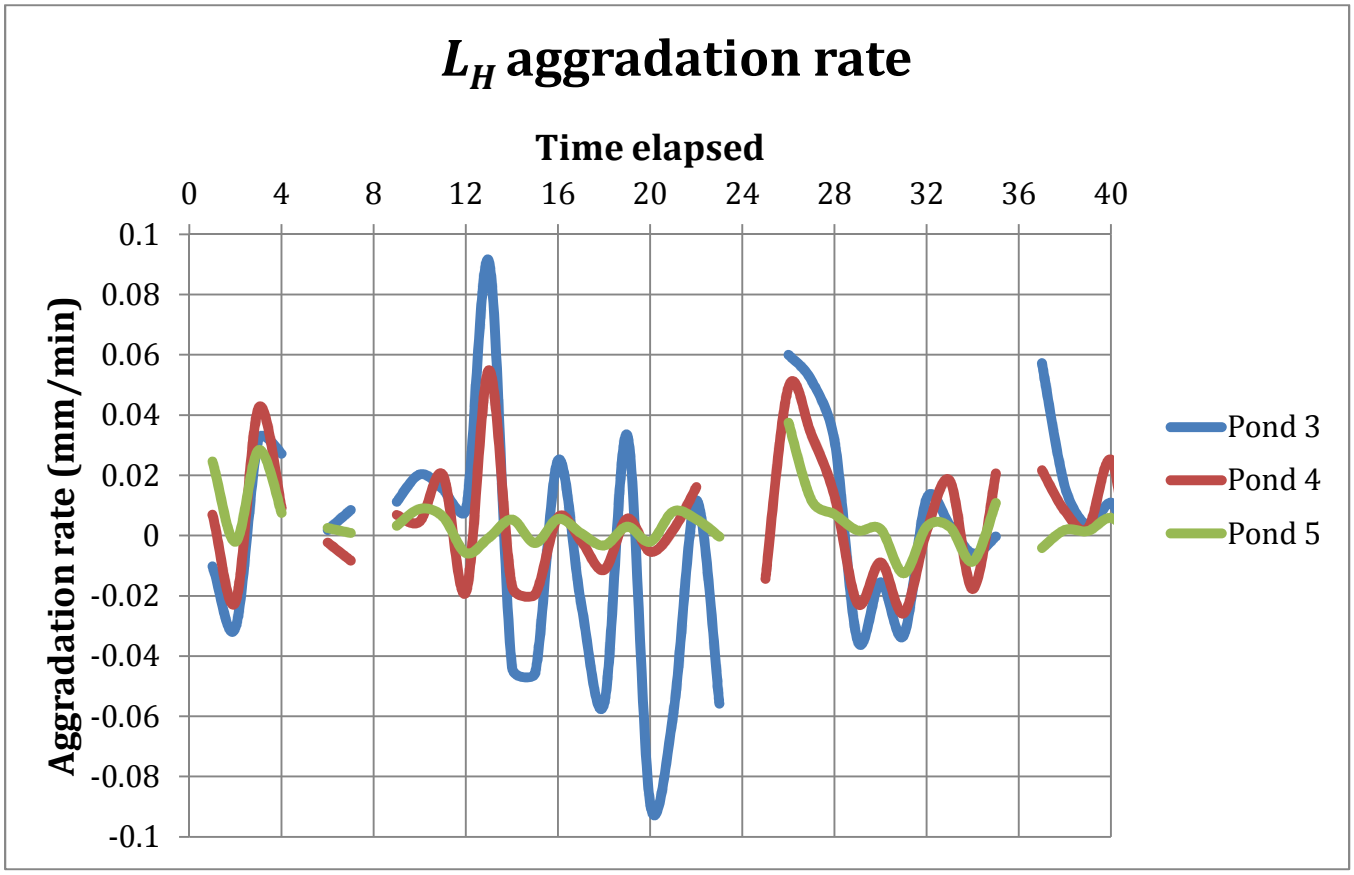

Figures 8.5: Aggradation rate of steps for $S_H$. Rates fluctuate similarly to pond aggradation rates.

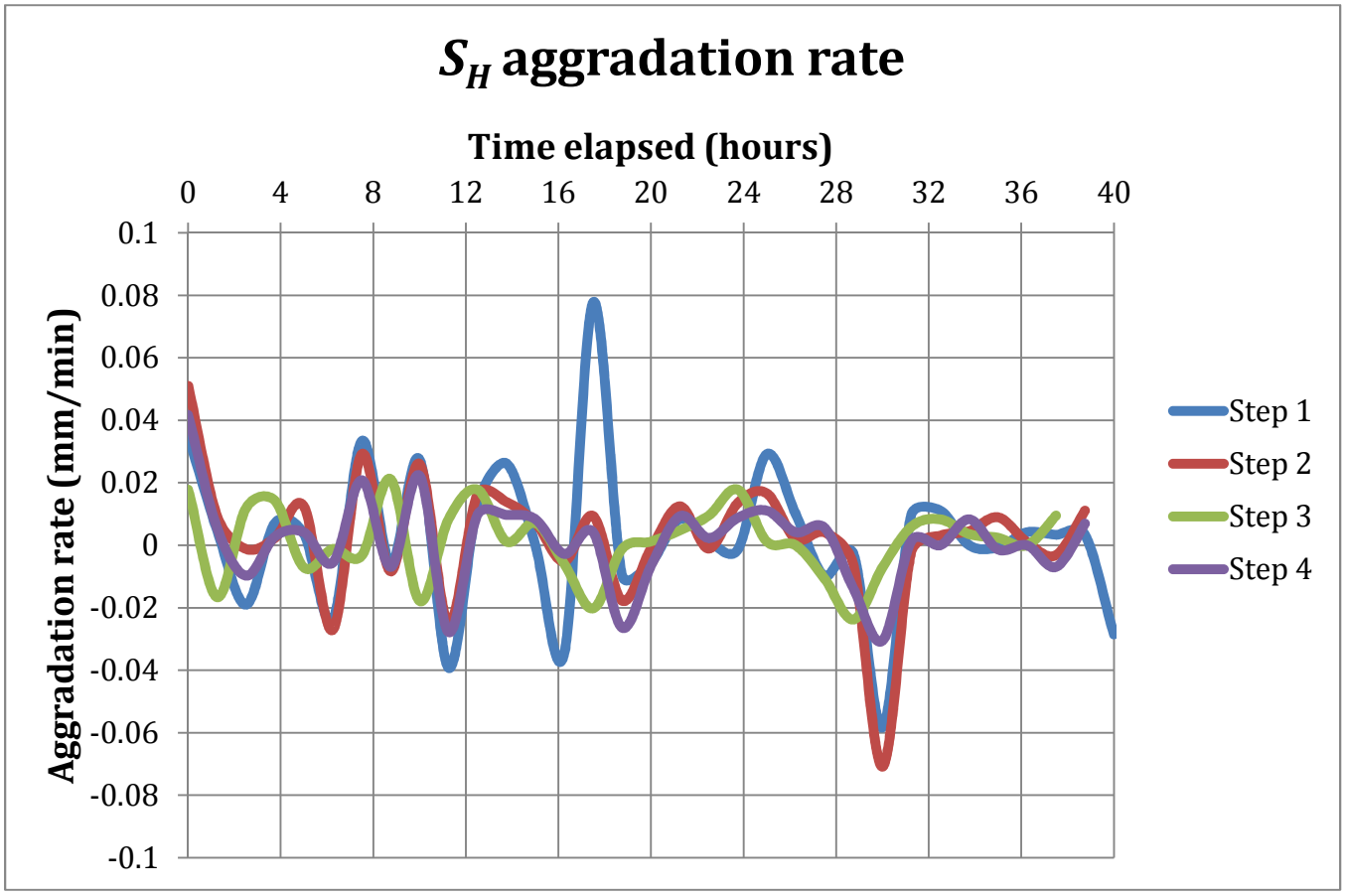

Figures 8.6: Aggradation rate of steps for $S_C$.

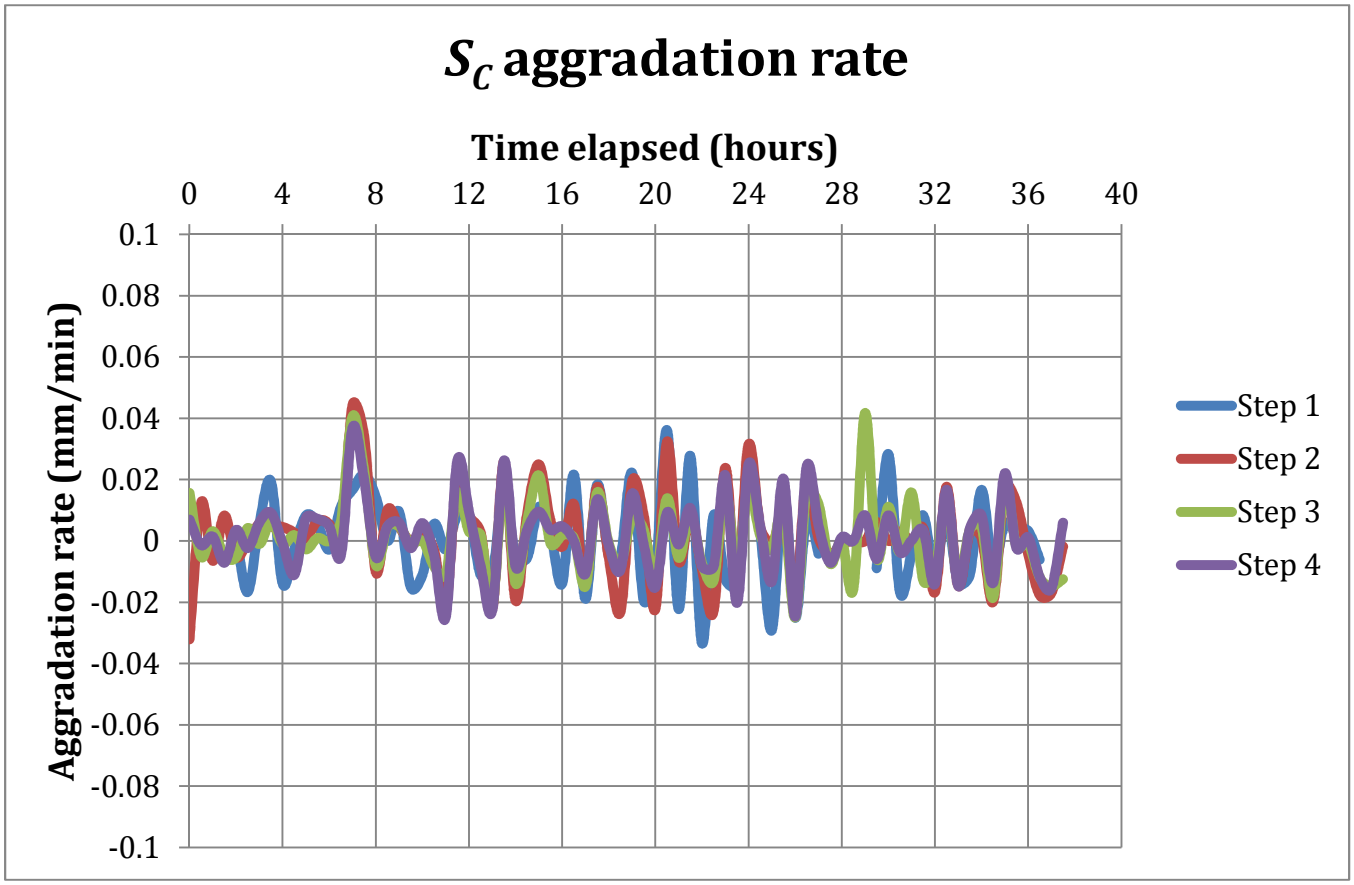

Figures 8.7: Aggradation rate of steps for $L_C$.

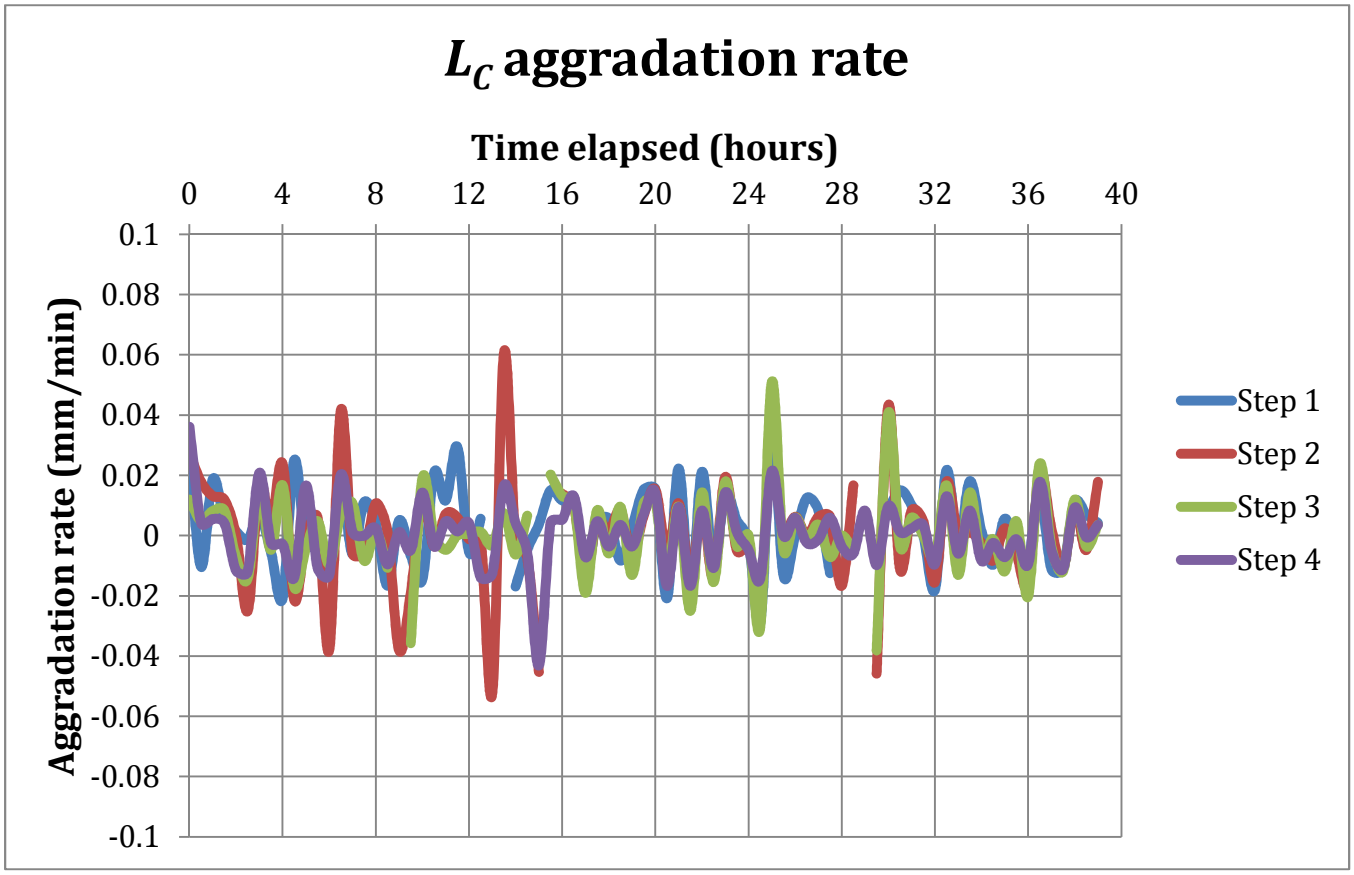

Figures 8.8: Aggradation rate of steps for $L_H$.

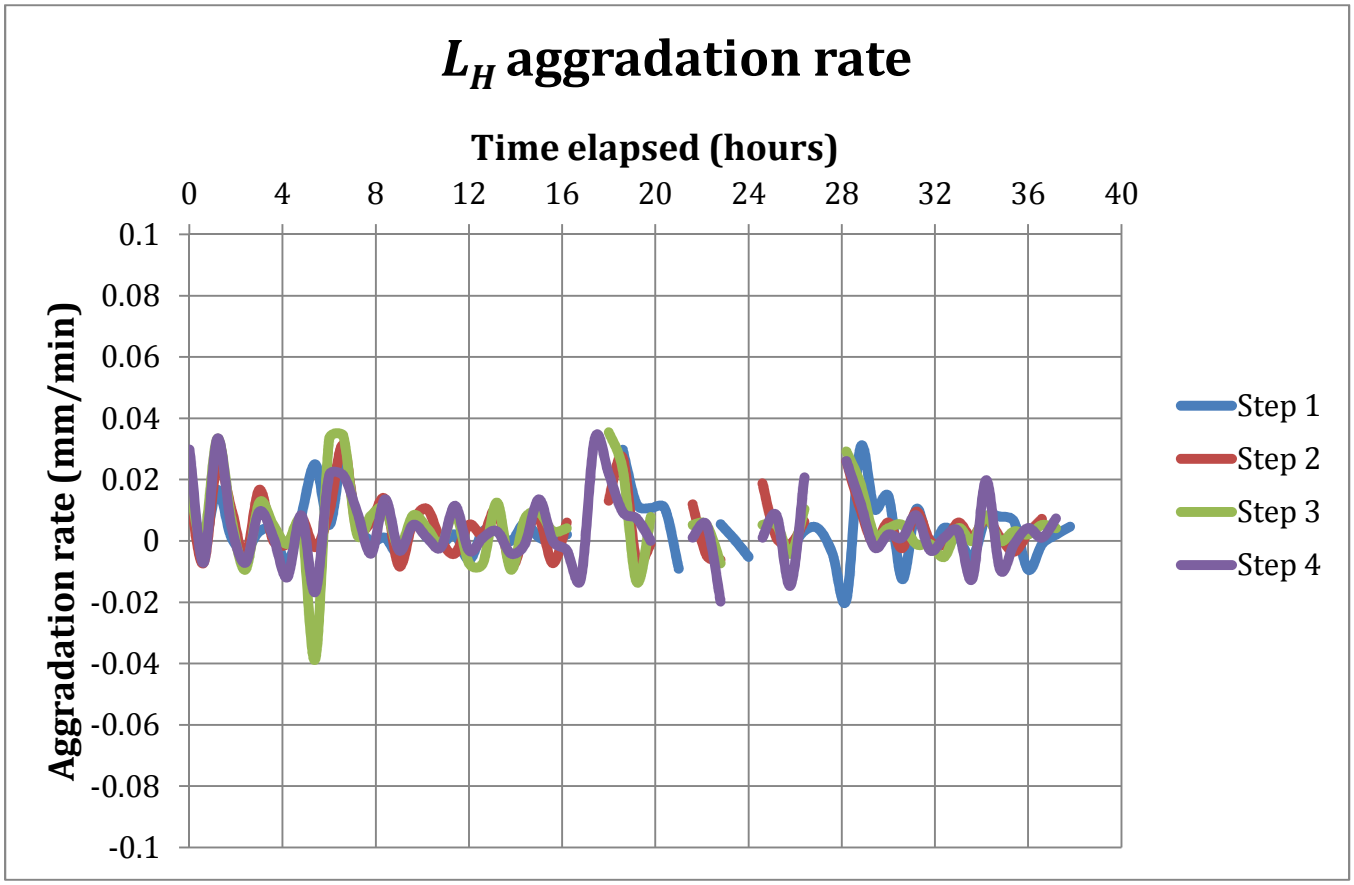

# References


Bargar, K.E. (1978). Geology and thermal history of Mammoth Hot Springs, Yellowstone National Park, Wyoming, U.S. U.S. Geological Survey Bulletin, 1444, 1-54.

Buhmann, D. and Dreybrodt, W. (1984). The Kinetics of Calcite Dissolution and Preciptation in Geologically Relevant Situation of Karst Areas. Chemical Geology, 48, 189-211.

Chafetz, H. S. and Folk, R. L. (1984). Travertines: Depositional Morphology and the Bacterially Constructed Constituents. Journal of Sedimentary Petrology, 54, 289-316.

Chen, J., Zhang, D. D., Wang, S., Xiao, T., and Huang, R. (2004). Factors controlling tufa deposition in natural waters at waterfall sites. Sedimentary Geology, 166, 353-366.

Fouke, B.W., Farmer, J. D., Des Marais, D. J., Pratt, L., Sturchio, N. C., Burns, P. C., Discipulo, M.K. (2000). Depositional Facies and Aqueous-Solid Geochemistry of Travertine-Depositing Hot Springs (Angel Terrace, Mammoth Hot Springs, Yellowstone National Park, U.S.A.). Journal of Sedimentary Research, 70, 565-585.

Frankel, R. B, and Bazylinski, D. A. (2003). Biologically induced mineralization by bacteria; Biomineralization. Reviews in Mineralogy and Geochemistry, 54, 95-114.

Goldenfeld, N., Chan, Y. C., and Veysey, J. (2006). Dynamics of Precipitation Pattern Formation at Geothermal Hot Springs. Physical Review Letters, 96, 254501-1-254501-4.

Hammer, O., Dysthe, D. K., and Jamtveit, B. (2007). The dynamics of travertine dams. Earth and Planetary Science Letters, 256, 258-263.

Hammer, O. (2008). Watch your step. Nature Physics, 4, 255-256.

Kandianis, M.T., Fouke, B. W., Veysey, J. and Inskeep, W. P. (2008). Microbial biomass; a catalyst for $CaCO_3$ precipitation in advection-dominated transport regimes. Geological Society of America Bulletin, 120, 442-450.

Lu, G., Zheng, C., Donahoe, R. J., and Berry Lyons, W. (2000). Controlling processes in a $CaCO_3$ precipitating stream in Huanglong Natural Scenic District, Sichuan, China. Journal of Hydrology, 230, 34-54.

Mann, S. (2001). Biomineralization: Principles and Concepts in Bioinorganic Materials Chemistry. Oxford University Press, Oxford, 201 pp.

Pentecost, A. and Viles, H. (1994). A Review and Reassessment of Travertine Classification. Geography Physique et Quaternaire, 48, 305-314.

Renaut, R. W., and Jones, B. (1997). Controls on aragonite and calcite precipitation in hot spring travertines at Chemurku, Lake Bogoria, Kenya. Canadian Journal of Earth Sciences, 34, 801-818.

Sant' Anna, L. G., Riccomini, C., Rodrigues-Francisco, B.H., Sial, A.N., Carvalho, M.D. and Moura, C. A. V. (2004). The Paleocene travertine system of the Itaborai basin, Southeastern Brazil. Journal of South American Earth Sciences, 18, 11-25.

Schlager, W. (2003). Benthic carbonate factories of the Phanerozoic. International Journal of Earth Sciences, 92, 445-464.

Sorey, M. L., and Colvard, E. M. (1997). Hydrologic investigation in the Mammoth Corridor, Yellowstone National Park and vicinity, U.S.A. Geothermics, 26, 221-249.

Zaihua, L., Svensson, U., Dreybrodt, W., Daoxian, Y., and Buhmann, D. (1995). Hydrodynamic control of inorganic calcite precipitation in Huanglong Ravine, China: Field measurements and theoretical prediction of deposit rates. Geochimica et Cosmochimica Acta, 59, 15, 3087-3097.

Stelmach, K (2011). Thesis. 20 p. B.S. thesis, University of Illinois, Champaign-Urbana.

Vescogni, H. R. (2009). Microbial Biomarkers: Mineralogy, Crystal Fabric and Chemistry of Calcium Carbonate Mineralization. 69 p. M.S. thesis, University of Illinois, Champaign-Urbana.

Veysey, J. and Goldenfeld, N. (2008). Watching Rocks Grow. Nature Physics, 4, 2310-313.